

Doctoral Dissertation (Shinshu University)

**PVC gel based artificial muscle development and
its application on walking assist wear**

March 2016

Yi Li

CONTENTS

Abstract

Chapter 1	Introduction	1
1.1	Background	2
1.2	State of the art.....	3
1.2.1	Robots, orthoses and exoskeletons.....	3
1.2.2	Soft robotic assist wears.....	8
1.2.3	Polymer and textile materials based assist wear	12
1.2.4	Polymer materials based artificial muscles	13
1.3	Study purpose	16
1.4	Outline	16
	PVC gel artificial muscles	23
Chapter 2	PVC gel artificial muscles	24
2.1	Composition and preparation of PVC gels.....	24
2.2	Electrical response of PVC gels.....	25
2.2.1	Deformation of PVC gels.....	25
2.2.2	Mechanism of deformation	26
2.3	Structure and principal of PVC gel artificial muscles.....	27
2.4	Characterizations of PVC gel artificial muscles	30
2.4.1	Displacement measurement.....	30
2.4.2	Generation force measurement	32
2.4.3	Electrical current measurement.....	39
2.4.4	Response rate measurement	41
2.4.5	Cycle life evaluation.....	41
2.4.6	Thermal stability evaluation	43
2.5	Proposal of actuation modular constructions of PVC gel artificial muscles.....	46
2.5.1	Compression type actuation module structure.....	47
2.5.2	Stretching type actuation module structure	48
2.5.3	Compression-Stretching type actuation module structure.....	49
2.5.4	A prototype of stretching type actuation module of PVC gel artificial muscles	50
2.6	Modeling of static characteristics of PVC gel artificial muscles.....	54
2.6.1	Hill's muscle model.....	54
2.6.2	Model of characteristics based on Hill's equation.....	55
2.7	Chapter summary	58
Chapter 3	Proposal of a lightweight walking assist wear using PVC gel artificial muscles .	63

3.1	Biomechanics of walking	63
3.1.1	Walking gait cycles	63
3.1.2	Motion definition of lower limbs	65
3.1.3	Angle, moment and power of lower limb joints	66
3.2	Proposal of a walking assist wear with PVC gel artificial muscles	67
3.3	Walking assistance method with the assist wear	68
3.4	Chapter summary	71
Chapter 4	Design and prototyping of the proposed walking assist wear	73
4.1	Actuation modules	73
4.1.1	Specification design of PVC gel artificial muscles	73
4.1.2	Structure of the actuation modules	75
4.1.3	Structure of electrodes and wiring	77
4.1.4	Fabrication of actuation modules	79
4.2	Walking motion detector	80
4.2.1	Sensors selection and calibration	81
4.2.2	Design and fabrication of walking motion detector	82
4.3	Controller	84
4.3.1	NI myRIO and its calibration	84
4.3.2	Control system construction	86
4.4	Prototype of the PVC gel artificial muscles based walking assist wear	87
4.5	Chapter summary	89
Chapter 5	Characterization and performance of the fabricated walking assist wear	92
5.1	Basic characteristics of the assist wear	92
5.1.1	Displacement	92
5.1.2	Output force	93
5.1.3	Response time	95
5.1.4	Current	96
5.2	Performance of the walking assistance system	97
5.2.1	Insole force sensors measurement	97
5.2.2	Walking gait cycles detection and output control	97
5.3	Comparisons with the other assist wears	101
5.4	Chapter Summary	103
Chapter 6	Walking experiments using the assist wear system	106
6.1	Purpose and hypotheses	106
6.2	Methods and conditions	106
6.2.1	Subject characteristics	106

6.2.2	Experimental methods and devices	107
6.3	Results and discussions.....	111
6.3.1	Walking motion detection and assist wear control	111
6.3.2	Walking speed and length of steps	112
6.3.3	Acceleration and angular velocity of the upper body	114
6.3.4	Surface EMG of the muscles	116
6.3.5	Impression evaluation questionnaires.....	119
6.4	Chapter summary	121
Chapter 7	Conclusion	123
Acknowledgement	126
List of publications	128

List of Figures

Fig. 1.2.1. Exoskeletons for human augmentation.....	4
Fig. 1.2.2. Robotic wears and exoskeletons for rehabilitation, medical assistance.....	6
Fig. 1.2.3. Soft robotic wears for assistance and rehabilitation..	9
Fig. 1.2.4. Polymer and textile materials based assist wears for human support.....	13
Fig. 1.2.5. Polymer materials based artificial muscles..	14
Fig. 2.1.1. Preparation of PVC gel.....	25
Fig. 2.2.1. A bending deformation of PVC gels under an electric field. [13].....	26
Fig. 2.2.2. Deformation of a PVC gel membrane under a DC field in a front view.....	26
Fig. 2.2.3. (a) A result of space-charge measurement of a PVC gel. (b) Deformation mechanism (left part) and FEM analysis result of PVC gels (right part) [18].....	27
Fig. 2.3.1. Structure and deformation of PVC gel artificial muscles.....	29
Fig. 2.4.1. Method of displacement measurement. (a) Illustration. (b) Real device.	30
Fig. 2.4.2. Displacement of PVC gel artificial muscles with different number of stacked layers.	31
Fig. 2.4.3. Displacement of PVC gel artificial muscles with different number of stacked layers..	32
Fig. 2.4.4. Contraction force measurement of PVC gel artificial muscles.....	33
Fig. 2.4.5. Result of the contraction force before a separation happens.	33
Fig. 2.4.6. Proposed method of recovery force measurement.	34
Fig. 2.4.7. Relation between displacement and output force under different applied DC voltages.	37
Fig. 2.4.8. Relation between strain and output stress under different applied DC voltages.....	38
Fig. 2.4.9. Method of electrical current measurement of PVC gel artificial muscles.....	39
Fig. 2.4.10. A raw data of current variation of a 10-layer PVC gel artificial muscle at an input voltage of 400V.	39
Fig. 2.4.11. Equivalent circuit of PVC gel artificial muscle.	40
Fig. 2.4.12. Current of PVC gel artificial muscle with different number of stacked layers.	40
Fig. 2.4.13. Response rate of PVC gel artificial muscles.....	41
Fig. 2.4.14. Durability evaluation of PVC gel artificial muscles.....	42
Fig. 2.4.15. Characteristics variation of PVC gel artificial muscles during a long-term experiment.	45
Fig. 2.4.16. Displacement variation of 10-layer PVC gel artificial muscles under a DC voltage	

of 400V, a frequency of 1Hz with a duty ratio of 12.5%.....	46
Fig. 2.5.1. Illustration of compression type actuation modules.....	47
Fig. 2.5.2. Illustration of stretching type actuation modules.....	48
Fig. 2.5.3. Illustration of compression-stretching type actuation.....	49
Fig. 2.5.4. A prototype of stretching type actuation modules.....	50
Fig. 2.5.5. (a) Illustration of performance measurement of contraction force and recovery force. (b) Method of contraction force. (c) An example of a separation happens among the stacked layers when the applied load is 0.35kg.....	52
Fig. 2.5.6. Definition of response time of contraction and expansion.....	53
Fig. 2.5.7. Performance comparison of contraction force and recovery force measurement. ...	53
Fig. 2.6.1. Hill's force-velocity relationship, where P_m is maximum isometric force or force with zero velocity, S_m is the highest possible velocity, a and b are constant force and constant velocity.....	55
Fig. 2.6.2. Results of constant coefficients at different voltages. (a) a_f . (b) b_x . (c) c	56
Fig. 2.6.3. Simulation result based on the proposed model.	56
Fig. 2.6.4. Relation between the number of stacked layers and the output stress at a desired displacement of (a) 0.5mm and (b) 1.0mm.....	57
Fig. 3.1.1. Simulation result based on the proposed model.	64
Fig. 3.1.2. (a) Description of the anatomical planes. (b) A kinematic model of the leg with the positive direction of each joint indicated.....	65
Fig. 3.1.3. Representative angles, moments, and power of the leg flexion/extension joints over the gait cycle. Data are adapted from [4].....	66
Fig. 3.2.1. Structure of the proposed walking assist wear with PVC gel artificial muscles.....	68
Fig. 3.3.1. (a) Muscular activities variation during swing phase (adapted from [1]). (b) Muscles of the leg.....	69
Fig. 3.3.2. Method of walking assistance in walking gait cycles.....	70
Fig. 4.1.1. (a) Model of human body with the assist wear in the sagittal plane, the length of the assist wear is varying during walking gait cycles. (b) The results of the slack (ΔL) generated during a walking gait cycle with different thickness of the edge profile (X_b) of the waist belt while the height between the Greater trochanter and waist belt (Y_b) is about 20 mm.	74
Fig. 4.1.2. Structure of the actuation modules.....	76
Fig. 4.1.3. Structure of the electrodes.....	77
Fig. 4.1.4. (a) Traditional method of wiring for a multilayered artificial muscle, with a fabricated sample (80-layer). (b) Proposed method of wiring for a multilayered artificial muscle, with a fabricated sample (80-layer). (c) Photographs show the easy handle of a	

80-layer PVC gel artificial muscle with the new wiring.	78
Fig. 4.1.5. Results of the comparisons between the traditional wiring method and the proposed one.	79
Fig. 4.1.6. The fabricated prototype of actuation modules with PVC gel artificial muscles.	80
Fig. 4.2.1. Calibration of the force sensors.	81
Fig. 4.2.2. Fabrication of the walking motion detector.	83
Fig. 4.3.1. (a) Overview of the NI myRIO-1900 device. (b) NI myRIO-1900 hardware block diagram.	85
Fig. 4.3.2. Results of calibration of the analog input (MXP A/B) and analog output channels (MSP C).	86
Fig. 4.3.3. Control system of the walking assist wear.	87
Fig. 4.4.1. Prototype of the walking assist wear with PVC gel artificial muscles.	88
Fig. 4.4.2. Photographs of several basic motions of an elderly subject with the fabricated prototype of assist wear.	89
Fig. 5.1.1. Displacement and contraction strain of the assist wear.	93
Fig. 5.1.2. Output force measurement of the assist wear.	94
Fig. 5.1.3. Response time of the actuation modules of the assist wear.	95
Fig. 5.1.4. Electrical current of the assist wear.	96
Fig. 5.2.1. Force measurement using the insole force sensors.	97
Fig. 5.2.2. Results of the force measurement and output voltage control I.	98
Fig. 5.2.3. Results of the force measurement and output voltage control II.	99
Fig. 5.2.4. Estimation of assistance force of control method C1 and C2 during a walking gait cycle.	100
Fig. 6.2.1 Illustration of a to-and-fro straight line walking for about 10m.	108
Fig. 6.2.2. Arrangement of the EMG electrodes.	109
Fig. 6.2.3. Measurement method of acceleration and angular velocity.	109
Fig. 6.2.4. (a) Overview of wearing the PGAMs assist wear. (b) Overview of the walking experiment.	111
Fig. 6.3.1. Results of the walking motion detection and assist wear control.	112
Fig. 6.3.2. Results of the walking speed in the four types of walking.	113
Fig. 6.3.3. Results of the step length in the four types of walking.	113
Fig. 6.3.4. Results of the acceleration of the upper body during walking.	115
Fig. 6.3.5. Results of the angular velocity of the upper body during walking.	115
Fig. 6.3.6. Results of the integrated electromyogram (IEMG) variation during a walking gait cycle.	117
Fig. 6.3.7. (a) IEMG of the Rectus femoris muscle. (b) IEMG of the Sartorius muscle. (c)	

IEMG of the Hamstring. (d) IEMG of the Gastrocnemius.	118
Fig. 6.3.8. (a) %IEMG of the Rectus femoris muscle. (b) %IEMG of the Sartorius muscle. (c) %IEMG of the Hamstring. (d) %IEMG of the Gastrocnemius.	118
Fig. 6.3.9. (a) %MVC of the Rectus femoris muscle. (b) %MVC of the Sartorius muscle. (c) %MVC of the Hamstring. (d) %MVC of the Gastrocnemius.	119
Fig. 6.3.10. Five degree with a score from -2 to 2 for impression evaluation questionnaires.	120

List of Tables

Table 3.3.1. Muscular activities variation during swing phase (%GC) (adapted from [1])	69
Table 4.2.1 Dimension of each portion of foot (items from Fig. 4.2.2 (c))......	84
Table 5.3.1. Comparisons of the degree of freedom of movement between the PVC gel artificial muscles based assist wear and the motors based assist wear.	102
Table 5.3.2. Comparisons of the weight and power consumption between the PVC gel artificial muscles based assist wear and the motors based assist wear.	102
Table 6.2.1 Characteristics of the subject in the walking experiment.	107
Table 6.3.1. Result of the impression evaluation questionnaires.	120

Abstract

The rapid aging of global population has brought a situation in which more and more elderly people need to be cared for by the other elderly family members or professional caretakers. Aging may cause reduced mobility, which leads to loss of independence and muscular atrophy. And the spontaneous walking speed and pace length decrease due to the gait disorders and lower-limb impairments which may lead to a fall during walking.

Walking assistance for the elderly or the people with walking disabilities has received serious attention in the field of robotics and mechatronics in recently years. A large number of wearable robots, suits or devices have been developed over the years, usually with the purpose of assisting or augmenting human walking. Most of them are exoskeletons using electric motors with rigid links in parallel with the body that can impart torques to the joints and support compressive forces. However, exoskeletons still present some ongoing challenges, such as a heavy load, a bulky structure, high stiff rigid frames, which could be a burden for the elders with weakened muscles and the rigid frames may restrict the natural movements of the wearers.

Our long term goal is to develop a wearable assistive device that can be used for a daily life to support the elders with some weakened muscles or to lighten the muscular burdens of the healthy people during walking. In addition to have the function of lightening the burden of the wearers during walking, the devices should have low impedance, high flexibility, be comfortable and safe to wear and easy to don and doff. Therefore, some innovative technologies are needed to support the daily activities of elderly people and to lighten the heavy burden of nursing in the aging society. And we think the technology of artificial muscle based soft actuators should be one of the key issues for developing such technologies.

Polymer materials based artificial muscles have the properties of being soft, lightweight and flexible which are similar to the nature muscular actuators, have attracted great attention these years. However, most of artificial muscles so far are being challenged by the characteristics improvement to reach or exceed the level the nature muscles for a successful commercialization and a wide use. That is to achieve a large strain and stress, a fast response rate and a long cycle life with a low power consumption. We have developed a soft artificial muscle using the plasticized polyvinyl chloride (PVC) gel which has many positive characteristics, such as being soft and lightweight, having a stable actuation in the air with a high output, a notable response rate, a low power consumption and no noise, which showed a great potential for practical applications among all the candidates of artificial muscles.

In this thesis, we developed a novel lightweight, flexible wearable walking assistive wear using PVC gel artificial muscles. Compared to other prior motors based wearable assistive devices, the

proposed assist wear had the features of no rigid mechanical structures, minimal weight, compact and high flexibility which made the assistive device possibly be wearable like a clothing. The main works concern two aspects as development of PVC gel artificial muscles and application on the walking assist wear.

For the development of PVC gel artificial muscles, we have improved the characteristics of PVC gel artificial muscles from several aspects, from the gel membranes to artificial muscle fabrication to make it almost close to the level of the biological muscles. And we have proposed an improved approach to measure the output force of PVC gel artificial muscles that can accurately measure the characteristics than the former method which made a great sense in present and future development of PVC gel artificial muscle technologies. Also we have proposed three types of modular constructions to make the PVC gel artificial muscles become robust actuation devices for different kinds of applications, which are very important elements for the standardization of PVC gel artificial muscles. Furthermore, the model of the static characteristics developed in this study which showed a good agreement with the experimental data could be an effective element for the specific design and control of the proposed modular constructions in an application.

For the application on a walking assist wear, we have proposed a novel lightweight wearable assistive wear using PVC gel artificial muscles, according to the biomechanics of walking. The assist wear is able to assist the lower limb during the swing phase, from the moment that the toe leaves the ground, providing an assistance over 10% of the maximum moment on the hip to support the motion of the hip joint until the moment of the heel initially contact to the ground, so as to reduce the burden of the leg muscles in the flexion motion. And we have designed and prototyped the walking assist wear using PVC gel artificial muscles, and developed a smart and cost effective walking motion detector and a competent controller. We used a stretching-type structure to make the assist wear be robust to avoid a break and to obtain a high output force. A frame-only structure, a curved surface shape together with a compact new wiring design of the actuation modules makes the assist wear getting a good fitting to the body and makes it more compact. And we used some cheap but smart insole force sensors to construct a walking motion detector for supporting the control of the assist wear, together with a portable computer NI (National Instruments Corporation) myRIO to make the system be multifunctional and cost effective. The characteristics evaluation experimental results of the system were almost consistent with the desired results which indicated the effectiveness of the designed walking assistance system with PVC gel artificial muscles.

And we have conducted experiments to validate the effectiveness of the walking assist wear system, founding that, with the assistance of the PVC gel artificial muscles based assist wear the walking speed increased about 10% and the step length of the assisted leg increased about

2.8cm during walking.

Also we obtained about 17% maximum decrease of the muscular activity for the Rectus femoris muscle, about 11% maximum decrease for the Sartorius, about 5% maximum decrease for the Hamstring with a significant difference of 1% which shows that the assist wear can reduce the burden of the muscles of the lower limb during walking.

And the assist wear is compact and lightweight, showing no impedance to the natural movement of the wearer during walking, and it allowed the wearer walking freely like a clothing.

Therefore, the proposed PVC gel artificial muscles based assist wear could be reasonable for a daily life use, for the advantages of a simple structure, compact and lightweight, flexible, good in fitting and easy to put on and take off.

Chapter 1
Introduction

Chapter 1 Introduction

1.1 Background

Aging society has becoming a global social issue especially in Japan, of which 26.6% of the population is aged 65 or above, 12.9% aged 75 or above, as of April 2015 [1], which is thought to be outweigh all the other nations. The rapid aging of global population has brought a situation in which more and more elderly people need to be cared for by the other elderly family members or professional caretakers after suffering a stroke, developing senile dementia or being hit by age-related disabilities. In some cases, the caretakers become physically exhausted and stressed out due to the heavy burden to help these elderly people [2].

Walking is one of the main motions of human which is the key factor of doing the daily activity of doing physical exercise, shopping and public activities outdoors. Aging may cause reduced mobility, which leads to loss of independence and muscular atrophy [3-6]. The spontaneous walking speed decreases by about 1% per year from age 60 onward, and even greater in the maximum walking speed [7]. Gait disorders and lower-limb impairments are also common and often devastating companions of aging which showed a 35% prevalence of gait disorders among persons over age 70, and 80% over 85 years of age [8]. Fall is one of the most serious consequences of mobility impairment for the elders, one third of people aged 65 years or older fall each year [9], and the death rates from falls is about 10% and 60% for the people aged over 65 years and 74 years, respectively [10].

Walking assistance for the elderly or the people with walking disabilities has received serious attention in the field of robotics and mechatronics in recently years. A large number of wearable robots, suits or devices have been developed over the years, usually with the purpose of assisting or augmenting human walking [11-13]. Meanwhile, some novel technologies (e.g. artificial muscle actuators) were emerged in this field. We will introduce the state of the art in the following sections.

1.2 State of the art

1.2.1 Robots, orthoses and exoskeletons

The history of researches in powered human exoskeleton devices for motion assistance can date back to the 1960s in the United States [14] and in the former Yugoslavia [15], where the former was primarily focused on developing technologies to augment the abilities of able-bodied humans, often for military purposes, while the latter was intent on developing assistive technologies for physically challenged persons. Even though different purposes they have, they face many of the same challenges and constraints, particularly those related to portability and interfacing closely to a human operator [16]. Until 1971, General Electric Research developed and tested a full-body powered prototype man-amplifier called the Hardiman [17-19], as shown in Fig. 1 (a). Although it could lift 340kg and responded according to specification, it weighted 750kg and ran into fundamental technological limitations, such as a low speed of computer processing, heavy and bulky energy supplies and actuators.



Fig. 1.2.1. Exoskeletons for human augmentation. (a) General Electric’s Hardiman exoskeleton [19]. (b) The University of California at Berkeley’s BLEEX exoskeleton [21]. (c) The Berkeley Robotics and Human Engineering Laboratory’s ExoHiker™ robotic exoskeleton [24]. (d) French engineering company RB3D’s Hercule exoskeleton [25]. (e) Raytheon Sarcos’s XOS exoskeleton [26]. (f) MIT’s lower limb exoskeleton [27]. (g) NASA X1 exoskeleton [28]. (h) The Cyberdyne Inc.’s HAL exoskeleton [29].

Nowadays, orthoses and exoskeletons for human augmentation, rehabilitation and medical assistance have been developed prosperously, in different types of mechanical structures, actuators, interfaces and control strategies [11, 12].

For human augmentation exoskeletons, a big progress has achieved since a five-year program sponsored by the DARPA (American Defense Advanced Research Projects Agency) called Exoskeletons for Human Performance Augmentation (EHPA), of which the goal is to develop devices and machines to increase the speed, strength, and endurance of soldiers in combat

environments [20].

The Berkeley BLEEX [21-23], developed by the University of California, featured more than forty sensors and actuators to make the exoskeleton to function much like a human nervous system. It has been demonstrated to support up to 75 kg, walk at speeds up to 1.3 m/s [23]. After developing BLEEX, ExoHiker, and ExoClimber, Berkeley Bionics and his team created HULC (Human Universal Load Carrier), which has almost the same appearance with ExoHiker (Fig. 1.2.1 (c)) [24]. HULC incorporates the features of ExoHiker and ExoClimber exhibiting two independent characteristics. One is that it can take up to 200 pounds (about 100kg) without impeding the wearer (Strength Augmentation) and another is that it decreases its wearer's metabolic cost (Endurance Augmentation). Besides, Hercule exoskeleton (Fig. 1.2.1 (d)) [25], developed for the French Army, claimed to be lighter, easier to use and more agile than rival systems. No special training needed to wear the exoskeleton to do tasks for the users. The electrical power source was different from the rival systems that using some combustion or hydraulic engines. The battery can provide an about 20 km walking at a regular walking pace, with a load of 100 kg. And the XOS exoskeleton (Fig. 1.2.1 (e)) [26] by Ratheon Sarcos, Utah, was developed for military and civilians use. It can allow the users to lift heavy loads up to 200 pounds repetitively without tiring and to carry heavy cargos on long distances. The biomechatronics group at Massachusetts Institute of Technology (MIT) developed an exoskeleton which would reduce the burden for soldiers and others who carry heavy packs and equipment, a prototype as shown in Fig. 1.2.1 (f) [27]. The prototype weighs about 11.8 kg and is powered by a 48 V battery pack. It found that though the load borne by the wearer's back was lightened significantly, the wearer consumed 10% more oxygen than usual for the extra effort that required to compensate for gait interference. The NASA X1 exoskeleton (Fig. 1.2.1 (g)) [28] is uniquely aiming to improve crew health both aboard the space station and during future long-duration missions to an asteroid or Mars. It could keeping the astronauts healthy in microgravity by replicating the common crew exercises. Furthermore, the Robot Suit Hybrid Assistive Limb (HAL) exoskeleton (Fig. 1.2.1 (h)) [29, 30], is aimed at a range of uses including training doctors and physical therapists, assisting the disabled, allowing workers to carry heavier loads and as an aid in emergency rescues. It does not detect the user's motion but uses sensors on the skin to detect directly the bio-electrical signals of the muscles. This has the advantage of allowing people suffering spinal cord injuries or with paralyzed limbs be able to use the suit. The suit weighs 23 kg and is powered by electric motors running from a 100 V AC battery that lasts about 3 hours.



Fig. 1.2.2. Robotic wears and exoskeletons for rehabilitation, medical assistance. (a) The New Zealand REX Bionics Ltd.’s REX exoskeleton [31]. (b) Argo ReWalk™ exoskeleton [32]. (c) The Berkeley Bionics’ eLEGS exoskeleton [33]. (d) Vanderbilt’s exoskeleton [34]. (e) The Cyberdyne Inc.’s HAL exoskeleton for rehabilitation [30]. (f) Honda’s robotic device [35]. (g) The Toyota Technological Institute’s exoskeleton [36]. (h) The ShinShu University’s robotic wear CURARA® [37].

For rehabilitation and medical assistance, many types of robotic wears and exoskeletons were developed to supply additional energy for daily-life movements of healthy young and elderly people and those suffering from lower-limb muscular weakness or disabilities.

The New Zealand’s REX exoskeleton (Fig. 1.2.2 (a)) [31] has been designed from the outset to provide mobility to non-ambulatory wheelchair users rather than to support the abled individuals. It is composed of a pair of robotic legs which could help the people suffering from paraplegia to stand, walk, move sideways, turn around and go up and down stairs. The system is

powered by a rechargeable battery that typically provides two hours of active use on a full charge. Argo ReWalk exoskeleton (Fig. 1.2.2 (b)) [32], is also designed to help paraplegics. Battery-powered system features a light, wearable exoskeleton with motors at the hip and knee joints. An on-board computer and motion sensors realize a self-initiated walking without any switches to begin a step. A forward tilt of the upper body is sensed by the system, which leads up the first step. It controls movement using subtle changes in center of gravity and repeated body shifting generates a sequence of steps which mimics natural gait and provide functional walking speed. The Berkeley Bionics' another exoskeleton eLEGS (Fig. 1.2.2 (c)) [33] also can help the people with a wheelchair to walk once again. It uses a gesture-based human robot interface to determine the user's intentions. The Vanderbilt exoskeleton (Fig. 1.2.2 (d)) [34] has been developed to provide gait assistance to the stroke and spinal cord injured (SCI) population, is controlled by the person shifting the body's center of gravity, like the ReWalk. But weighs only 27 pounds (12 kg) that is lighter than the ReWalk (about 23.3kg). Besides, the mobile exoskeleton HAL (Fig. 1.2.2 (e)) [30], which was originally developed as a strength augmentation exoskeleton, but has applications in the rehabilitation. HAL utilizes biofeedback through EMG signals from the surface of the skin, which makes it applicable for some injury types where muscle signals can still be read. However, the upper-body exoskeleton is mainly focused on strength augmentation for lifting. Honda developed a robotic device (Fig. 1.2.2 (f)) [35] to help people with mobility problems, especially for the elderly people. Two motors are used to help lift each leg at the thigh as it moves forward and backward. The aim is to lengthen the user's stride, making it easier to cover longer distances at a greater speed. It weighs 2.8kg including a 22.2V battery, which can provide about 2 hours' action. The Toyota Technological Institute proposed a versatile upper and lower body exoskeleton (Fig. 1.2.2 (g)) [36] that can be potentially utilized in robotic rehabilitation and power augmentation tasks. The exoskeleton utilizes off-the-shelf joint-level compensation techniques developed for robot manipulators to achieve sensor less control while handling exoskeleton-based robotic rehabilitation and power augmentation tasks. Furthermore, a robotic wear CURARA[®] (Fig. 1.2.2 (h)) [37] for human assistance and rehabilitation is developed at ShinShu University. The key design of the structure is that it uses the skeletal system of the human body to support the weight of the each part of the wear at the joints. Unlike the other systems (each part of the exoskeleton is connected by a rigid frame), CURARA[®] uses no full-body rigid frames to transfer the power, so called a non-exoskeletal structure which makes the robotic wear much lighter (total weight of about 10 kg) and allows the wearer to move more naturally and freely. This could be one big step to make the general exoskeletons possible for a widespread use.

Some other exoskeletons and devices, such as the LOPES device [38], the Kanagawa Institute of Technology's Power Suit [39], MINA orthoses for paraplegics [40] and MIT RoboWalker

[41] are also doing efforts in this field. And each of these systems' effectiveness has been confirmed due to a large number of clever and innovative design features and control strategies.

However, for a widespread use, exoskeletons still present challenges such as large interaction loads occurs due to the misalignments between human limbs and exoskeleton [42] and exoskeletons may require bulky self-aligning mechanisms [42, 43]. Even though the weight of the exoskeleton is supported by the exoskeleton itself, the inertia is still felt by the user. Besides, the motors based actuators were too stiff, heavy, bulky and noisy, which should have some innovative improvement in the future. Furthermore, most if not all of the exoskeletons would restrict some other natural movements that don't need the assistance, which could bring a burden to the users [37].

1.2.2 Soft robotic assist wears

Soft robotic assist wears could have some tremendous advantages over with the rigid exoskeletons:

1. Soft robotic assist wears are flexible and compliant.
2. It could be easier for the soft robotic assist wear to fit an individual user's body due to their high flexibility, while the rigid exoskeletons have to prepare different types of metal suits for different persons.
3. Soft robotic assist wears could be more compact, much lighter and require less energy to consume.
4. Soft robotic assist wears could provide fewer limitations to the wearers' joints so as to be easier to wear.
5. Soft robotic assist wears could be possibly worn underneath clothing, which would be adapted by the general public much faster. This could make a great sense as that in general, current exoskeletons are viewed as ugly and unattractive.
6. Soft robotic assist wears could be significantly less expensive than rigid frame exoskeletons.

However, since the soft robotic assist wears have no external rigid frames which means that the wearable devices will have difficulty transferring power from any area of the body to the ground. Motors and sensors will be more difficult to mount due to the complex structure of human body. Therefore, unlike the traditional exoskeletons, barely a soft robotic assist wear has been commercialized and wide used so far due to different reasons. But many researches have been done in this field.

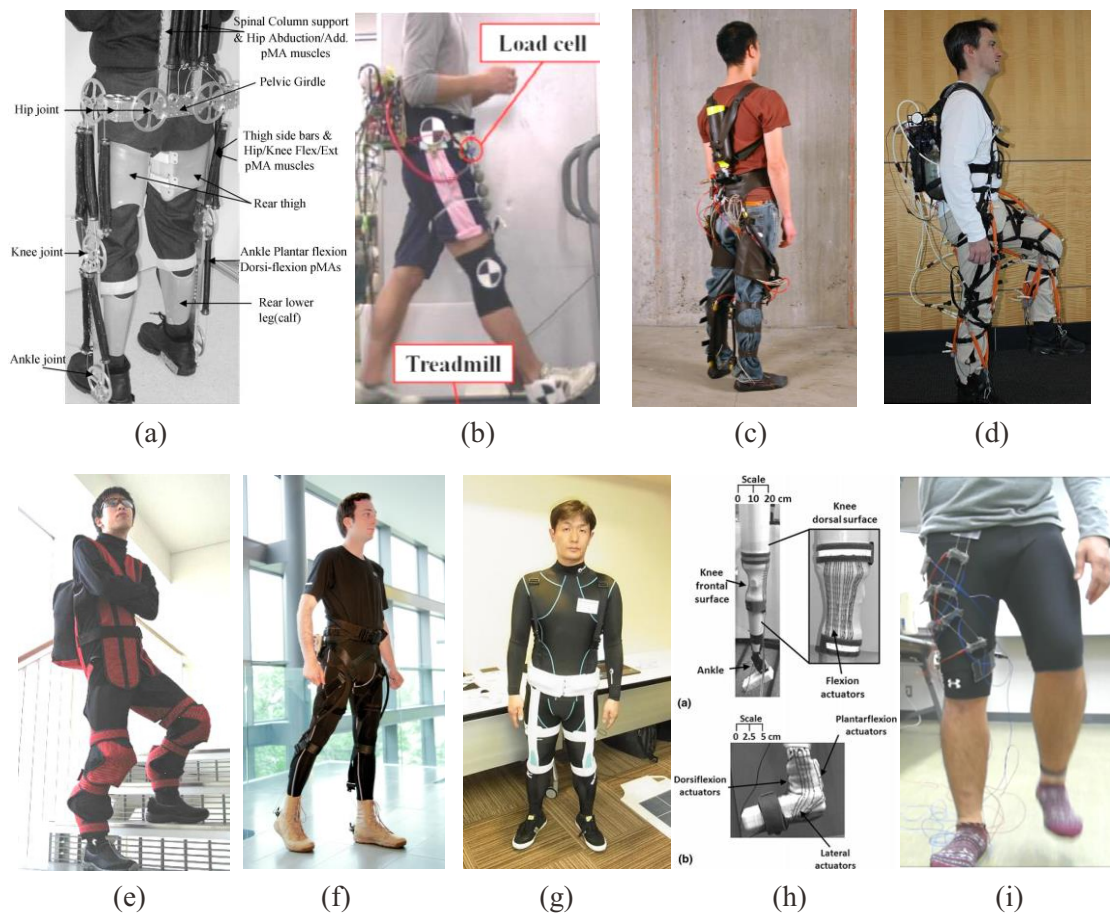


Fig. 1.2.3. Soft robotic wears for assistance and rehabilitation. (a) Powered Lower Limb Orthosis by N. Costa [46]. (b) Power assist wear by T. Kawamura [47]. (c) The ITP.NYU's Soft Pneumatic Exoskeleton [49]. (d) Harvard's Wyss Institute's pneumatically-powered Soft Exosuit [50]. (e) Power assist wear by D. Sasaki [51]. (f) Harvard's Wyss Institute's Soft Exosuit [53]. (g) Sumitomo Riko Company Limited's latest soft robotic wear [54]. (h) Shape Memory Alloy Wire for an Active, Soft Orthotic by Leia Stirling [56]. (i) The variable stiffness PVC gel spats by Y. Maeda [58].

So far, most of the soft robotic assist wears are constructed by the Pneumatic Muscle Actuators (PMAs) [44, 45] which have the advantages of high force to weight ratio, lightweight, low cost and flexibility. N. Costa et al. [46] proposed a powered lower limb orthosis for rehabilitation using PMAs (Fig. 1.2.3 (a)). A pair of PMAs are connected antagonistically around each joint through a pulley (by a cable-driven) to provide a moment to assist the joint motion. The system is flexible and compliant that can easily deal with the tolerance for mechanical misalignments. It found that the orthosis can

perform almost the same range of motion of an abled-individual. However, the prototype weighs 11 kg not including the air source which showed little advantage over the traditional exoskeletons. T. Kawamura et al. [47] developed a flexible power walking assistant system based on pneumatic artificial muscle (Fig. 1.2.3 (b)), which can provide a 40mm stroke with a load of 40N that corresponding to torque of about 5% of the nominal biological moment at the hip during unloaded walking. When applied it on a healthy subject during walking, it was found that the EMG of the sartorius muscle decreased and the average step length increased about 23mm with the assistance of the assist wear. However, the system needed to be improved for an accurate control and a compact and lightweight structure which was proposed in [48]. A team from ITP of NYU developed a Soft Pneumatic Exoskeleton (Fig. 1.2.3 (c)) [49] to help the wearer to lift heavier loads as well as walking. It is powered by a small scuba-diving bottle worn on the back, and is triggered when the user flexes his muscles. A force sensor under the foot and a flex sensor behind the knee activate the air muscles around the calf and quads, respectively. The attractive benefit of the Pneumatic Soft Exoskeleton is its light weight (about 3 kg, including the five-pound scuba tank) and flexibility. But the capability of a continuous performance using the limited air source is not verified. Besides, as shown in a video online, the response speed of the muscles seems a little slower than that of human motion. Michael Wehner et al. [50] proposed a lightweight soft exosuit for gait assistance using soft McKibben style pneumatic actuators (Fig. 1.2.3 (d)) to augment the normal muscle work of healthy individuals by applying assistive torques at the wearer's joints with the goal of reducing the metabolic cost of transport of the wearer. Compared to traditional exoskeletons, the exosuit presented provides minimal additional mechanical impedance and kinematic restrictions with a weight of about 7kg not including the air cylinder. It was found that there was a 10.2% reduction in average metabolic power when comparing the powered and optimally tuned suit to the passive unpowered suit. Another PMAs based assist wear for locomotion assistance was presented by D. Sasaki (Fig. 1.2.3 (e)) [51]. It is a trousers-like power assist wear where the pneumatic actuators are composed by three balloon and circular actuators, one on the knee, one on the rear of thigh and one on the rear of the shank, which are attached by a hook-and-loop fastener between the outer and inner wears. The whole weight of this system is about 3.7 kg. And the system can be driven for almost 1 hour by driving air pumps intermittently. Experiments with one subject showed that the peak of subject's EMG decreased during walking upstairs, but some extra peaks were recorded while walking downstairs.

And some other pneumatic muscle-type actuators based assistive rehabilitation

robotics systems, with different designs and control schemes are reported in [52]. Nevertheless, pneumatic muscles based system seems to have challenges on the volume change of actuators with the on and off actuations which may make the device bulky, and the pneumatic power supply system could bring a burden and noise.

To overcome such problems, Harvard University proposed a soft clothing-like Soft Robotic Exosuit which was actuated by geared motors driving Bowden cables (Fig. 1.2.3 (f)) [53]. Unlike the traditional exoskeletons, the Exosuit does not consist of a rigid frame but a series of webbing straps, and uses geared motors to pull a Bowden cable which is connected to the suit in proximity of the ankle joint. The suit tension is controlled and augmented and torques acting on the hip and knee joints are as well increased owing to the curved path of the straps. The total system weighed 6.5kg including the textile exosuit, and consumed 65W in the multiarticular load path and 72W at the hip during walking at 1.79m/s (4.0mph). Primary results with a healthy subject showed that the Exosuit could apply powered torques to the hip and ankle joints, around 18% of the normal human walking torques. Another soft walking assist wear that has the similar principal with the Harvard Exosuit was proposed by Sumitomo Riko Company Limited and Kyusyu University, as shown in Fig. 1.2.3 (g) [54]. The assist wear was actuated by geared motors driving Soft Elastic Belts to assist a flexing motion of the user's hip joint during walking using elastic force generated by elongating the belt. The motors actuated according to the gait cycle change which was detected by two Smart Rubber (SR) sensors. The system weighs 2.2 kg, without an output force of 40 N. Experimental results showed the EMG of the gastrocnemius was decreased up to 17% by walking with the device.

Besides, a shape-memory alloy (SMA) [55], as a replacement of conventional actuators such as electric motors, pneumatics and hydraulics due to their unique characteristics and ability to react directly to environmental stimuli, has many applications in biomedical and robotics. Leia Stirling et al. presented a primary work on development of an active, soft orthotic for the knee using NiTi shape memory alloy (SMA) wires (Fig. 1.2.3 (h)) [56]. They found that the SMA spring actuators made possible a full range of knee motion, but with a slow response and high power consumption. Moreover, a heat problem could be happened when using more SMA wires to construct a Clothes-type orthosis [57].

In our previous study, we focused on walking assistance for daily life and presented a preliminary work of developing novel poly vinyl chloride (PVC) gel actuators based light-weight and soft wearable assistive spats (Fig. 1.2.3 (i)) [58, 59] for supporting the walking motion of human. The PVC gel devices are incorporated in the generally used

spats. And the stiffness of the gel spats can be actively varied with the applied DC field turned on and off. The gel spats have the characteristics of a simple structure, a light weight, easy to put on and take off and with a high flexibility. A prototype was tested in the motions of lifting a foot and walking. It was found that the integrated electromyogram (IEMG) and maximal voluntary contraction (%MVC) values of the rectus femoris muscle reduced up to about 6% with the assistance of the gel spats, which demonstrated the potential of the gel spats as a device for walking assistance. Though the prototype gel spats have a very light weight of about 0.3 kg (not including a power source and control), the variable stiffness spats has a small generation force that is less than 10N which might insufficient to provide a moment for the hip joint. Also in order to get the generation force, an initial strain should be set to the gel spats beforehand which should cause a burden to human muscles. Furthermore, the structure has a lower robustness to external forces.

1.2.3 Polymer and textile materials based assist wear

Some polymer materials based functional clothes (without any actuators) are also being studied for walking assistance or locomotion support, such as the functional spats (Fig. 1.2.4 (a)) for walking assistance proposed by Akio Shizukai et al. [60], the Morita Group's lumbar support wear RAKUNIE (Fig. 1.2.4 (b)) [61] and the Wacoal Holding Corporation's conditioning wear CW-X (Fig. 1.2.4 (c)) [62]. These types of assist wears can only support motion passively, may not provide individualized control so as to assist the muscles more appropriately, which might result in a limitation of applications.



Fig. 1.2.4. Polymer and textile materials based assist wears for human support. (a) Functional clothes for walking assistance by A. Suzukai [60]. (b) Morita Group's lumbar support wear RAKUNIE [61]. (c) Wacoal Holdings Corporation's CW-X® Conditioning Wear [62].

As mentioned above, the soft robotic assist wears demonstrate a very high potential to bring a revolutionary change to the human assistance and rehabilitation. However, they still meet many ongoing challenges, such as to construct a more efficient and robust structure for the wear according the biological structure of human body, to minimize the power source size and enhance the energy efficiency, to use some new actuators to make the system more smart and have a higher power to weight ratio and to make the assist wear much more attractive, with a high affinity to human.

Some innovative technologies are needed to meet the requirements of such applications in human motion assistance. And we think the polymer material based artificial muscles could be one of the key issues of developing such technologies. We will introduce the development of artificial muscles in the next section.

1.2.4 Polymer materials based artificial muscles

Polymer materials based artificial muscles have the properties of being soft, lightweight and flexible which are similar to the nature muscular actuators, have attracted great attention these years [63, 64].

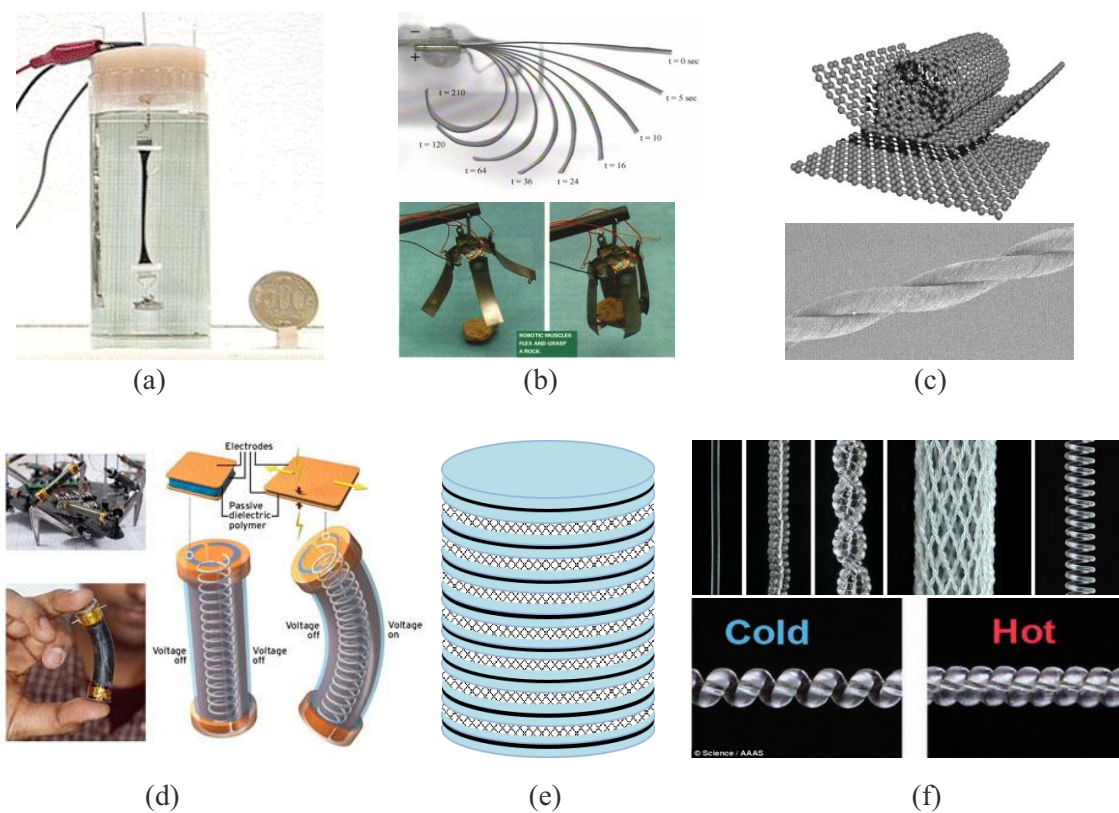


Fig. 1.2.5. Polymer materials based artificial muscles. (a) Conducting polymer artificial muscle [68]. (b) Ionic Polymer-Metal Composite (IPMC) artificial muscle [70]. (c) Carbon nanotube (CNT) artificial muscle (a graphene sheet rolled into a nanotube and a twist-spun MWNT yarn) [72]. (d) Dielectric elastomer actuator (DEA) artificial muscle [73]. (e) The PVC gel artificial muscle (PGAM) [76]. (f) Fishing line and sewing thread artificial muscle [78].

A variety of electronic, ionic, and photoactivated artificial muscles are proposed that exhibit large strain in length and volume, high response rate, and high output power, which is the primary similarity with muscle [65, 66]. Since each artificial muscle is defined according to the physical theory on which its legitimacy is founded, a general theory of artificial muscles does not exist. Each one has its own composition, mechanism, motion type and mechanical structure. Polymer artificial muscles can be divided into three major groups based on their actuation mechanism: In the first group of polymer artificial muscles is a class of materials in which the presence and movement of ions is necessary to make actuation possible. For the second group, dimensional change (actuation) is in response to an electric field. These are commonly known

as electronic or electric electroactive polymers (EAPs). And in the third group of polymer artificial muscles the dimensional change (actuation) is in response to heat. Most of the artificial muscles developed so far are being challenged by the characteristics improvement to reach or exceed the level the nature biological muscles which have a contraction rate of 20%-40%, a stress of 0.1-0.3MPa and a response rate of 10Hz [67].

Conducting polymers (Fig. 1.2.5 (a)) are typically semiconducting when undoped and conducting when doped with donor or acceptor ions [68]. They can achieve a high strain (10-40%) and high stress (~49 MPa) under a voltage of 1.5 V [69]. However, they have to be operated in a solution which brings a major challenge to a practical application. Ionic polymer-metal composites (IPMCs) (Fig. 1.2.5 (b) [70, 71] can make a bending movement under a step voltage of several volts due to solvated mobile cations move toward the oppositely charged electrode, producing a big bending strain and a high stress (as high as 30 MPa). However, the response rate is not notable and there is a need to maintain their wetness like the conducting polymer which poses a major design challenge for application of IPMC artificial muscles. Another ionic artificial muscle is Carbon nanotube (CNT) (Fig. 1.2.5 (c)) [72]. Since the CNTs are extremely stiff (tensile strength is thought to be 20-40 GPa), the strains are low (<2%).

Dielectric elastomer actuators (DEAs) are one of the most studied EAP actuators and numerous applications are being developed including electroactive fluid pumps, conformal skins for Braille screens and insect-like robots [73-75]. When a voltage is applied, a Maxwell stress happens between the electrodes, which compresses and elongates the dielectric as shown in Fig. 1.2.5 (d), with a large strain and stress that most closely emulate human muscles. However, the challenge for this type of actuators is their use of a high voltage (> 1 kV typical) due to the high electric fields that are needed (> 100V/ μm). While the PVC gel based artificial muscles (Fig. 1.2.5 (e)) [76, 77] can be actuated using a medium electric field (< 20V/ μm) with a good strain (> 10%), notable response rate (up to 9 Hz) in air, and high electric efficiency together with a long cycle life (over 5 million times) which will be introduced in detail in the next Chapter.

A number of other artificial muscle technologies exist that respond to heat, of which the artificial muscles from fishing line and sewing thread (Fig. 1.2.5 (f)) [78-80] have been attracted attentions recently. They are very cheap but strong, have an excellent strain and stress that exceeds the biological muscles. However, the heating and cooling could be the challenge for a high response rate for an application on motion assistance. Besides, Shape memory polymers (SMPs) [81, 82] can be developed into multifunctional materials actuated by various methods, such as thermal-induced, electro-activated and magnetic-actuated SMPs. They can achieve a high strain and stress but a low response rate (sec to min).

All in all, among all the candidates of artificial muscles, PVC gel based artificial muscles showed a great potential for practical applications.

1.3 Study purpose

Our long term goal is to develop a lightweight wearable assistive device that can be used for a daily life to support the elders with some weakened muscles. In addition to have the function of lightening the burden of the wearers during walking, the devices should have low impedance, high flexibility, be comfortable and safe to wear and easy to don and doff. PVC gel artificial muscles, as a candidate of next generation soft actuators instead of the traditional electrical motors, exhibiting many positive properties which demonstrates the feasibility of constructing such a wearable assist wear.

In this PhD Thesis, we proposed a novel approach to make a high-performance light-weight walking assist wear using the PVC gel artificial muscles. And we constructed a new walking assist system to control the walking assist wear. The effectiveness of the whole system was verified from several aspects in this study.

We used the contraction-expansion movement and output force for motion assist to get a bigger generation force. We proposed a new measurement method to evaluate the characteristics of PVC gel artificial muscles, along with an analytical model for the static characteristics of PVC gel artificial muscles. A new stretching-type structure unit together with some structure improvement of PVC gel artificial muscles were introduced to make the assist wear more robust to external factors (e.g. an external force). For the walking motion detection, we used some flexible force sensors to integrate into the insole to detect the gait changes during walking. And we used a portable and smart controller to construct the whole control system.

The proposed walking assist wear has the advantages of a light weight, a good flexibility and good-fitting and a simple structure that can be easy to don and doff. We think it is feasible to use for a daily life support during walking.

1.4 Outline

After the introduction of this Chapter 1, this PhD Thesis is organized as follows:

In Chapter 2, the PVC gel artificial muscles are introduced and developed. The basic concerns about PVC gels, including the composition, fabrication and movement principal will be described. Then the development of PVC gel artificial muscles, concerning about the structure,

actuation mechanism, and characterizations will be presented.

In Chapter 3, the novel lightweight walking assist wear with PVC gel artificial muscles will be proposed. And the structure, function and assistance method will be addressed.

In Chapter 4, a prototype of walking assist wear using PVC gel artificial muscles will be designed, fabricated and a walking motion detector and a controller will be constructed.

In Chapter 5, the characterizations and performances of the walking assist wear, the walking motion detector and the controller system will be evaluated.

In Chapter 6, walking experiments with the whole walking assist wear system will be conducted from several aspects and the effectiveness of the whole system will be discussed.

In Chapter 7, the conclusions of the main contributions will be remarked and some remained works will be discussed.

References

- [1] Population Estimates, Statistics Bureau, 1 April 2015. Available on line: <http://www.stat.go.jp/english/data/jinsui/tsuki/index.htm>.
- [2] The elderly who need help, The Japan Times, Available on line: <http://www.japantimes.co.jp/opinion/2014/08/04/editorials/elderly-need-help/#.VhJ692zouM9>.
- [3] A.H. Snijders, B.P. van de Warrenburg, N. Giladi, B.R. Bloem, Neurological gait disorders in elderly people: clinical approach and classification, *The Lancet Neurol.* 6 (1) (2007) 63-74.
- [4] J. Verghese, A. LeValley, C.B. Hall, M.J. Katz, A.F. Ambrose, R.B. Lipton, Epidemiology of gait disorders in community-residing older adults, *J. Am. Geriatr. Soc.* 54 (2) (2006) 255-261.
- [5] R.S. Wilson, J.A. Schneider, L.A. Beckett, D.A. Evans, D.A. Bennett, Progression of gait disorder and rigidity and risk of death in older persons, *Neurology* 58 (12) (2002) 1815-1819.
- [6] Ronenn Roubenoff, The Pathophysiology of Wasting in the Elderly, *The Journal of Nutrition*, (129) 1999 256S-259S.
- [7] J.A. Ashton-Miller, Age-associated changes in the biomechanics of gait and gait-related falls in older adults, in: J.M. Hausdorff, N.B. Alexander (Eds.), *Gait Disorders: Evaluation and Management*, Taylor & Francis, Boca Raton, 2005, pp. 63-100.
- [8] *Dtsch Arztebl Int* 2010, 107 (17): 306-16 DOI: 10.3238/arztebl.2010.0306

- [9] Kyle C. Moylan, Ellen F. Binder, Falls in Older Adults: Risk Assessment, Management and Prevention, *The American Journal of Medicine* (2007) 120, 493-497.
- [10] Albert B. Schultz, Mobility impairment in the elderly: Challenges for biomechanics research, *J. Biomechanics*, Vol.25, No.5, pp.519-528, 1992.
- [11] T. Yan, M. Cempini, C.M. Oddo and N. Vitiello, "Review of assistive strategies in powered lower-limb orthoses and exoskeletons," *Robotics and Autonomous Systems*, 64 (2015) 120-136.
- [12] H. Herr, Exoskeletons and orthoses: classification, design challenges and future directions, *J. Neuroeng. Rehabil.* 6 (2009) 21.
- [13] A.M. Dollar, H. Herr, Lower extremity exoskeletons and active orthoses: challenges and state-of-the-art, *IEEE Trans. Robot.* 24 (2008) 144-158.
- [14] R.S. Mosher, Handyman to Hardiman, Technical Report, SAE Technical Paper, 1967.
- [15] M. Vukobratovic, B. Borovac, D. Surla, D. Stokic, *Biped Locomotion*, Springer-Verlag, 1990, p. 349.
- [16] A.M. Dollar, H. Herr, Lower extremity exoskeletons and active orthoses: challenges and state-of-the-art, *IEEE Trans. Robot.* 24 (2008) 144-158.
- [17] K. E. Gilbert, "Exoskeleton prototype project: Final report on phase I," General Electric Company, Schenectady, NY, GE Tech. Rep. S-67-1011, 1967.
- [18] K. E. Gilbert and P. C. Callan, "Hardiman I prototype," General Electric Company, Schenectady, NY, GE Tech. Rep. S-68-1081, 1968.
- [19] B. R. Fick and J. B. Makinson, "Hardiman I prototype for machine augmentation of human strength and endurance: Final report," General Electric Company, Schenectady, NY, GE Tech. Rep. S-71-1056, 1971.
- [20] E. Garcia, J. M. Sater, and J. Main, "Exoskeletons for human performance augmentation (EHPA): A program summary," *J. Robot. Soc. Japan*, vol. 20, no. 8, pp. 44-48, 2002.
- [21] H. Kazerooni, "Exoskeletons for human power augmentation," *IEEE/RSJ International Conference on Intelligent Robots and Systems (IROS2005)*, pp. 3459-3464, 2005.
- [22] A. Zoss, H. Kazerooni, and A. Chu, "On the mechanical design of the berkeley lower extremity exoskeleton (bleex)," *IEEE/RSJ International Conference on Intelligent Robots and Systems (IROS2005)*, pp. 3465-3472, 2005.
- [23] A. Zoss, H. Kazerooni, and A. Chu, "Biomechanical design of the berkeley lower extremity exoskeleton (bleex)," *IEEE/ASME Transactions on Mechatronics*, vol. 11, no. 2, pp. 128-138, 2006.
- [24] <http://bleex.me.berkeley.edu/research/exoskeleton/hulc/>
- [25] <http://www.defense.gouv.fr/actualites/economie-et-technologie/l-exosquelette-hercule-le-futur-a-nos-portes.>

- [26] Mone G, Building the real Iron Man. Popular Science 2008. Available on line: <http://www.popsci.com/node/20689>.
- [27] A. M. Dollar and H. Herr, "Lower extremity exoskeletons and active orthoses: challenges and state-of-the-art," IEEE Transactions on Robotics, vol. 24, no. 1, pp. 144-158, 2008.
- [28] R. Rea, C. Beck, R. Rovekamp, M. Diftler, and P. Neuhaus, "X1: A robotic exoskeleton for in-space countermeasures and dynamometry," 2014.
- [29] Y. Sankai, "Leading edge of cybernics: robot suit hal," in SICE-ICASE International Joint Conference, pp. P-1-P-2, 2006.
- [30] Y. Sankai, "Hal: Hybrid assistive limb based on cybernics," in Robotics Research, pp. 25-34, Springer, 2011.
- [31] <http://www.rexbionics.com/products/rex/>
- [32] G. Zeilig, H. Weingarden, M. Zwecker, I. Dudkiewicz, A. Bloch, A. Esquenazi, et al., "Safety and tolerance of the rewalk exoskeleton suit for ambulation by people with complete spinal cord injury: A pilot study," The journal of spinal cord medicine, vol. 35, no. 2, pp. 96-101, 2012.
- [33] K. A. Strausser and H. Kazerooni, "The development and testing of a human machine interface for a mobile medical exoskeleton," IEEE/RSJ International Conference on Intelligent Robots and Systems (IROS2011), pp. 4911-4916, 2011.
- [34] S. Murray, K. Ha, C. Hartigan, and M. Goldfarb, An Assistive Control Approach for a Lower-Limb Exoskeleton to Facilitate Recovery of Walking following Stroke, IEEE Transactions on Neural Systems and Rehabilitation Engineering, vol. 23, no. 3, 2015.
- [35] K. Yasuhara, K. Shimada and T. Koyama, "Walking assist device with stride management system," Honda R&D technical review, vol. 21, no. 2, pp. 54-62, Oct. 2009.
- [36] <http://www.toyota-ti.ac.jp/english/research/laboratories/elec/post-5.html>
- [37] H. Tanaka and M. Hashimoto, Development of a Non-Exoskeletal Structure for a Robotic Suit, International Journal of Automation Technology, Vol.8, No.2, pp. 201-207, 2014.
- [38] J. F. Veneman, R. Kruidhof, E. E. Hekman, R. Ekkelenkamp, E. H. Van Asseldonk, and H. van der Kooij, "Design and evaluation of the lopes exoskeleton robot for interactive gait rehabilitation," IEEE Transactions on Neural Systems and Rehabilitation Engineering, vol. 15, no. 3, pp. 379-386, 2007.
- [39] M. Ishii, K. Yamamoto, and K. Hyodo, "Stand-alone wearable power assist suit-development and availability," Journal of robotics and mechatronics, vol. 17, no. 5, p. 575, 2005.
- [40] P. D. Neuhaus, J. H. Noorden, T. J. Craig, T. Torres, J. Kirschbaum, and J. E. Pratt, "Design and evaluation of mina: A robotic orthosis for paraplegics," IEEE International Conference on Rehabilitation Robotics (ICORR2011), pp. 1-8, 2011.

- [41] E. Guizzo and H. Goldstein, "The rise of the body bots [robotic exoskeletons]," *IEEE Spectrum*, vol. 42, no. 10, pp. 50-56, 2005.
- [42] Schiele, "Ergonomics of exoskeletons: Objective performance metrics," *IEEE World Haptics Conference, 2009 (WHC 2009)*, Salt Lake City, UT, USA, pp. 103-108.
- [43] M. A. Ergin and V. Patoglu, "A self-adjusting knee exoskeleton for robotassisted treatment of knee injuries," *IEEE/RSJ International Conference on Intelligent Robots and Systems (IROS2011)*, pp.4917-4922, 2011.
- [44] F. Daerden, D. Lefeber, B. Verrelst and R. Van Ham, Pleated pneumatic artificial muscles: actuators for automation and robotics, in: *Proceedings of 2001 IEEE/ASME International Conference on Advanced Intelligent Mechatronics, 2001*, pp.738-743.
- [45] F. Daerden, D. Lefeber, *Pneumatic artificial muscles: actuators for robotics and automation*, *Eur. J. Mech. Environ. Eng.* 47 (2002) 11-21.
- [46] Costa, N., Bezdicek, M., Brown, M., Gray, J.O., Caldwell, D.G. Joint motion control of a powered lower limb orthosis for rehabilitation. *Int. J. Autom. Comput.* 2006, 3, 271-281.
- [47] T. Kawamura, K. Takanaka, T. Nakamura and H. Osumi, Development of an orthosis for walking assistance using pneumatic artificial muscle: A quantitative assessment of the effect of assistance, *Proceedings of 2013 IEEE International Conference on Rehabilitation Robotics, (ICORR 2013)*, Poster E9, June 24-26, Seattle, Washington USA, 2013.
- [48] Takuma Kawamura, Marie Noma, and Taro Nakamura, Development of a Passive Switching Cam Mechanism for Walking Assistance Using Pneumatic Artificial Muscle, *IEEE/ASME International Conference on Advanced Intelligent Mechatronics (AIM2014)*, pp. 1486-1491, France, July 8-11, 2014.
- [49] <http://cwwang.com/2008/04/08/soft-pneumatic-exoskeleton/>
- [50] Wehner M, Quinlivan B, Aubin PM, Martinez-Villalpando E, Baumann M, Stirling L, Holt K, Wood R, Walsh C, "A lightweight soft exosuit for gait assistance," *IEEE International Conference on Robotics Atomation (ICRA)*, Karlsruhe, Germany, May 6-10, pp.3362-3369, 2013.
- [51] D. Sasaki, T. Noritsugu, M. Takaiwa, Development of pneumatic lower limb power assist wear driven with wearable air supply system, *IEEE/RSJ International Conference on Intelligent Robots and Systems (IROS2013)*, pp. 4440-4445, 2013.
- [52] Mohd Azuwan Mat Dzahir and Shin-ichiroh Yamamoto, "RecentTrends in Lower-Limb Robotic Rehabilitation Orthosis: Control Scheme and Strategy for Pneumatic Muscle Actuated Gait Trainers,"*Robotics*, Vol 3, pp.120-148, 2014.
- [53] Alan T. Asbeck, Stefano Marco Maria De Rossi, Ignacio Galiana, Ye Ding, Conor J. Walsh: Stronger, Smarter, Softer: Next-Generation Wearable Robots. *IEEE Robot. Automat. Mag.* 21(4): 22-33 (2014).

- [54] M. Sato, S. Takasugi, K. Masumoto, T. Komastu, K. Hashimoto and M. Yamamoto, Study of a Walking Assistance Method using Elastic Belts based on Phase Information of Hip Joint, LIFE2012, pp. GS1-1-1. (in Japanese)
- [55] Jani J. M., Leary M., Subic A., Gibson M. A., "A Review of Shape Memory Alloy Research, Applications and Opportunities". *Materials & Design*. Volume 56, pp. 1078-1113, 2014.
- [56] L. Stirling, C. Yu, J. Miller, R. J. Wood, E. Goldfield and R. Nagpal, "Applicability of shape memory alloy wire for an active, soft orthotic," *J. Mater. Eng. Perform.*, vol. 20, no. 4-5, pp. 658-662, 2011.
- [57] M. Nakayama, Y. Matsumoto, Y. Nakashima, T. Ando, Y. Kobayashi and M. G. Fujie, Development of a Clothes-Type Orthosis with Multiple Shape Memory Alloy Actuators for Stumbling Prevention, -Derivation of the Relationship between the Arrangement of Actuators and Hip Joint Moment in Clothes-Type Orthosis-, in the 20th Robotics Symposia, 2015, pp. 489-495.
- [58] Y. Maeda, Y. Li; K. Yasuda and M. Hashimoto, "Development of Variable Stiffness Gel Spats for Walking Assistance ", The 2013 IEEE/RSJ International Conference on Intelligent Robots and Systems (IROS2013), Tokyo, Japan, 2013, pp.5404-5409.
- [59] Y. Li, Y. Maeda and M. Hashimoto, "Light-weight, Soft Variable Stiffness Gel Spats for Walking Assistance", *International Journal of Advanced Robotic Systems*, Vol. 12, No. 175, pp. 1-11, 2015.
- [60] S. Akio, M. Takashi, K. Ryu, M. Soichiro and Y. Hiroshi, "Walking assist by functional clothes with highly elastic fabric," in 28th Annu. Conf. Robotics Society Japan, pp. ROMBUNNO.2J1-8, 2010. (in Japanese)
- [61] T. Kusaka, T. Tanaka, H. Nara, T. Yamagishi and S. Ogura, Development of a Semi-active Type Power Assist Suit for 3-Dimensional Motion based on KEIROKA-Technology, in the 13th SICE system integration division annual conference (SI2012), pp.1092-1093. 2012.
- [62] <http://cw-x.com/Default.aspx>.
- [63] T. Mirfakhraia, J. D.W. Maddena, R. H. Baughman, Polymer artificial muscles, *Mater. Today* 10 (2007) 30-38.
- [64] K. Asaka, H. Okuzaki, Soft actuators, materials, modeling, applications and future perspectives, *Polymer science*, 2014.
- [65] S. Sherrit, X. Bao and Y. Bar-Cohen, Methods of testing and characterization, in: Bar-Cohen, Y., (Ed.), *Electroactive Polymer (EAP) Actuators as Artificial Muscles*, 2nd Edition, SPIE Press, Vol. PM136, 2004, pp. 467-526.
- [66] Y. Nabetani, H. Takamura, Y. Hayasaka, T. Shimada, S. Takagi, H. Tachibana, D. Masui, Zhiwei T. and H. Inoue, A photoactivated artificial muscle model unit: reversible, photoinduced sliding of nanosheets, *J. Am. Chem. Soc.* 133 (2011) 17130-17133.

- [67] R.H. Baughman, Playing nature's game with artificial muscles, *Science* 308 (2005) 63-65.
- [68] Skotheim, T. A., et al., *Handbook of Conducting Polymers*. Marcel Dekker, New York, (1998).
- [69] <http://www.eamex.co.jp/features/koubunshi/koubunsi/>
- [70] S. Nemat-Nasser and Y. Wu, Comparative experimental study of ionic polymer-metal composites with different backbone ionomers and in various cation forms, *J. Appl. Phys.* 93 (2003) 5255-5267.
- [71] S. G. Lee, H. C. Park, Surya D. Pandita, and Y. Yoo, Performance improvement of IPMC (Ionic Polymer Metal Composites) for a flapping actuator, *Int. J. Control Autom.* 4 (2006) 748-755.
- [72] Baughman, R. H., et al., Carbon nanotube actuators, *Science* (1999) 284, 1340
- [73] Y. Bar-Cohen, Electroactive polymers as artificial muscles: capabilities, potentials and challenges, *Handbook on biomimetics*, NTS Inc., Aug. 2001, pp.134.
- [74] R. Pelrine, R. Kornbluh, Q. Pei, S. Stanford, S. Oh, and J. Eckerle, Dielectric elastomer artificial muscle actuators: toward biomimetic motion, *Smart Structures and Materials 2002: Electroactive Polymer Actuators and Devices*, Y. Bar-Cohen, Editor, in: *Proceedings of SPIE*, San Diego, 2002, pp. 126-137.
- [75] Y. Liu, L. Liu, Z. Zhang and J. Leng, Dielectric elastomer film actuators: characterization, experiment and analysis, *Smart Mater. Struct.* 18 (2009) 095024.
- [76] M. Yamano, N. Ogawa, M. Hashimoto, M. Takasaki and T. Hirai, "A Contraction Type Soft Actuator Using Poly Vinyl Chloride Gel," in *Proc. IEEE Int. Conf. Robotics and Biomimetics (ROBIO2008)*, Bangkok, Thailand, 2009, pp.745-750.
- [77] Y. Li and M. Hashimoto, "PVC gel based artificial muscles: Characterizations and actuation modular constructions", *Sensors and Actuators A-Phys.*, Vol 233, No. 1, pp.246-258, 2015.
- [78] Marcio D. Lima et al., Electrically, Chemically, and Photonically Powered Torsional and Tensile Actuation of Hybrid Carbon Nanotube Yarn Muscles, *Science*, 338 (2012) 928-932.
- [79] Carter S. Haines et al., Artificial Muscles from Fishing Line and Sewing Thread, *Science*, 343 (2014) 868-872.
- [80] Michael C. Yip and Gunter Niemeyer, "High-Performance Robotic Muscles from Conductive Nylon Sewing Thread", *The 2015 IEEE International Conference on Robotics and Automation (ICRA 2015)*, Seattle, USA, pp.2313-2318, 2015.
- [81] J. Leng, X. Lan, Y. Liu, S. Dua. Shape-memory polymers and their composites: Stimulus methods and applications. *Prog. Mater. Sci.* 56 (2011) 1077-1135.
- [82] Y. Liu, H. Du, L. Liu and J. Leng, Shape memory polymers and their composites in aerospace applications: a review, *Smart Mater. Struct.* 23 (2014) 1-22.

Chapter 2

PVC gel artificial muscles

Chapter 2 PVC gel artificial muscles

In our previous study, we have developed a contraction and expansion type PVC gel artificial muscle, using the meshed anode and foil cathode [1]. And we evaluated and improved its characteristics [2-6], modeled it as a control element [7]. The PVC gel artificial muscle has the advantages of stable movement in the air with a large strain and an output stress with a high response rate and stability on thermal influence. Some applications, such as a massage device for lymphedema care [8], a motor brake [9], walking assist gel spats [10] and a breath control device [11] are implemented so far.

In this Chapter, we introduce the PVC gel artificial muscles, including the composition, fabrication and movement mechanism. We propose a new measurement method to evaluate the characteristics of PVC gel artificial muscles, and some most updated basic characterizations will be presented along with an analytical model for the static characteristics of PVC gel artificial muscles. Besides, some new types of actuation modular constructions together with some structure improvement of PVC gel artificial muscles will be proposed to make the PVC gel artificial muscle as a robust actuation device for robotics and mechatronics.

2.1 Composition and preparation of PVC gels

Poly (vinyl chloride) (PVC) is one of the most widely produced synthetic plastic polymer. It comes in two basic forms: rigid and flexible. The rigid form of PVC is used in construction for pipe and in profile applications, such as doors and windows. And the flexible form is obtained by the addition of plasticizers which is used in plumbing, electrical cable insulation, imitation leather, and many applications where it replaces rubber [12]. When increasing the amount of plasticizers we can get a softer form that we called it PVC gels.

PVC gels are made from commercial PVC powder (degree of polymerization is 3200) plasticized by dibutyl adipate (DBA) plasticizer. Fig. 2.1.1 (a) shows the process of preparation of PVC gels. Firstly, mix the PVC powder in the DBA with a certain weight ratio. Secondly, put the mixture into the tetrahydrofuran (THF) solvent and cast the solution in Petri dishes. Finally we can obtain the PVC gel membranes after the evaporation of the THF at a room temperature for two to five days. The fabricated PVC gel membrane is one kind of soft dielectric elastomers which is soft, lightweight and with a very high degree of transparency (Fig. 2.1.1 (b)). We can

get a PVC gel membrane that has a thickness from several hundreds of micrometers to several millimeters. And the material characteristics of the PVC gel membranes can be changed by adjusting the weight ratio of PVC and DBA. In this study, the weight ratio of PVC and DBA is 1:4.

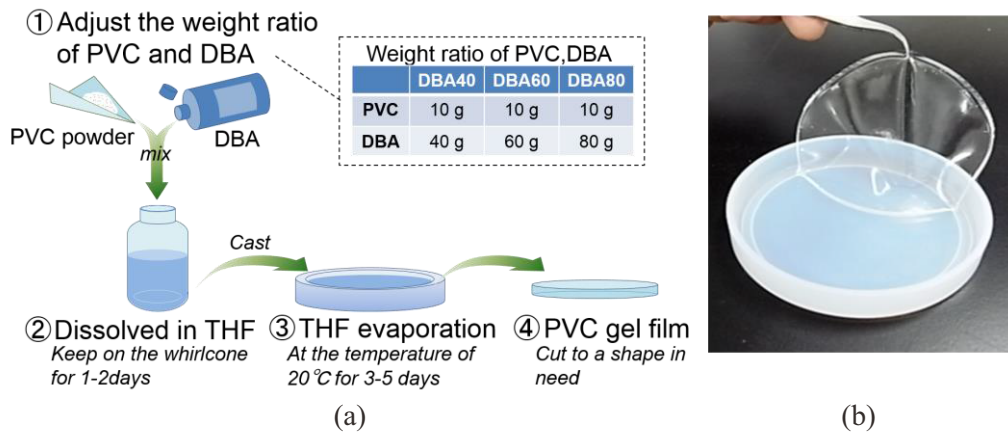


Fig. 2.1.1. Preparation of PVC gel, (a) process of fabrication and (b) an actual PVC gel membrane

2.2 Electrical response of PVC gels

2.2.1 Deformation of PVC gels

A PVC gel is one kind of electroactive polymers which has a response to the electrical stimuli. T. Hirai et al. [13, 14] firstly found the bending deformation of PVC gels under an electric field, as shown in Fig. 2.2.1. The local deformation illustration of PVC gel can be seen in Fig. 2.2.2 (a), when PVC gel is sandwiched between electrodes, creep deformation takes place between the gel and the anode when the electric field is charged. And with the electric field is turned off, the gel returns to its original shape quickly by its own elasticity. This was confirmed by an electron microscope [15] that when a DC field was applied to the gel, a creep deformation just only took place on the anode electrode surface, as shown in Fig. 2.2.2 (b). No such phenomenon occurred on the cathode surface.

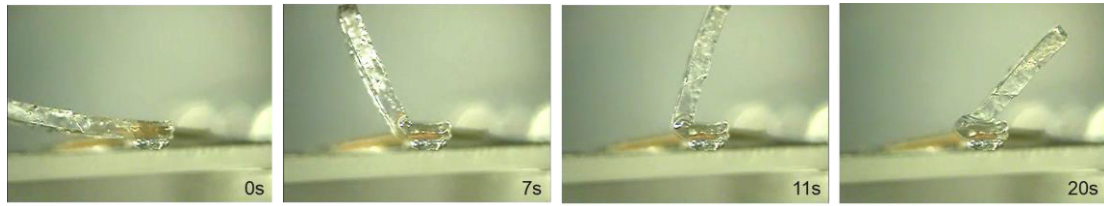


Fig. 2.2.1. A bending deformation of PVC gels under an electric field. [13]

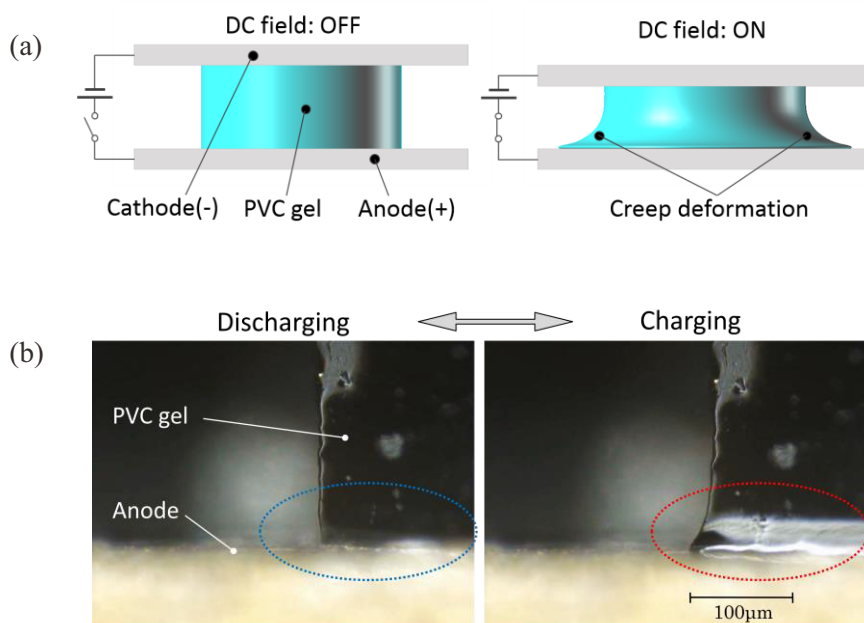


Fig. 2.2.2. Deformation of a PVC gel membrane under a DC field in a front view. (a) Illustration. (b) Experimental result.

2.2.2 Mechanism of deformation

A phenomenon that an accumulation of negative charges on the gel surface near the anode was confirmed by space-charge measurement [16], an example shown in Fig. 2.2.3 (a). It was also found that PVC gels were separated to two layers obviously after applied an electrical field, of which the layer near the anode was thinner and softer than other layer due to the transfer of plasticizer to the anode [17]. Therefore, we believe that when an electric field is turned on,

electrons are injected from the cathode into the gel, and migrate toward the anode. Due to the Maxwell force, the PVC gel will be deformed asymmetrically and results in creep deformation along the anode. Based on this hypothesis, our research group simulated the deformation of PVC gel by finite element method (FEM) and got the same creep deformation (Fig. 2.2.3 (b)) [18].

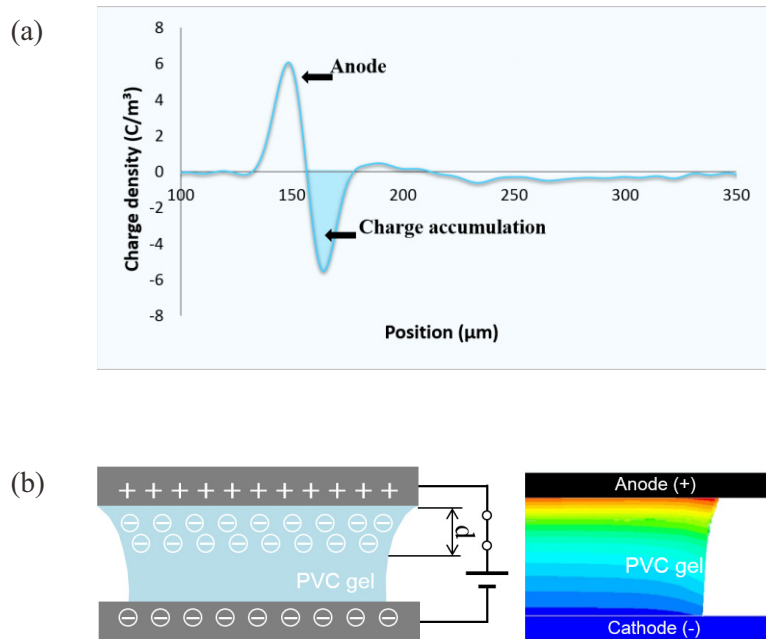


Fig. 2.2.3. (a) A result of space-charge measurement of a PVC gel. (b) Deformation mechanism (left part) and FEM analysis result of PVC gels (right part) [18].

2.3 Structure and principal of PVC gel artificial muscles

To emulate natural biological muscle, we think it is necessary to create a contraction and expansion movement. Based on the unique phenomenon and mechanism of PVC gel at the side of anode of electrode, we have developed a contraction and expansion type PVC gel artificial muscle, using the meshed anode and foil cathode [1].

As shown in Fig. 2.3.1 (a), the PVC gel is sandwiched between stainless steel mesh as an anode and a foil cathode. When a DC field is applied, the PVC gel creeps up the anode and moves into the holes in the mesh. As a result, the artificial muscle shrinks in the thickness direction. When the DC field is removed, the elasticity of the gel causes it to rapidly return to its

original shape. Thus it performs the contraction and expansion deformation that similar to a human muscle. Fig. 2.3.1 (b) shows an actual deformation of a single-layer structure PVC gel artificial muscle. By increasing the number of stacked layers of the single structure units (Fig. 2.3.1 (c)), we can get a multilayered contraction and expansion type artificial muscle with more displacement. Fig. 2.3.1 (d) shows an example of a deformation of a 50-layer artificial muscle.

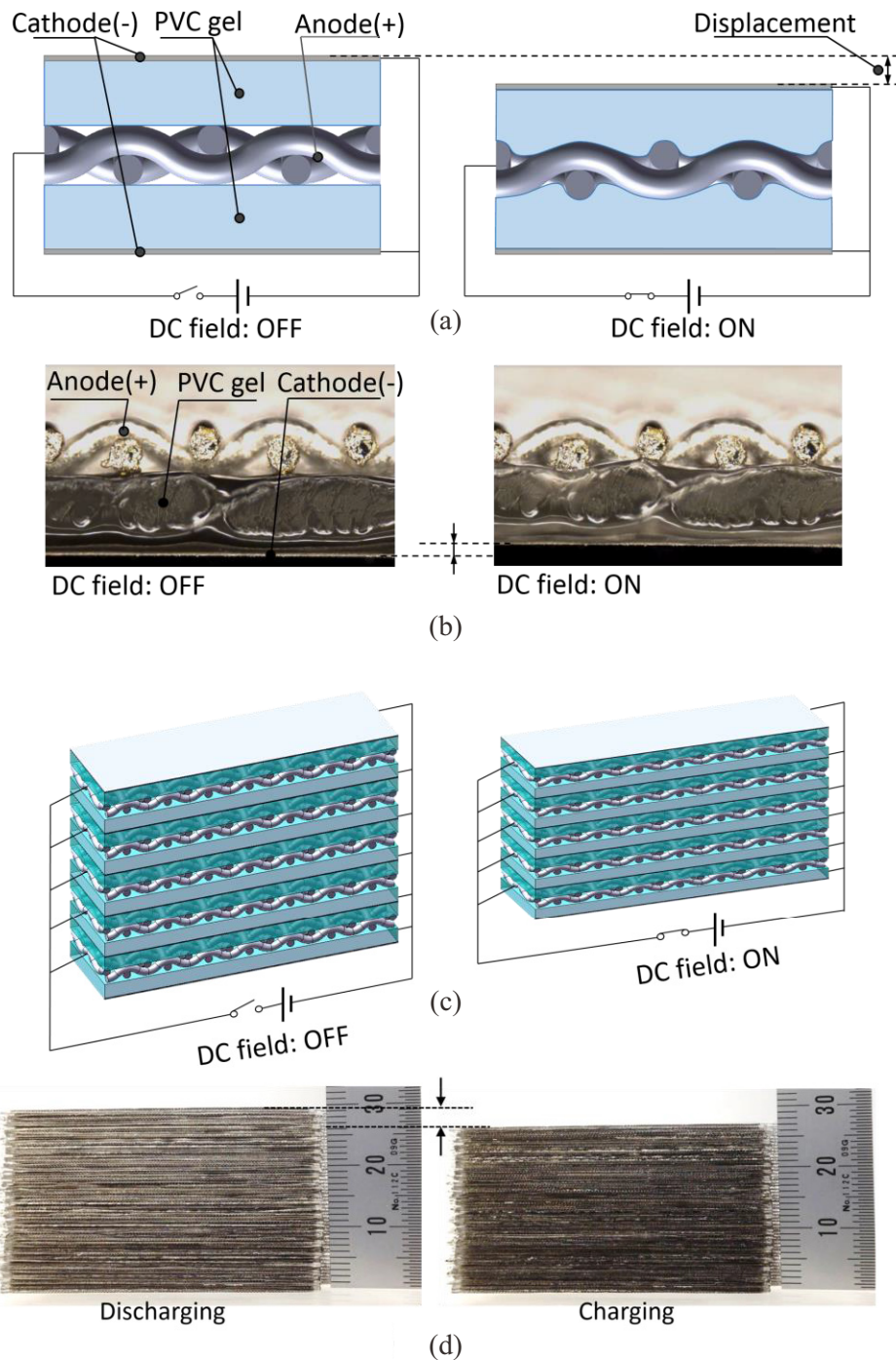


Fig. 2.3.1. Structure and deformation of PVC gel artificial muscles. (a) Single-layer structure and deformation mechanism under an applied DC field. (b) A multilayered structure (5-layer) PVC gel artificial muscle and an actual sample of 50-layer artificial muscle (with a size of 50mm×10mm×30mm).

2.4 Characterizations of PVC gel artificial muscles

With the aim of developing a new PVC gel artificial muscle that be capably to practically use in an application, we investigated the basic characteristics of displacement, generation force, electrical current, response rate and durability.

2.4.1 Displacement measurement

The displacement was measured by a laser displacement sensor (IL-065, Keyence, JAPAN) (see in Fig. 2.4.1). The PVC gel membrane in each layer was about 0.2 mm in thickness and 50×10 mm in size. The mesh size of the stainless steel mesh anode was 100 (each inch has 100 wires), with a thickness of about 0.18 mm. And a 0.01 mm thick foil electrode was used as the cathode. The total thickness of each single-layer artificial muscle was about 0.6 mm and it weighed about 0.5 g. In this study, we measured the displacement of several single-layer, 5-layer and 10-layer PVC gel artificial muscles with the applied DC voltage from 80V to 400V and a pre-load of 20g (about 400Pa) on the top.

As described in section 2.3, under an applied DC field, the gel creeps up the anode and moves into the holes of the mesh, causing the artificial muscle to shrink in the thickness direction with a displacement. Considering this mechanism, we think that the displacement should be directly proportional to the number of stacked layers, while the contraction strain should be constant under a certain applied DC field.

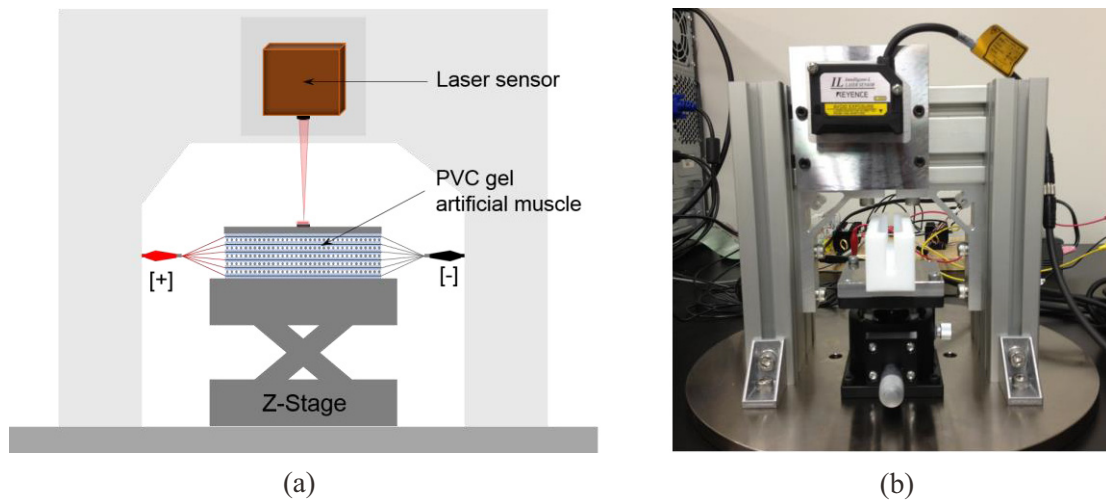


Fig. 2.4.1. Method of displacement measurement. (a) Illustration. (b) Real device.

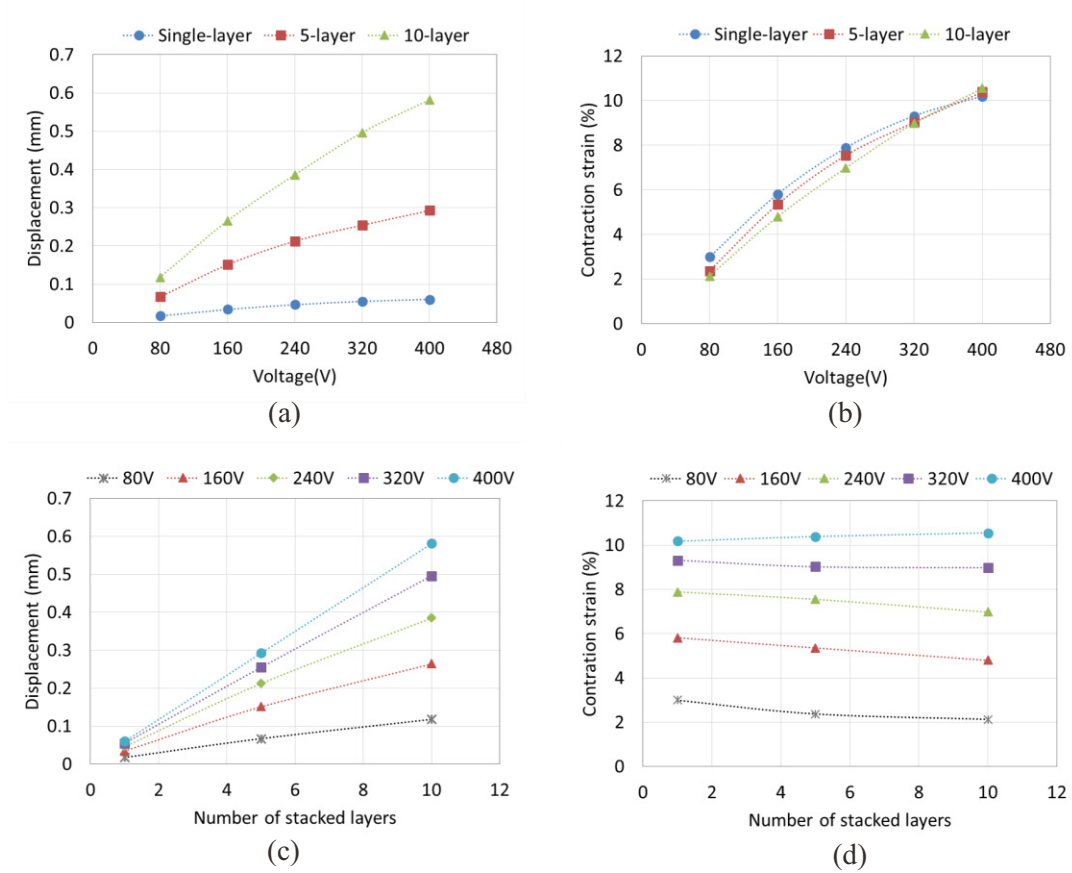


Fig. 2.4.2. Displacement of PVC gel artificial muscles with different number of stacked layers. (a) Displacement with different applied DC voltages. (b) Contraction strain with different applied DC voltages. (c) Displacement with different number of stacked layers. (d) Contraction strain with different number of stacked layers.

Fig. 2.4.2 shows the relationship between the displacement and number of stacked layers of PVC gel artificial muscles, under different applied DC voltages. The displacement increases almost linearly (and reach a saturation when most of the mesh holes been full filled) with the increase of the applied DC voltage. In the case of an applied voltage of 400V the displacement of the 10-layer artificial muscles is about 0.6mm (Fig. 2.4.2 (a)), and the contraction strain is about 10.5% (Fig. 2.4.2 (b)). And the displacement increases almost linearly with the number of stacked layers as expected (Fig. 2.4.2 (c)), therefore, the contraction strain remains almost constant with different number of stacked layers (Fig. 2.4.2 (d)).

2.4.2 Generation force measurement

PVC gel artificial muscles have two forms of generation forces, as shown in Fig. 2.4.3. One is the force generated by the applied DC field, defined as a contraction force (Fig. 2.4.3 (a)). Another one is the force generated when the DC field is turned off, defined as a recovery force (Fig. 2.4.3 (b)). That is, when the DC field is applied to the PVC gel artificial muscles, an accumulation of negative charges on the gel surface near the anode happens, resulting in a creep deformation of PVC gels on the anode surface due to the Maxwell force between the gels and anode electrodes. Consequently the artificial muscle generates a contraction force $F_{Contraction}$ to the outside. Then, when the DC field is turned off, the deformed PVC gels recover to their original shape by their elasticity. As a result, the artificial muscle generates a recovery force $F_{Recovery}$ to the outside. Both the contraction force and the recovery force are determined by the applied DC field, and we think that theoretically they have the same value under a certain DC field.

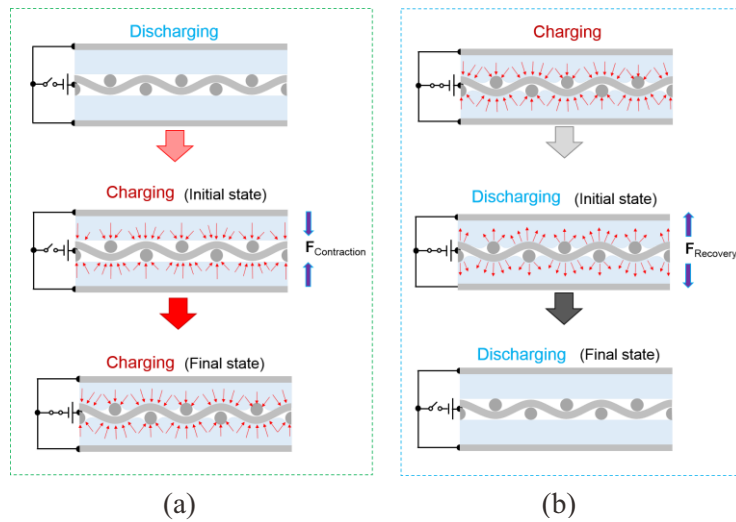


Fig. 2.4.3. Displacement of PVC gel artificial muscles with different number of stacked layers. (a) Displacement with different applied DC voltages. (b) Contraction strain with different applied DC voltages.

As shown in Fig. 2.3.1 (b), the multilayered PVC gel artificial muscles are just simply stacked by the unit structures of PVC gels, mesh anodes and foil cathodes. And each of the artificial muscle units moves independently under the electric fields. As long as a micro non-uniform structure of mesh anodes or PVC gels happens, the multilayered artificial muscles separate from

one layer to the others when being pulled by a certain force under the electric fields. Therefore we failed to measure the maximum contraction force using a force sensor as the traditional method (Fig. 2.4.4 (a)) due to a separation happened. In this study, we proposed an improved approach for investigating the maximum contraction force before a break happens, as shown in Fig. 2.4.4 (b).

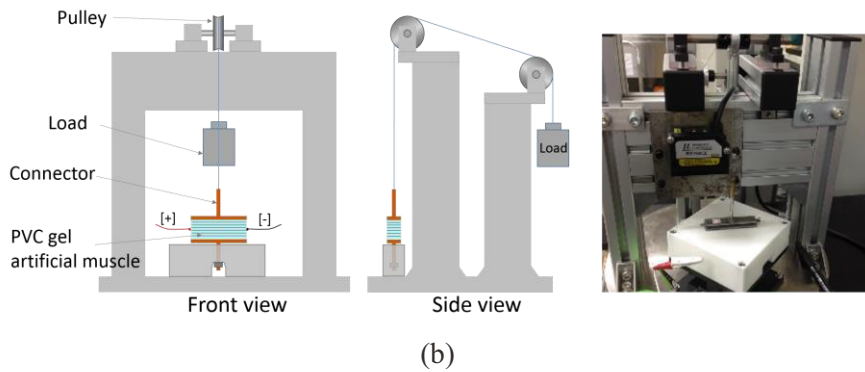
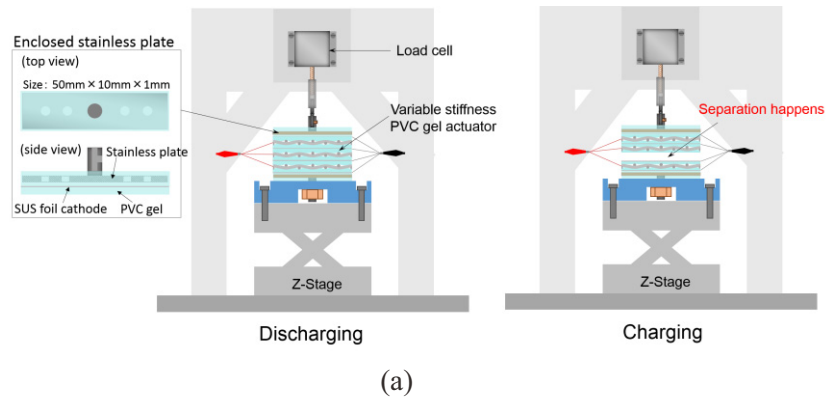


Fig. 2.4.4. Contraction force measurement of PVC gel artificial muscles. (a) Traditional method. (b) Proposed method.

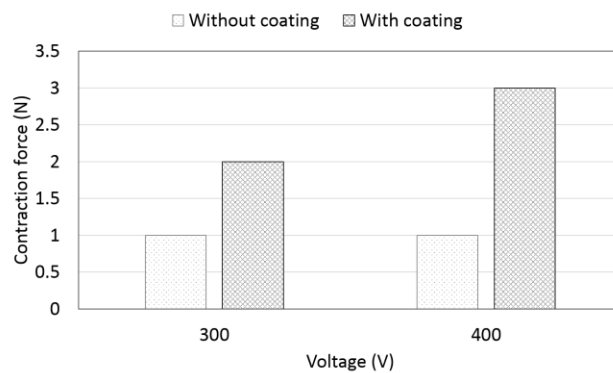


Fig. 2.4.5. Result of the contraction force before a separation happens.

We measured the 5-layer PVC gel artificial muscle with and without a PVC gel film coating outside around the surface. Fig. 2.4.5 shows the results of the contraction force under the DC voltages of 300V and 400V. As we can see that the force increases with the increase of applied voltage when there is a coating around and the contraction force increases from 1N to 3N before a break happens at the applied voltage of 400V. Considering the break happens among the stacked layers due to the non-uniform structure of the components, we think the contraction force generated under the electric fields could not be efficiently utilized in the practical applications.

As for the recovery force measurement, since a strain gauge type force sensor has a deformation up to several tens of micrometers when measuring a force as we measured, and considering the displacement of the PVC gel artificial muscles was small (several tens of micrometers to several hundreds of micrometers), we did not use a load cell to measure the recovery force. In this study, we proposed a new approach to measure the recovery force as shown in Fig. 2.4.6 (a).

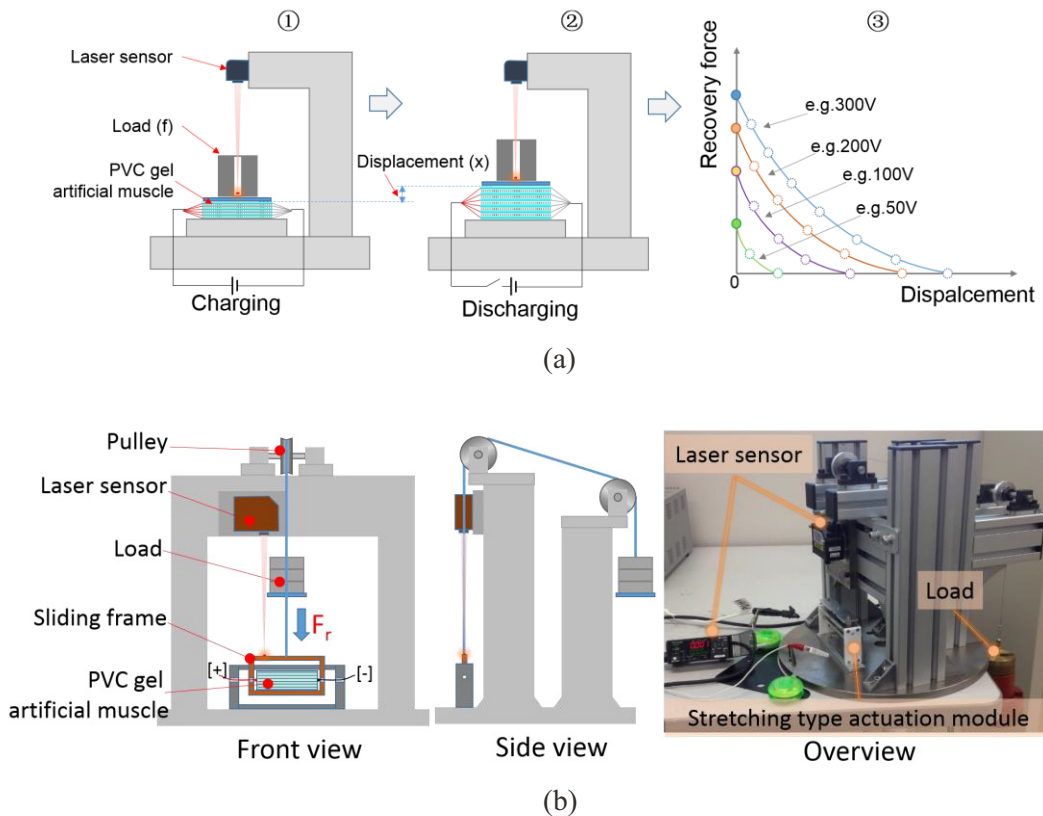


Fig. 2.4.6. Proposed method of recovery force measurement. (a) Mechanism. (b) Illustration of measurement and the actual device.

We measured the relation between the output force and displacement with different applied DC fields. When the DC field is applied, the artificial muscle shrinks and we directly put a weight on the top of artificial muscle. When the DC field is turned off, the artificial muscle recovers to its original shape by its elasticity and lift the weight upward. Then we use a laser displacement sensor to measure the displacement of the artificial muscle when turn off the DC field. By adjusting the applied weight and DC field we can get the relation between output force and displacement of the artificial muscle. With the applied weight increases, the displacement decreases. And we define the force that when the displacement becomes 0 as the maximum generation force of the PVC gel artificial muscles. To apply the loads on the small surface of the artificial muscles in a balanced way, we used a stretching type structure with two pulleys to adjust the applied loads, as shown in Fig. 2.4.6 (b). Several single-layer, 5-layer and 10-layer PVC gel artificial muscles, with the same conditions of material and size as mentioned in section 2.4.1, were used in this experiment. We measured the relation between displacement and output force with the applied DC voltages from 80V to 400V.

Fig. 2.4.7 shows the results of the relation between displacement and output force of PVC gel artificial muscles with different number of stacked layers and under different applied voltages. An inversely proportional relationship (as part of a rectangular hyperbola) was confirmed between displacement and output force. At the same applied voltage, with the increase of the displacement, the output force decreases. And for the same displacement (or output force), with the increase of number of stacked layers, the output force (or displacement) increases. Besides, with the increase of the applied voltage, the maximum displacement and output force increase. Furthermore, we found that there is a little hysteresis between the on-load and off-load due to the viscoelasticity of PVC gel. The maximum output force at an applied DC voltage of 400V is about 45N (about 90kPa), which is about fifteen times bigger than the maximum contraction force that we measured, and is almost 20 times as much as that reported in the prior literatures [2-5] and 10 times as much as that reported in [6] which used a load cell (strain gauge type force sensor).

Fig. 2.4.8 shows the results of relation between strain and output stress of PVC gel artificial muscles with different number of stacked layers and under different applied DC voltages. As shown in the results, for all the applied voltages, the curves of the single layer, 5-layer artificial muscles are almost the same as that for the 10-layer artificial muscles, except some results of the single layer under a strain of 0.005. This should due to the displacement of the single layer under a strain of 0.005 is extremely small (under several micrometers) that made it difficult to measure. Therefore, under a certain applied DC voltage, with a same strain of the artificial muscles, the output forces are the same in spite of the different number of stacked layers. This indicates that, under a certain applied DC voltage, the displacement of PVC gel artificial

muscles is linear proportional to the number of stacked layers which is consistent with the result that we got in the displacement measurement. And the output stress remains constant with the variation of the number of stacked layers but could be linear proportional to the area of the single layer structure, which is different from the prior literatures [5, 6].

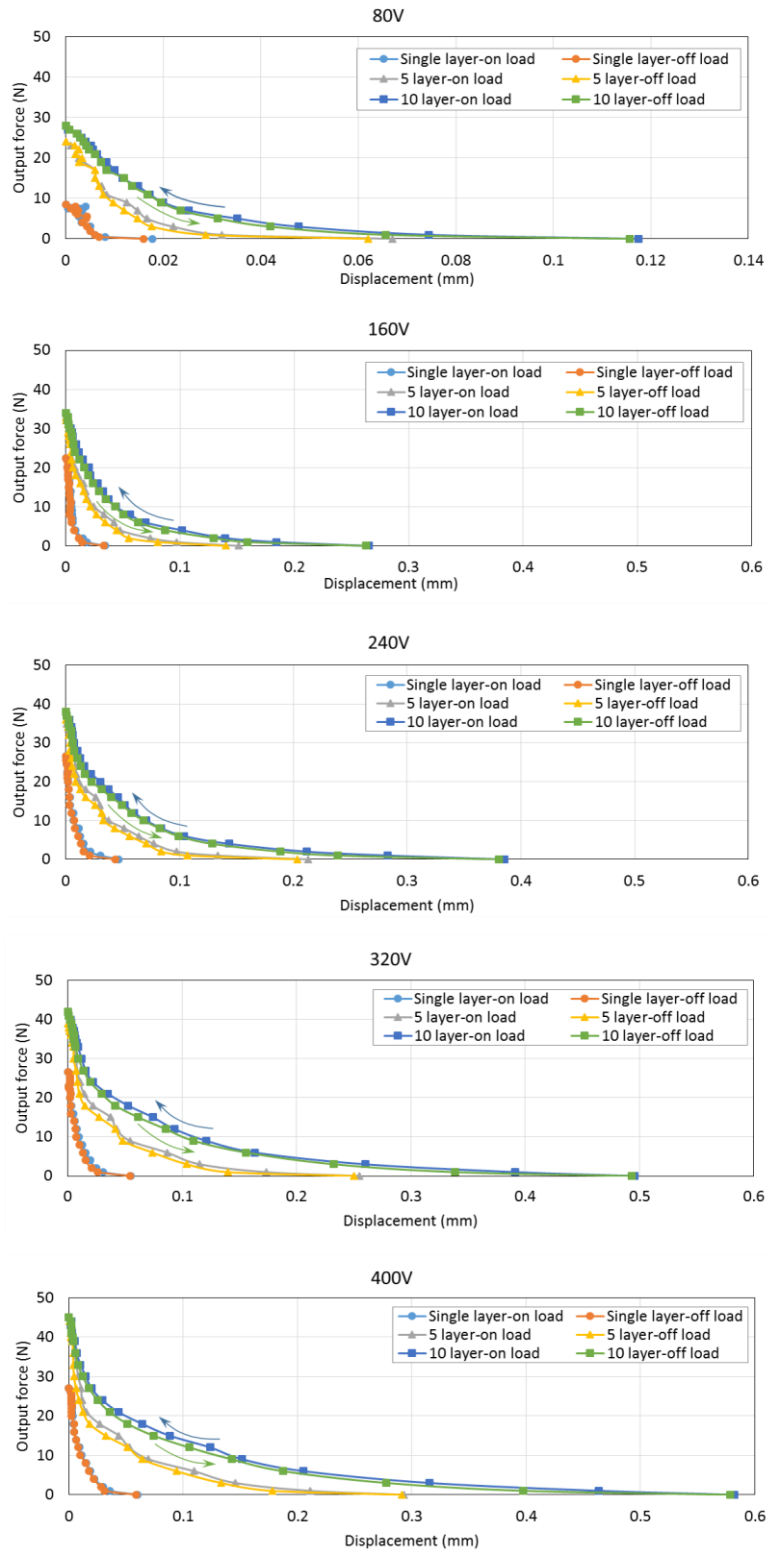


Fig. 2.4.7. Relation between displacement and output force under different applied DC voltages.

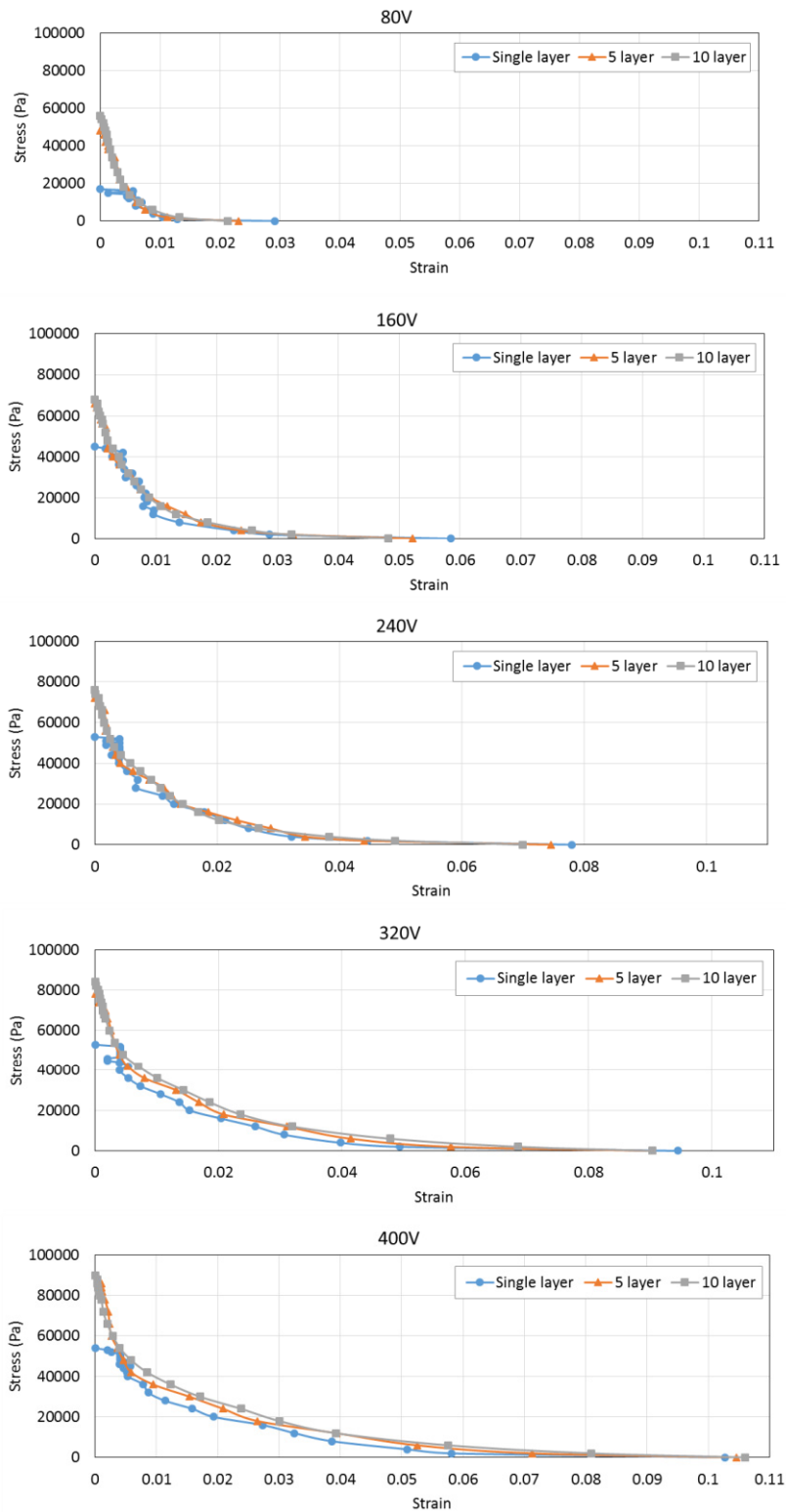


Fig. 2.4.8. Relation between strain and output stress under different applied DC voltages.

2.4.3 Electrical current measurement

As one of the evaluation criteria of artificial muscles, the power consumption becomes an important parameter. We measured the current of PVC gel artificial muscles as shown in Fig. 2.4.9. We introduced a series resistor of $1\text{ k}\Omega$ to evaluate the electrical current of PVC gel artificial muscles. The voltage of the $1\text{ k}\Omega$ resistor was detected through a 16bit interface board in the computer. We measured the currents of the single-layer, 5-layer and 10-layer PVC gel artificial muscles under the applied DC field from 80V to 400V .

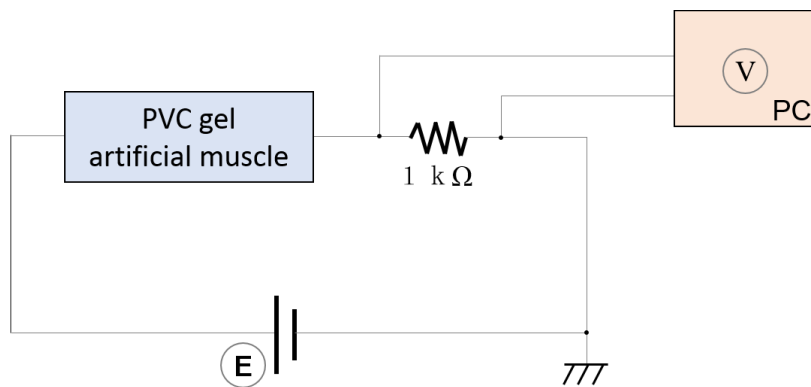


Fig. 2.4.9. Method of electrical current measurement of PVC gel artificial muscles.

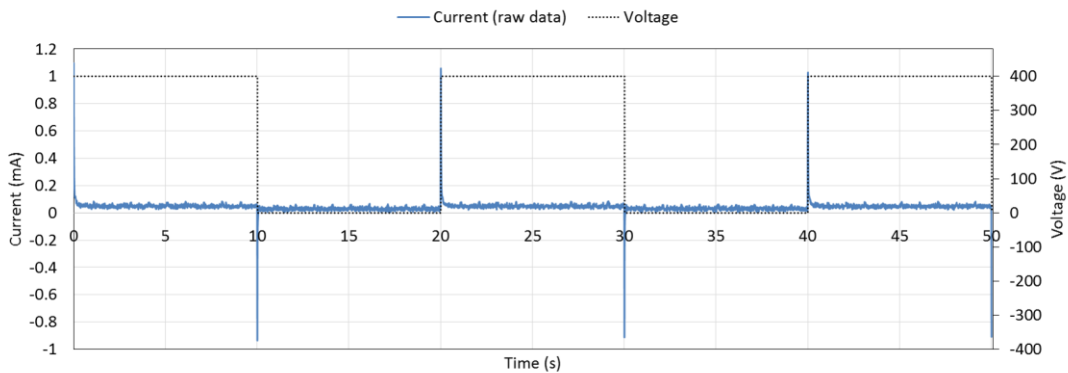


Fig. 2.4.10. A raw data of current variation of a 10-layer PVC gel artificial muscle at an input voltage of 400V.

Fig. 2.4.10 shows a result of current variation of a 10-layer PVC gel artificial muscle under a DC voltage of 400V . As shown in Fig. 2.4.10 that an instantaneous inrush current occurs when

the DC field is turned on and decrease dramatically to a stable current, and a negative inrush current occurs when the DC field is turned off and decrease to zero quickly. This is due to the charge and discharge of the capacitance of PVC gel which is consistent with the result of the equivalent circuit of PVC gel artificial muscles in prior literature (Fig. 2.4.11) [7].

Fig. 2.4.12 shows the variation of the stable current of PVC gel artificial muscles with different number of stacked layers. The electrical current increases with the increase of the applied DC voltages (Fig. 2.4.12 (a)) and the number of stacked layers (Fig. 2.4.12 (b)). As we can see that the current is not linearly proportional to the number of stacked layers, we think this might due to the contact status between the PVC gel and mesh anode electrodes is not equal in each layer. The average current of the 10-layer artificial muscles is about 0.036 mA (the power consumption is about 14.4mW) under an applied DC voltage of 400V which indicates that the PVC gel artificial muscles have a low power consumption.

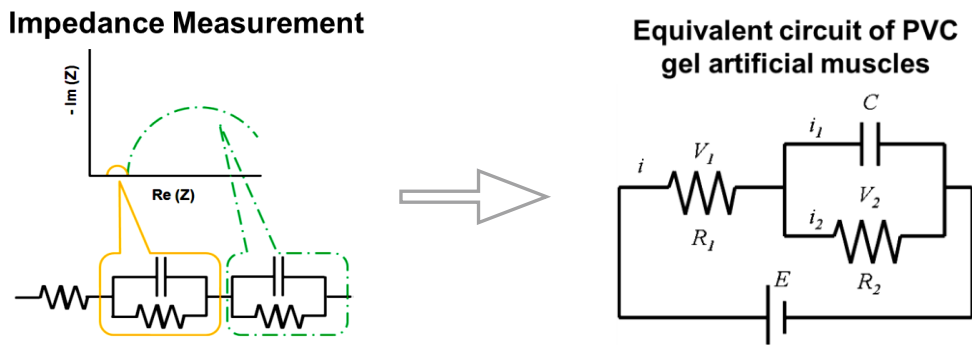


Fig. 2.4.11. Equivalent circuit of PVC gel artificial muscle.

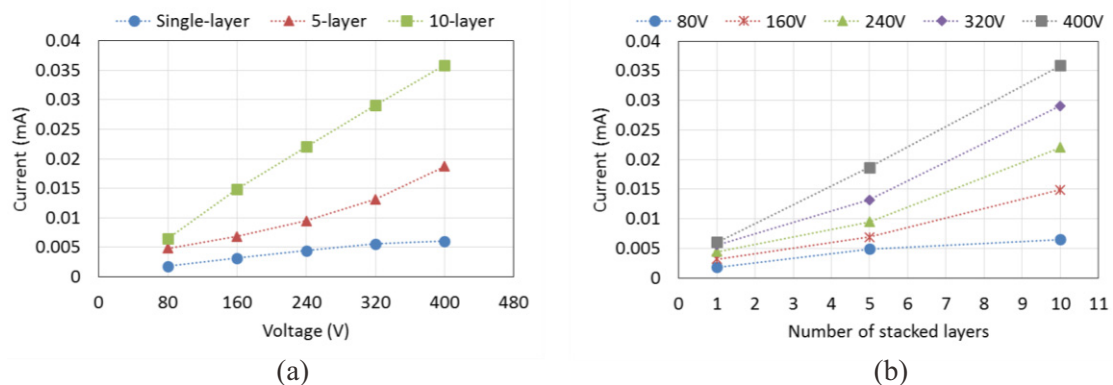


Fig. 2.4.12. Current of PVC gel artificial muscle with different number of stacked layers. (a) Relation between current and applied DC voltages. (b) Relation between current and number of stacked layers.

2.4.4 Response rate measurement

The response rate was investigated by the frequency response method. The input signal to the artificial muscles was rectangular pulses with the frequencies from 0.1Hz to 10Hz. The applied DC voltage of the rectangular pulse was 400V. Fig. 2.4.13 shows the bode diagram of the displacement. The band width (-3dB) of the PVC gel artificial muscles is 9Hz which reaches the same level of biological muscles [19].

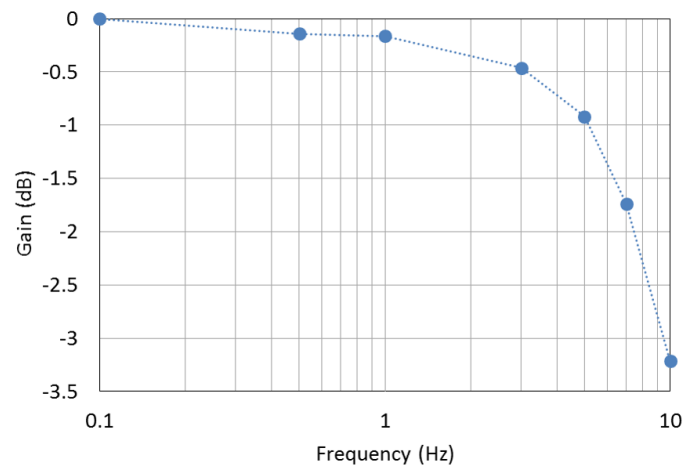


Fig. 2.4.13. Response rate of PVC gel artificial muscles.

2.4.5 Cycle life evaluation

In recently decades, a variety of artificial muscles that exhibit substantial deformations in response to different external stimulus have been developed. However, a very few of them have demonstrated exceptional cycle life, which should be one of the reasons that no single artificial muscle technology that has received wide-spread adoption as an artificial skeletal muscle so far. Among the few artificial muscles, a swaged pneumatic artificial muscle [20] and a fishing line based artificial muscle [21] exhibit a cycle life over 1 million actuation cycles.

In this study, we evaluated the durability of the PVC gel artificial muscle under a continuous electric field for a long period to ensure that its cycle life is sufficient for practical applications. Fig. 2.4.14 shows the method of the durability experiment. Three single-layer PVC gel artificial muscles were placed in a thermostatic chamber at a room temperature of 20 °C. The displacement and current of the three samples were measured simultaneously by three laser sensors with a repeatability of 0.002 mm. We used a computer (LabVIEW, cDAQ, NI) for data acquisition and analog-digital conversion.

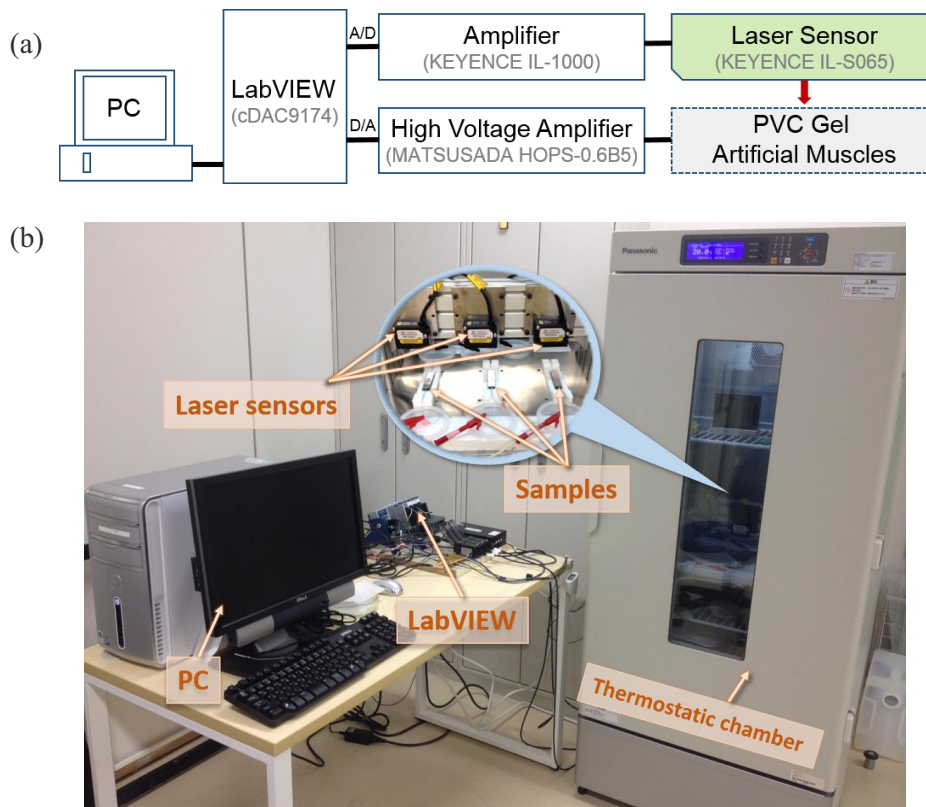


Fig. 2.4.14. Durability evaluation of PVC gel artificial muscles. (a) Measurement system. (b) Photograph of the measurement system.

The applied electric field was a shifted sine wave where the origin was shifted from zero to 160 V so that the minimum and maximum voltages became 0 and 320 V, respectively. The electric field was applied to the PVC gel artificial muscle continuously at a frequency of 2 Hz for about 31 days (about 5.4 million cycles). The recovery stress was measured before and after the durability experiment.

Fig. 2.4.15 (a) shows the result of displacement variation during the durability experiment. The displacements of the three samples decreased to about 64% of the maximum displacement after 6 hours, 50% after 168 hours (7 days) and remained constant until 600 hours (25 days). The limited variation of displacement shows that the PVC gel artificial muscles possess reasonable durability under an applied electric field. We also found an increasing trend of displacement after a break time, which can be attributed to the recovering shape of PVC gel from a long-term deformation due to the complex structure of the stainless mesh anode. Besides, we can minimize the decrease of the displacement during the continuous drive of PVC gel artificial muscles by adjusting the driving conditions, such as the type of waveform, duty ratio

and driving voltage. For example, Fig. 2.4.16 shows the average displacement variation of three 10-layer artificial muscles, under the driving condition of a 1Hz (with a duty ratio of 12.5%) square wave of a DC voltages of 0V and 400V. We can see that the displacement only decreased by about 16% and the contraction strain only decreases by 2% after about 1000 times driving and remains constant until 10000 times (about 3 hours) driving.

To determine the variation of recovery stress of the PVC gel artificial muscle after long-term driving under an electric field, we investigated the recovery stress of the artificial muscle before and after the durability experiment. The recovery stress was measured manually by a force sensor. The applied DC voltage was a square wave of 320 V. When the DC field was turned off, the artificial muscle returned to its original shape through its elasticity and the recovery stress was measured by the force sensor. Fig. 2.4.15 (c) shows the recovery stress of the artificial muscles before and after the durability evaluation experiment. The recovery stress after the experiment is almost the same as that before.

Power consumption is an important parameter to evaluate the efficiency of an artificial muscle during long-term operation. We measured the current of three single-layer PVC gel artificial muscles using a resistance of 1 k Ω . Fig. 2.4.15 (b) shows the current variation of the three artificial muscles. After 6 hours, the currents of the three artificial muscles decreased to about 0.01 mA and remained constant until 600 hours (25 days), which indicates that the power consumption of the PVC gel artificial muscles is very low. In other words, the PVC gel artificial muscles possess outstanding energy efficiency.

Therefore it was confirmed that the PVC gel artificial muscles' cycle life is more than 5 million times at the state of continuous electric field driven (2Hz), which reaches a level closes to a mammalian skeletal muscle [22]. It shows a great advantage over many other artificial muscles, such as 3000 actuation cycles of IPMC [23].

2.4.6 Thermal stability evaluation

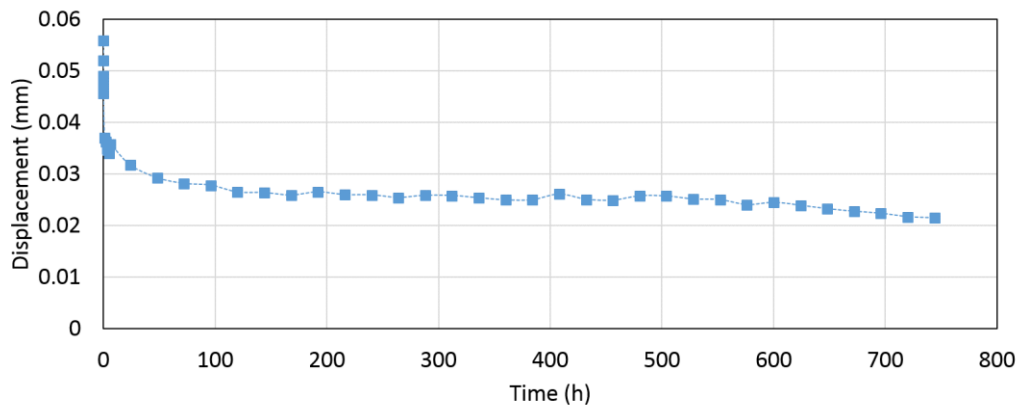
In our previous study [3], we have investigated the displacement of the artificial muscle under different temperatures. A windy oven (WFO-451SD, EYELA) was used to control the temperature of the artificial muscles. The displacement was measured by a laser displacement meter (LB-02, KEYENCE) which was settled at 25 degrees Celsius in the atmosphere.

It was found that the displacement increases around 70 degrees Celsius, and then it remained constant. It was supposed that the change of displacement was due to the elasticity change of PVC gel. And it was found that the height of PVC gel artificial muscles increased about 1% around 70 degrees Celsius which might due to the expansion of PVC gel with heat.

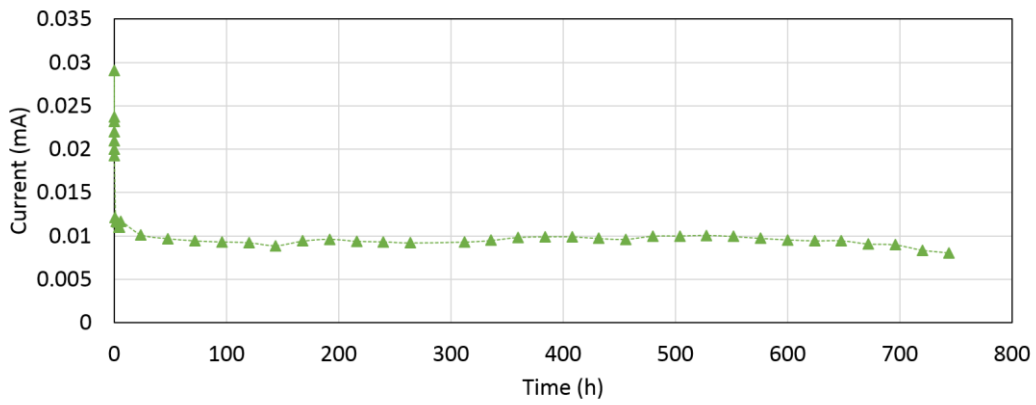
Besides, we used an infrared thermography device to investigated the surface temperature

change of the artificial muscles during the long-term cycle life evaluation experiment (as mentioned in section 2.4.5) and found no notable change on the surface temperature of the artificial muscles which indicated that the continuous actuation of the artificial muscles produce few heat to affect the characteristics.

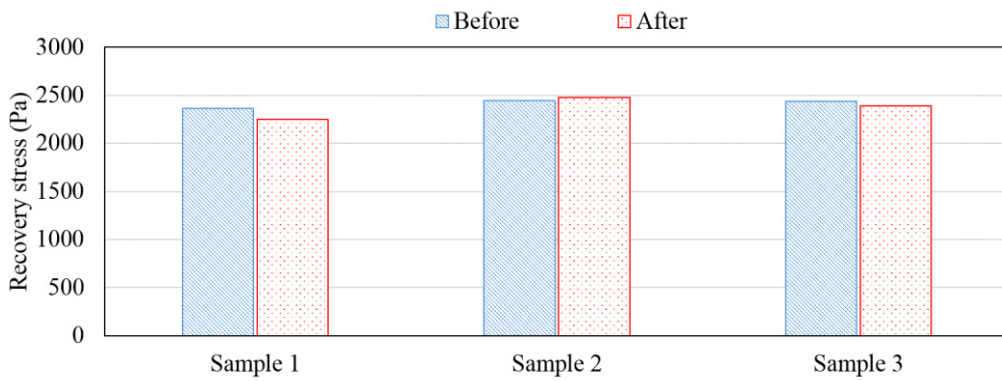
As all the properties mentioned above, the PVC gel artificial muscles are light in weight, having good performances of large displacement, high output force, low power consumption, long cycle life, and good thermal stability. Therefore, PVC gel artificial muscles are suitable for various of practical applications.



(a)



(b)



(c)

Fig. 2.4.15. Characteristics variation of PVC gel artificial muscles during a long-term experiment. (a) Displacement variation. (b) Current variation. (c) Output force variation.

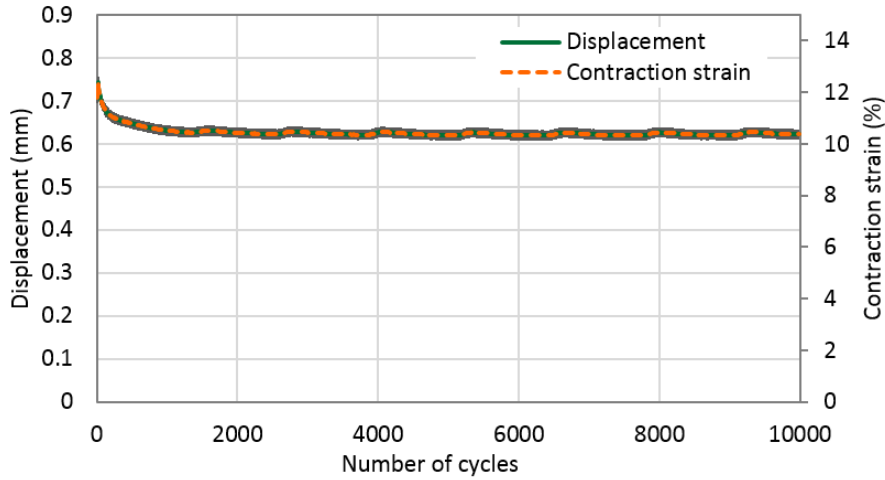


Fig. 2.4.16. Displacement variation of 10-layer PVC gel artificial muscles under a DC voltage of 400V, a frequency of 1Hz with a duty ratio of 12.5%.

2.5 Proposal of actuation modular constructions of PVC gel artificial muscles

As we mentioned in section 2.4.2 that the multilayered artificial muscles could separate from one layer to the others when being pulled by a certain force under the electric fields which may be due to the non-uniform structure of the stacked mesh anodes or PVC gels.

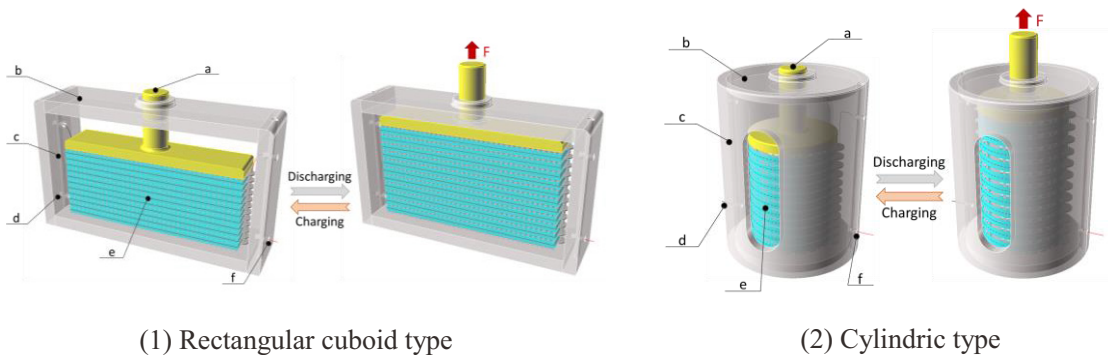
Though Ogawa et al [24] tried to solve this problem by enlarging the mesh anode of each layer and connecting them together to give a prepressing to enhance the contact between the gels and mesh anodes, it brought a big loss of strain and got an unsatisfactory contraction stress of 1.9 kPa. And we applied a thin coating of PVC gel on the surface of multilayered PVC artificial muscles to prevent the breaking, and tried to use the variable stiffness generated by the contraction force to develop PVC gel spats for walking assistance [10]. However, we only got a maximum tensile strain of 7%, with a generation force of 2.63 N (5.26 kPa) until a break happened. Therefore, we think that the contraction force generated under the electric fields cannot be efficiently utilized in the practical applications to provide a tensile force outside.

In this study, considering the drawback that mentioned above, we proposed to use the recovery force as the output force of PVC gel artificial muscles for the practical applications. Meanwhile, we proposed three types of actuation modular constructions to provide different types of forces outside, for different purposes of applications, so as to make PVC gel artificial muscles being robust actuation devices.

2.5.1 Compression type actuation module structure

The proposed compression type actuation module, as shown in Fig. 2.5.1, being defined as that the actuation module can generate a compressive force without a break under an external compressive force. The multilayered PVC gel artificial muscle is enclosed in a case, with the top layer connected to a force transferring unit. To avoid the separation between the artificial muscle and the transferring unit, we fixed two mesh anodes on the bottom sides of the transferring unit and the container, respectively.

When the DC field is on (left part of Fig. 2.5.1 (1), (2)), the artificial muscle shrinks in the direction of thickness. When the DC field is off, the artificial muscle recovers to the original shape and generate a force. The stroke and output force of the module can be controlled by the input voltage. The shape, size and other detailed design specifications of the case and artificial muscles can be adjusted according to the practical applications. Furthermore, we can get more displacement by the series connection of the actuation module units and bigger output force by the parallel connection of the actuation module units. In this case, the connection between each unit should be a rigid connection. Meanwhile, even though this type of actuation module units is not robust to the stretching force, we can make a more robust compressive and stretching actuation device by connecting the connector parts of the compression type actuation module units in I-shaped.



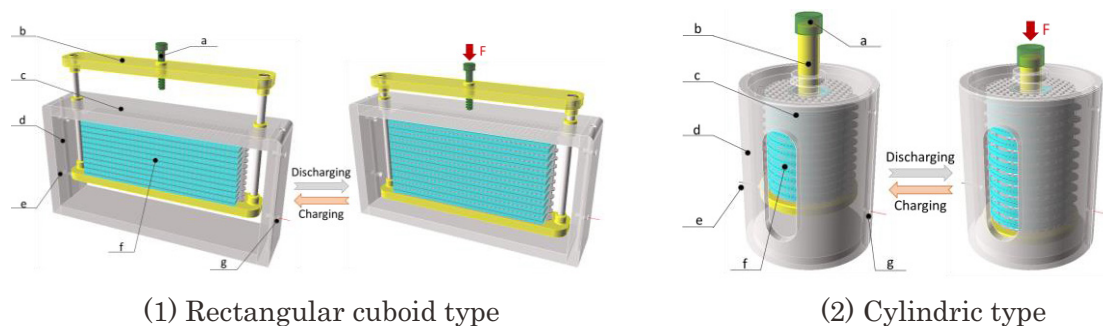
- a: connector and force transferring part;
- b: container and protector;
- c: pipeline for wiring and aeration (left and right);
- d: input of cathode (-);
- e: PVC gel artificial muscle;
- f: input of anode (+).

Fig. 2.5.1. Illustration of compression type actuation modules.

2.5.2 Stretching type actuation module structure

When the applications need a pulling force, for example, walking assist application, it is effective to design the actuation module as the structure shown in Fig. 2.5.2. It mainly contains a slide frame and a container. The multilayered PVC gel artificial muscle is placed on the slide frame, of which the height is adjusted to the thickness of artificial muscles so as to prevent a hardly break when bearing a compressive load. And we can adjust the part of the connector and force transferring ('a' of Fig. 2.5.2 (1), (2)) to control the preload to the artificial muscle. To avoid the separation among the layers of artificial muscles due to the self-weight of the slide frame, we fixed two mesh anodes on the top side and the bottom side of the container and the slide frame, respectively.

When the DC field is applied to the artificial muscle, it contracts and brings the slide frame an upward movement. And when the DC field is turned off, the artificial muscle occurs a downward movement and generate a tensile force without a break happens. Also, it is reasonable to connect the stretching actuation modules in a series connection or a parallel connection to adopt the practical applications. In this case, flexible connection is suitable for the connection among the modules, for example, using stainless wire. Although this type of actuation module units is not robust to the external compressive force, we can make a more robust compressive and stretching actuation device by connecting the connector parts of the stretching type actuation module units in I-shaped to make a device that is robust in both upward and downward movements.



(1) Rectangular cuboid type

(2) Cylindric type

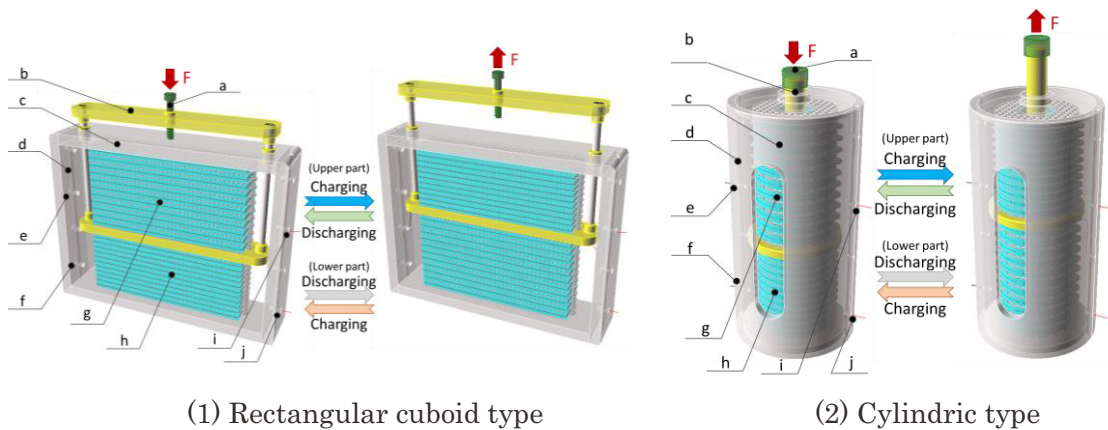
- a: connector and force transferring part;
- b: slide frame;
- c: container and protector;
- d: pipeline for wiring and aeration (left and right);
- e: input of cathode (-);
- f: PVC gel artificial muscle;
- g: input of anode (+).

Fig. 2.5.2. Illustration of stretching type actuation modules.

2.5.3 Compression-Stretching type actuation module structure

By combination of the compression type and stretching type actuation modules, we can make a compression and stretching type actuation module as shown in Fig. 2.5.3. The basic structure is the same as the stretching type that contains a slide frame and a container. Two multilayered PVC gel artificial muscles are arranged inside and outside of the slide frame. Both the top and bottom sides of the upper artificial muscle are fixed to the container and slide frame, respectively. And the top and bottom sides of the lower artificial muscle are fixed to the bottom side of slide frame and the container, respectively.

When the upper artificial muscle is charged and the lower artificial muscle is discharged at the same time, the actuation module produces a compressive force. Otherwise, when the upper artificial muscle is discharged and the lower artificial muscle is charged coinstantaneous, a pulling force occurs. The interaction force between the upper and lower artificial muscles can prevent the break in both the contraction and expansion movement of the slide frame. Therefore, this actuation module type is robust in the bidirectional assistance.



(1) Rectangular cuboid type

(2) Cylindric type

- a: connector and force transferring part;
- b: slide frame;
- c: container and protector;
- d: pipeline for wiring and aeration (left and right);
- e: input of cathode (-) of the upper artificial muscle;
- f: input of cathode (-) of the lower artificial muscle;
- g: upper PVC gel artificial muscle;
- h: lower PVC gel artificial muscle;
- i: input of anode (+) of the upper artificial muscle.
- j: input of anode (+) of the lower artificial muscle.

Fig. 2.5.3. Illustration of compression-stretching type actuation.

2.5.4 A prototype of stretching type actuation module of PVC gel artificial muscles

In this study, we made a prototype of stretching type actuation module to evaluate the effectiveness of the proposed modules. We investigated the advantages of using recovery force of PVC gel artificial muscles instead of contraction force using the fabricated stretching type actuation module, from two aspects of robustness and response time against the external loads. Furthermore, as a design and control element of the proposed modules in practical use, we developed a model of static characteristics of PVC gel artificial muscles based on the experimental data measured by the prototype of modules.

Fig. 2.5.4 shows the overview of the fabricated stretching type module unit. It mainly contains a slide frame that made of Aluminum plate and a container that made of Aluminum and Teflon plates. In order to decrease the friction force of sliding movement, we introduced a linear bearing (LMUF3, MISUMI, JAPAN) to the slide frame. And the length of the slide frame was adjustable so as to fit the thickness of artificial muscles.

A 10-layer multilayered PVC gel artificial muscle was fixed between the bottom of slide frame and the top of the container. The compositions and conditions of the artificial muscle was the same as mentioned in section 2.4.1. When making the actuation movement without an external load, to avoid the separation among the layers of artificial muscles due to the self-weight of the slide frame, we fixed two mesh anodes on the top side and the bottom side of the container and the slide frame, respectively.

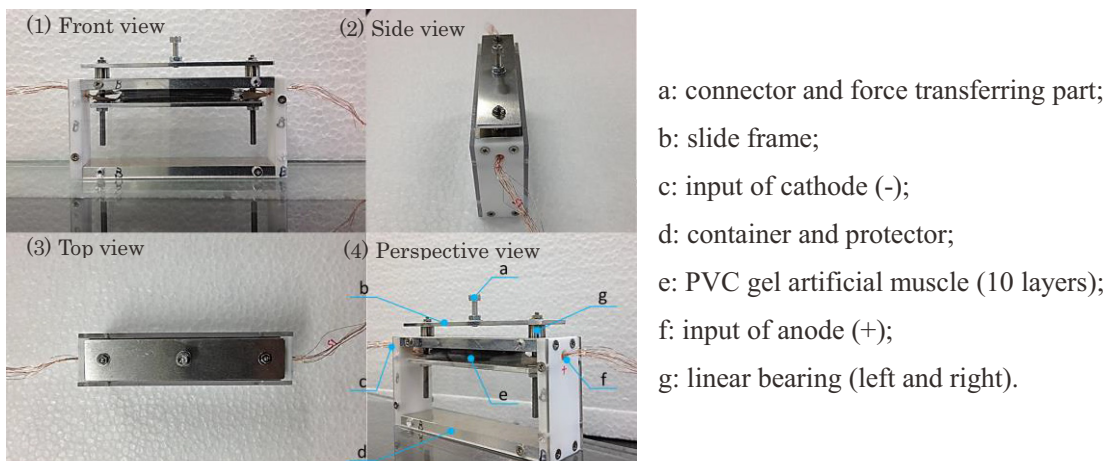


Fig. 2.5.4. A prototype of stretching type actuation modules.

In this study, based on the prototype of stretching type actuation module, we conducted a comparison experiment between the contraction force and recovery force to confirm the performances and advantages of the proposed actuation modules that using the recovery force of PVC gel artificial muscles. Fig. 2.5.5 shows the method of the evaluation experiment. As shown in Fig. 2.5.5 (b), to evaluate the performance of contraction force of the actuation module, we put the loads on the top of the slide frame of actuation module. When the DC field is applied to the artificial muscle, it shrinks and a contraction force F_c generated to lift the load upward. And it returns to its original shape due to the elasticity of PVC gel and the applied load when the DC field is turned off. A laser sensor is used to measure the displacement of the load. As we mentioned before that each of the artificial muscle units moves independently under the electric fields. With the increase of the applied loads, the displacement of the load decreases and the multilayered artificial muscle separates from one layer to the others when being compressed by a certain force due to the nonuniform structure of mesh anodes or PVC gels (Fig. 2.5.5 (c)). As a result, the contraction force generated before the break can be efficiently utilized in the practical applications.

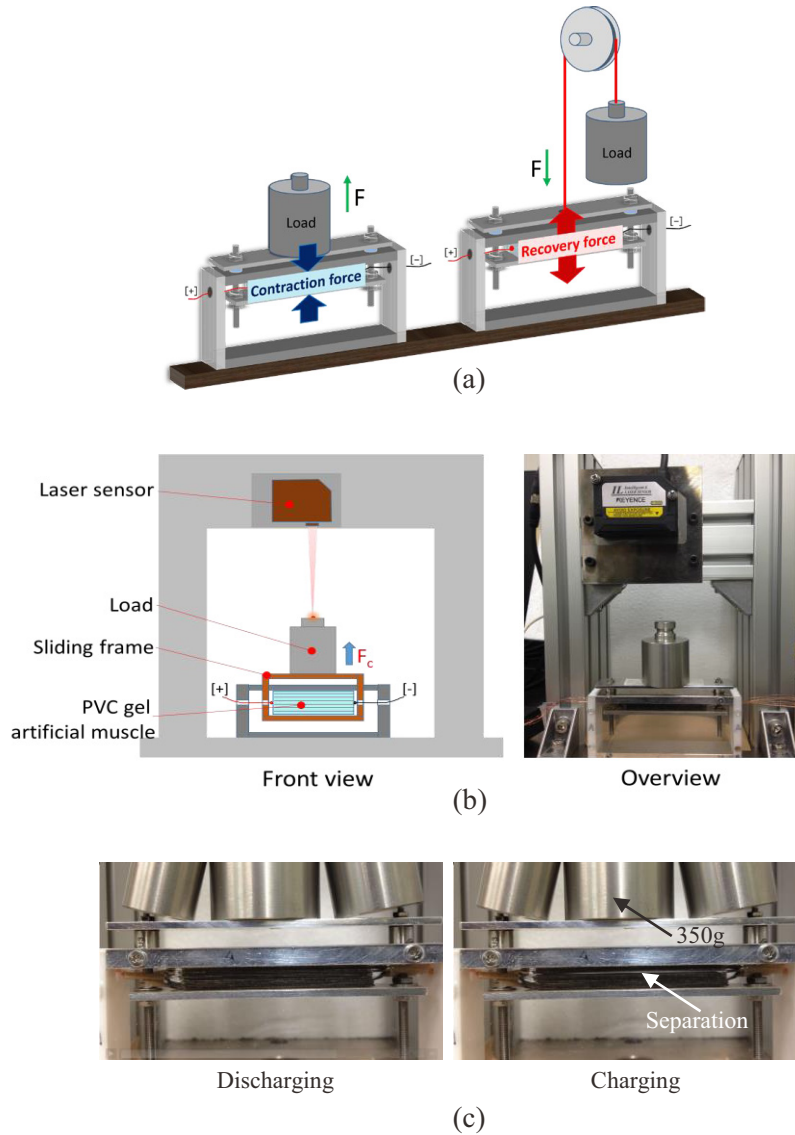


Fig. 2.5.5. (a) Illustration of performance measurement of contraction force and recovery force. (b) Method of contraction force. (c) An example of a separation happens among the stacked layers when the applied load is 0.35kg.

On the other hand, for the recovery force evaluation of the actuation module, we used the method that we proposed in section 2.4.2 (Fig. 2.4.6 (b)). The actuation module is connected to the applied load by stainless wire and pulleys. When a DC field is applied to the artificial muscle, it shrinks and brings a downward movement to the external load. And when the DC field is turned off, the artificial muscle recovers to its original shape by its elasticity very quick, generating a recovery force F_r and consequently lift the applied load upward. The displacement

of the applied load is measured by displacement of the slide frame. By this utilization of the stretching type actuation module, there will not be a break happens among the layers of PVC gel artificial muscles. With the applied load increases, the strain of artificial muscle decreases and the stress at the strain of 0% is the maximum recovery stress of PVC gel artificial muscles that we can efficiently utilize in the practical applications.

In this experiment, we compared the variation of both the contraction force and recovery force under a DC voltage of 400V. Also the response time of the two kinds of forces was investigated. As shown in Fig. 2.5.6, the response time of contraction force (t_c) and recovery force (t_r) is defined as the time from 10% to 90% of the contraction displacement and recovery displacement, respectively.

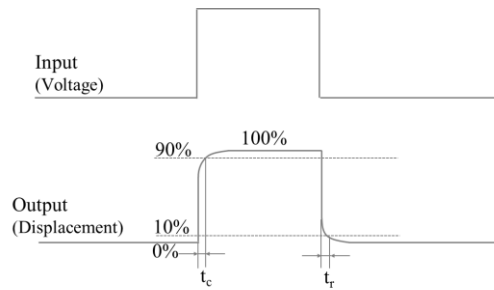


Fig. 2.5.6. Definition of response time of contraction and expansion.

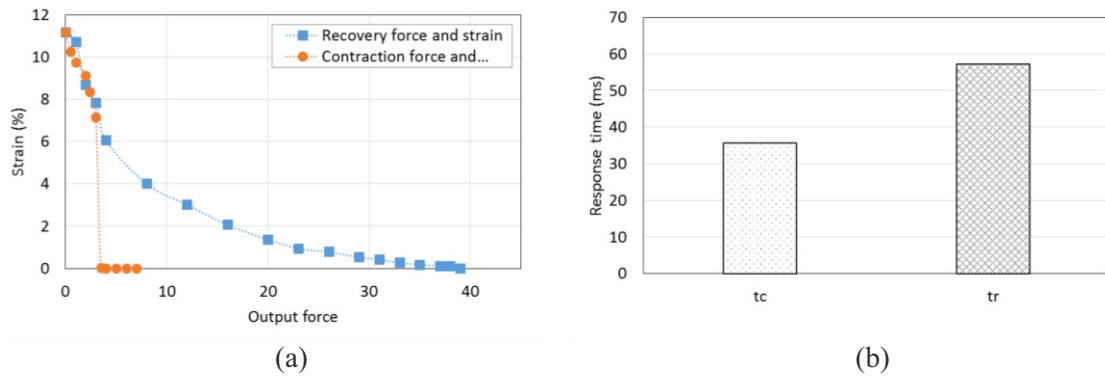


Fig. 2.5.7. Performance comparison of contraction force and recovery force measurement.

(a) Output force comparison. (b) Response time comparison.

Fig. 2.5.7 (a) shows the result of the comparison of contraction force and recovery force measurement. As shown in the result of contraction force and strain, the strain drops

dramatically to 0% at the applied load of 3.5N (7kPa) which shows that the maximum generation force that can be used before a break happens is below 3.5N. However, as for the recovery force and strain, we can see that the maximum generation force is about 38N (78kPa) at the strain of 0% which is about 11 times of the maximum contraction force.

Fig. 2.5.7 (b) shows the result of the response time of contraction force and recovery force. The response time t_r of recovery force is about 57ms, which is slow than that of contraction force t_c (about 36ms). But we don't consider it as a big difference in the practical applications. Since the response time of the recovery force is determined by the viscoelasticity of PVC gel, we can adjust the weight ratio of PVC and DBA to improve the response speed.

Therefore, as discussed above, it is obvious that the proposed module constructions are effective to utilize the properties of PVC gel artificial muscles so as to make the PVC gel artificial muscles as a kind of robust actuation devices in various applications from some micro machines to large scale devices.

2.6 Modeling of static characteristics of PVC gel artificial muscles

Considering practical applications of the proposed actuation modular constructions, as a design and control element, we modeled the static characteristics of PVC gel artificial muscles based on the experimental results that measured by the prototype of stretching type actuation module.

In this study, we developed a model to represent the relation between the applied DC voltages and output of displacement and force based on Hill's muscle model [25, 26].

2.6.1 Hill's muscle model

Hill demonstrated the relation between active force P and speed of shortening S in skeletal muscle can be adequately described as part of a rectangular hyperbola [25], as shown in Fig. 2.6.1. And the general equation of this relation given as the Hill muscle model as follows:

$$(P+a)(S+b) = (P_m+a)b = C, \quad (1)$$

$$\frac{P}{P_m} = \frac{S}{S_m} = \text{const} \tan t \quad (2)$$

where P and S are the muscle force and the contraction velocity, respectively. a , b and C are constants. P_m is the maximum force with zero velocity, and S_m is the maximum contraction velocity with zero force.

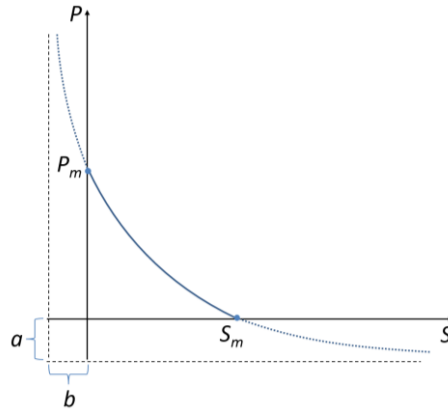


Fig. 2.6.1. Hill's force-velocity relationship, where P_m is maximum isometric force or force with zero velocity, S_m is the highest possible velocity, a and b are constant force and constant velocity.

2.6.2 Model of characteristics based on Hill's equation

As shown in Fig. 2.4.7 that the displacement and output force of PVC gel artificial muscles have an inversely proportional relationship (as part of a rectangular hyperbola). The curve of the displacement and output force is quite similar with the curve of Hill's muscle model (Fig. 2.6.1). Therefore, in this study we modeled the relation between displacement and output force of PVC gel artificial muscles as described in the following equation:

$$(F + a_f)(X + b_x) = (F_m + a_f)b_x = (X_m + b_x)a_f = c \quad (3)$$

where F and X are the output force and the displacement, respectively. a_f , b_x and c are constants. F_m is the maximum force with zero displacement, and X_m is the maximum displacement with zero force.

F and X can be obtained by the experimental data. a_f , b_x and c can be obtained by fitting Hill's hyperbolic equation to experimental data. Several methods have been used in the past for fitting a hyperbolic function to experimental force-velocity data, like the graphical fitting method [27], the parameters adjusting method [28] and the regression analysis method [29]. In this study, we chose the regression analysis method because it has an advantage over the previous method in that it is simpler and more convenient to use. Furthermore, the method is not based on the use of F_m which is therefore applicable to fitting a hyperbola to observations at low and intermediate forces.

The regression analysis of the variables F , X and FX in the hyperbolic equation can be performed in six steps [29]. We used the experimental data of 10-layer PVC artificial muscles to calculate the numerical values of the three constants. The obtained a_f , b_x and c with different

applied DC voltages are shown in Fig. 2.6.2.

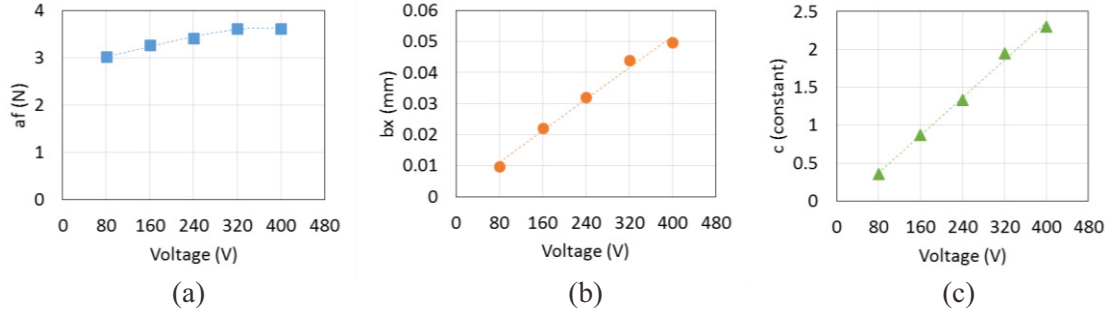


Fig. 2.6.2. Results of constant coefficients at different voltages. (a) a_f , (b) b_x , (c) c .

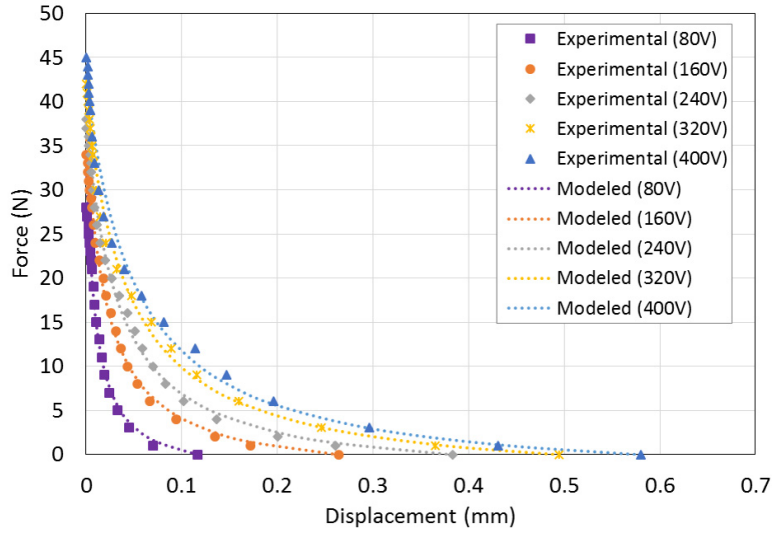


Fig. 2.6.3. Simulation result based on the proposed model.

The relation between the constants and applied DC voltages can be presented as follows:

$$A_f(v) = -5.0176 \times 10^{-6} v^2 + 4.3400 \times 10^{-3} v + 2.6956 \quad (4)$$

$$B_x(v) = 1.2700 \times 10^{-4} v + 9.7018 \quad (5)$$

$$C(v) = 6.2100 \times 10^{-3} v - 1.4925 \quad (6)$$

Therefore, we can model the relation between the applied DC voltages, displacement and output force of PVC gel artificial muscles by Eq. (7):

$$(F + A_f(v))(X + B_x(v)) = C(v) \quad (7)$$

Fig. 2.6.3 shows the simulation result of the model and the measured data of 10-layer artificial

muscles. This indicates a good agreement between the model and the measured data. For a practical application, once two of the desired parameters of applied DC voltage, displacement and output force in the model are defined, we can obtain the rest one. Since we have addressed in Fig. 2.4.2 and Fig. 2.4.8 that the displacement of PVC gel artificial muscles is linear proportional to the number of stacked layers and the output stress remains constant with the variation of the number of stacked layers, this model can be also effective to different number of stacked layers by simply normalize the displacement with the number of stacked layers.

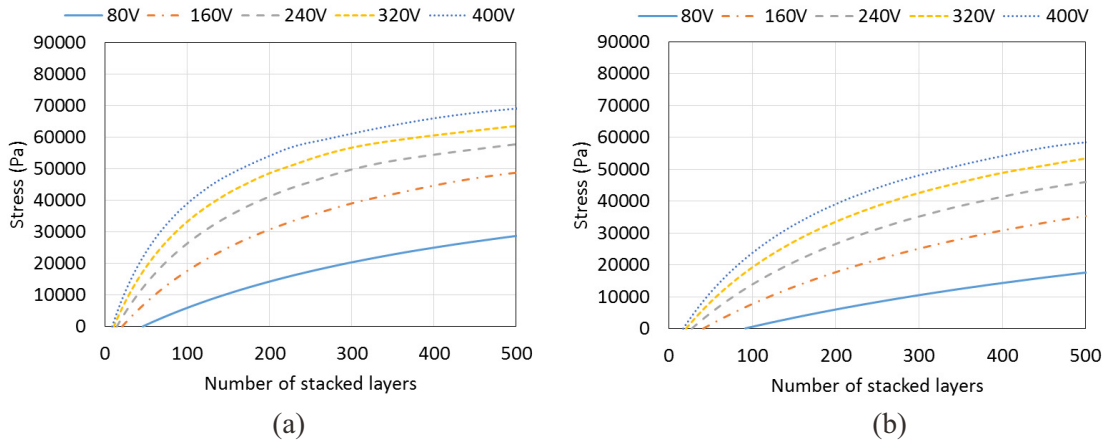


Fig. 2.6.4. Relation between the number of stacked layers and the output stress at a desired displacement of (a) 0.5mm and (b) 1.0mm..

When the requirement of an application is determined, we have to design the actuation module to satisfy it. Then we have to determine the structure and size of the actuation module according to the size of artificial muscles. PVC gel artificial muscles' size is determined by the number of stacked layers and the area of each layer. And the displacement is linear proportional to the number of stacked layers and the output force is linear proportional to the area of each layer. To find the relation between the number of stacked layers and the output stress, we can define the F and X of Eq. (7) as follows:

$$X = \frac{10X_{desire}}{N_{layer}} \quad (8)$$

$$F = A_{area}S_{stress} = 5 \times 10^{-4} S_{stress} \quad (9)$$

where X_{desire} is the displacement required by an application. N_{layer} is the number of stacked layers. A_{area} and S_{stress} are the area of one layer and the output stress, respectively. Then, the model of relation between number of stacked layers and output stress can be given as Eq. (10).

$$(5 \times 10^{-4} S_{stress} + A_f(v)) \left(\frac{10 X_{desire}}{N_{layer}} + B_x(v) \right) = C(v) \quad (10)$$

Fig. 2.6.4 shows the simulation result of a desired displacement of 0.5mm and 1.0mm. At the same number of stacked layers, with the increase of applied DC voltage, the output stress increases. And at the same applied DC voltage, with the increase of number of stacked layers, the output stress increases. The output force is determined by the area and stress and the height of artificial muscles is determined by the number of stacked layers. Therefore, using this model we can get an optimization design of the size of the actuation modular constructions for a practical application, for example, an application as a motor brake [9].

2.7 Chapter summary

Most of the artificial muscles that developed so far are being challenged by the characteristics improvement to reach or exceed the level the nature muscles for a successful commercialization and a wide use.

We have improved the characteristics of PVC gel artificial muscles from several aspects (e.g. gel membranes, electrodes and fabrication) to make it almost close to the level of the biological muscles, in terms of the stable contraction strain (> 10% vs 20-30%), response rate (up to 9Hz vs 10Hz) and the maximum output stress (about 0.09MPa vs 0.1-0.3MPa).

These advantages along with the satisfactory cycle life (over 5 million times) indicate that the PVC gel artificial muscles have a great potential to use as a candidate of artificial muscles in practical use.

We proposed a new approach to measure the output force of PVC gel artificial muscles that can accurately measure the characteristics than the former method.

We proposed three types of modular constructions in this study which are very important elements for the standardization of PVC gel artificial muscles (as one element for commercialization).

They make the PVC gel artificial muscles become robust actuation devices.

By combining them in different constructions with different functions we can realize various applications. For example, we can make a robust and lightweight walking assist wear by combining the stretching type actuation module units in a series connection so that we can support the walking motion by the output force generated with the DC field on and off, so as to lighten the load of human muscles.

Furthermore, the model of the static characteristics developed in this study which showed a good agreement with the experimental data could be an effective element for the specific design

and control of the proposed modular constructions in an application.

In summary, we believe that the PVC gel artificial muscles based actuation modular units will play an important role in the field of mechatronics, robotics, biomimetics and biomedicine in the future.

References

- [1] M. Yamano, N. Ogawa, M. Hashimoto, M. Takasaki and T. Hirai, "A Contraction Type Soft Actuator Using Poly Vinyl Chloride Gel," in Proc. IEEE Int. Conf. Robotics and Biomimetics (ROBIO 2008), Bangkok, Thailand, 2009, pp.745-750.
- [2] N. Ogawa, M. Hashimoto, M. Takasaki and T. Hirai, Characteristic Evaluation of a Multilayered PVC Gel Actuator, in the 9th SICE System Integration Division Annual Conference (SI2008), pp. 283-284. 2014.
- [3] N. Ogawa, M. Hashimoto, M. Takasaki and T. Hirai, Characteristics Evaluation of PVC Gel Actuators, in: The 2009 IEEE/RSJ Int. Conf. on Intelligent Robots and Systems (IROS2009), St. Louis, USA, 2009, pp.2898-2903.
- [4] N. Hayasaka, S. Mao, Y. Tsuchiya and M. Hashimoto, Structural improvement and performance of thin-type PVC gel actuators, in: The JSME conference on Robotics and Mechatronics, 2013, pp. 2P1-F09. (in japanese)
- [5] S. Mao, N. Hayasaka and M. Hashimoto, Development of an Artificial Muscle using PVC Gel Thin Films, The 17th World Congress on Biomimetics, Artificial Muscles and Nano-Bio (BAMN2013), 2013.
- [6] Y. Li, Y. Tsuchiya, A. Suzuki, Y. Shirai and M. Hashimoto, Influence of the Number of Stacked Layers on the Performance of PVC Gel Actuators, The 2014 IEEE/ASME International Conference on Advanced Intelligent Mechatronics (AIM2014), 2014, pp. 94-99.
- [7] M. Shibagaki, N. Ogawa, M. Hashimoto and T. Hirai, Modeling of contraction type PVC gel actuators, in: Proc. of the 2010 IEEE Int. Conf. Robotics and Biomimetics (ROBIO 2010), Tianjin, China, 2010, pp.1434-1439.
- [8] Y. Maeda and M. Hashimoto, Developing a massage machine using PVC-Gel actuator, The JSME conference on Robotics and Mechatronics. 1P1-P02 (1)-(4), 2011.

- [9] M. Shibagaki, T. Matsuki and M. Hashimoto, Application of a contraction type PVC gel actuator to brakes, in: Proc. of the 2010 IEEE Int. Conf. on Mechatronics and Automation (ICMA), Xian, China, 2010, pp.39-44.
- [10] Y. Li, Y. Maeda and M. Hashimoto, "Light-weight, Soft Variable Stiffness Gel Spats for Walking Assistance", International Journal of Advanced Robotic Systems, Vol. 12, No. 175, pp. 1-11, 2015.
- [11] H. Takase, Y. Tsuchiya and M. Hashimoto, Development of a Breath Entrainment Device using a PVC Gel Actuator, in the 16th Japan Society of Kansei Engineering, pp. F23, 2014.
- [12] https://en.wikipedia.org/wiki/Polyvinyl_chloride
- [13] T. Hirai, S. Kobayashi, M. Hirai, M. Yamaguchi, Md. Z. Uddin, M. Watanabe and H. Shirai, Bending induced by creeping of plasticized poly (vinyl chloride) gel, Proc. Of SPIE, 5385 (2004) 433-441.
- [14] Md. Zulhash Uddin, M. Watanabe, H. Shirai, and T. Hirai, Creeping and novel huge bending of plasticized PVC, J. Robotics and Mechatronics, 14 (2002) 161-166.
- [15] K. Yasuda and M. Hashimoto, Deformation Analysis of PVC Gel Using a Digital Microscope, in the 15th SICE System Integration Division Annual Conference (SI2014), pp. 672-673. 2014.
- [16] H. Xia, M. Takasaki and T. Hirai, Actuation mechanism of plasticized PVC by electric field, Sens. Actuators A 157 (2010) 307-312.
- [17] H. Xia, T. Ueki and T. Hirai, Electrical response and mechanical behavior of plasticized PVC actuators, Adv. Mater. Res. 79-82 (2009) 2063-2066.
- [18] K. Yasuda and M. Hashimoto, "Simulation of Electroactive PVC Gel using FEM," The JSME conference on Robotics and Mechatronics. 2A1-J05, 2014.
- [19] R.H. Baughman, Playing nature's game with artificial muscles, Science 308 (2005) 63-65.
- [20] B.K. Woods, M.F. Gentry, C.S. Kothera and N.M. Wereley, Fatigue life testing of swaged pneumatic artificial muscles as actuators for aerospace applications, J. Intel. Mat. Syst. Str. 23 (2012) 327-343.
- [21] C. S. Haines, M. D. Lima, N. Li, G. M. Spinks, J. Foroughi, J. D. W.Madden, S. H. Kim, S. Fang, M. Jung de Andrade, F. Göktepe, O. Göktepe, S. M. Mirvakili, S. Naficy, X. Lepr'o, J. Oh, M. E. Kozlov, S. J. Kim, X. Xu, B. J. Swedlove, G. G. Wallace, and R. H. Baughman, Artificial muscles from fishing line and sewing thread, Science 343 (2014) 868-872.
- [22] J. D. Madden, N. A. Vandesteeg, P. A. Anquetil, P. G. Madden, A. Takshi, R. Z. Pytel, and I. W. Hunter, Artificial muscle technology: Physical principles and naval prospects, IEEE J. Ocean. Eng. 29 (2004) 706-728.
- [23] E. Malone and H. Lipson, Freeform fabrication of ionomeric polymer-metal composite actuators, Rapid Prototyping J. 12/5 (2006) 244-253.

- [24] N. Ogawa, M. Hashimoto, M. Takasaki and T. Hirai, Development of an artificial muscle using PVC-gel, -Increasing force generation during the contraction-, in: The JSME conference on Robotics and Mechatronics, 2009, pp. 1A2-M03. (in japanese)
- [25] Hill, A.V.: The Heat of Shortening and the Dynamic Constants of Muscle. Proceedings of the Royal Society B, London, 126, pp.136-195. 1938.
- [26] Hill, A.V.: First and Last Experiments in Muscle Mechanics. Cambridge University Press, Cambridge, 1970.
- [27] KATZ B., The relation between force and speed of muscular contraction. Journal of Physiology 96(1939) 45-64.
- [28] EDMAN K.A.P., MULIERI L.A and SCUBON-MULIERI B., Non-hyperbolic force-velocity relationship in single muscle fibers, Acta Physiologica Scandinavica 98(1976) 143-156.
- [29] B. Wohlfart, K. A. P. Edman, Rectangular hyperbola fitted to muscle force-velocity data using three-dimensional regression analysis, Exp. Physiol. 79 (1994) 235-239.

Chapter 3

Proposal of a lightweight walking assist wear using PVC gel artificial muscles

Chapter 3 Proposal of a lightweight walking assist wear using PVC gel artificial muscles

The goal of this study is to develop a wearable, lightweight, flexible assist wear for a daily life support for the elders to lighten their burden during walking. This requires that the assist wear should have a low impedance not to impede the natural motion of the wearer, a natural interface and a simple structure to make it comfortable to wear and easy to don and doff. Furthermore, a good safety, a low power consumption and a long life should be taken into account. PVC gel artificial muscles have the properties of being soft and lightweight, with notable response rate, a high energy efficiency and a long cycle life which demonstrates a great potential to construct a walking assist wear for a daily life walking support.

Such a wearable assist wear consists of several segments that includes attachment points to the body, an actuation segment to provide tensile forces by changing its length in the assist wear, and some structured textile belts to transmit the forces across the body. Since these forces are offset from the joint centers of rotation due to the tissue and bone structure surrounding the joints, the assist wear is able to create moments around the joints to support the motion of human body.

This Chapter will propose the structure of a lightweight wearable assistive wear using PVC gel artificial muscles, and discuss the assistance method with the assist wear according to the walking gait analysis.

3.1 Biomechanics of walking

It is very important to understand the biomechanics of human walking for the design of exoskeletons, active orthoses and walking assist wears for the lower limbs. Therefore, before getting into the proposal of the assist wear in this study, we provide a brief background of the most relevant concepts about the biomechanics of human walking.

3.1.1 Walking gait cycles

Fig. 3.1.1 shows a diagram of human walking gait, with some gait terms that will be used

throughout this thesis.

The human walking gait cycle (GC) is typically represented as starting (0%) and ending (100%) at the point of heel strike on the same foot, with heel strike on the opposite foot occurring at approximately 50% of gait cycle [1, 2]. Each gait cycle can be described in the phasic terms of Stance Phase and Swing Phase. The Stance Phase is defined as the interval in which at least one foot is on the ground. This accounts for about 62% of the gait cycle. Generally, Stance Phase is divided into five phases as initial contact, loading response, mid stance, terminal stance and pre swing. Initial contact is an instantaneous point in time (0-2% GC) when the foot contacts the ground. Loading response (2-12% GC) is the phase that the foot comes in full contact with the ground, and body weight is fully transferred onto the stance limb. Also the initial double-limb support occurs in this phase. Mid stance (12-31% GC) represents the first half of single limb support and the terminal stance (31-50% GC) constitutes the second half of single limb support. Pre swing (50-62% GC) is the 2nd double-limb support period and occupies the last 12 percent of stance phase. During this period, the stance limb is unloaded and the body weight is transferred onto the opposite limb.

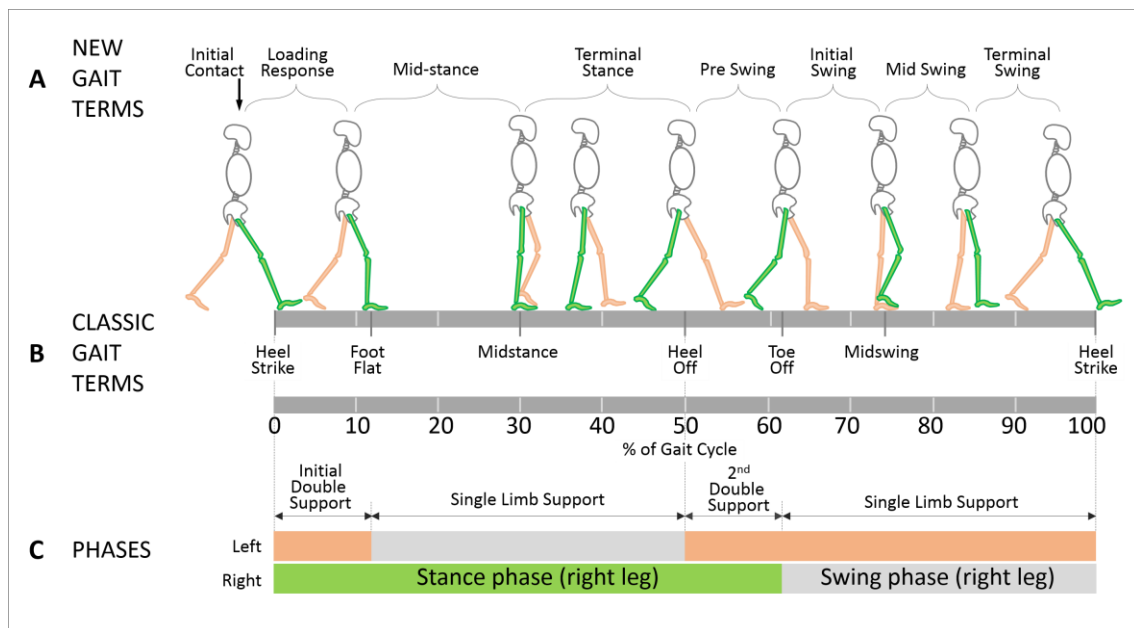


Fig. 3.1.1. Simulation result based on the proposed model.

Swing Phase is defined as the interval in which all portions of the foot are in forward motion in the air, constituting the remaining 38% of the gait cycle. Swing is usually divided into two phases as acceleration to mid swing and mid swing to deceleration. And the swing period can be

divided into three phases, initial swing, mid swing and terminal swing. Initial swing (62-75% GC) begins the moment the foot leaves the ground and continues until maximum knee flexion occurs. Mid swing (75-87% GC) occurs in the second third of the swing period. It begins from the maximum knee flexion and ends when the tibia is in a vertical position. Finally, in the terminal swing (87-100% GC), the tibia passes beyond perpendicular, and the knee fully extends in preparation for heel contact of another gait cycle.

3.1.2 Motion definition of lower limbs

Fig. 3.1.2 (a) shows a description of the human Anatomical Planes, as a Coronal Plane, a Sagittal Plane and a Transverse Plane. The Coronal Plane divides the body into dorsal and ventral (back and front, or posterior and anterior) portions. The Sagittal Plane is a plane parallel to the sagittal suture which divides the body into left and right, and the Transverse Plane divides the body into cranial and caudal (head and tail) portions [3]. Fig. 3.1.2 (b) shows a description of a kinematic model of the human leg in the sagittal plane, which is the dominant plane of motion during human locomotion.

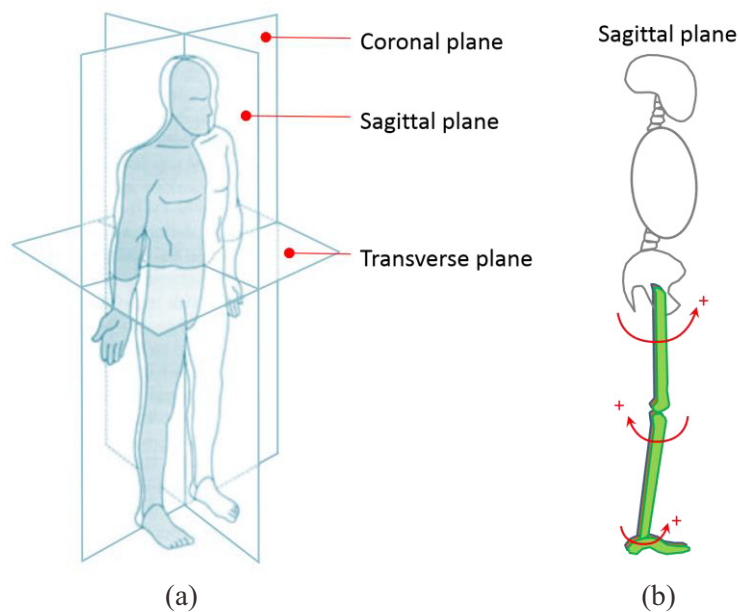


Fig. 3.1.2. (a) Description of the anatomical planes. (b) A kinematic model of the leg with the positive direction of each joint indicated.

Human lower limb can be thought of as a 7 DOF structure, with three rotational DOFs at the hip, one at the knee, and three at the ankle. In this thesis, hip joint motion in the Sagittal Plane is

simply referred to as flexion (positive direction) and extension (negative direction) (Fig. 3.1.2 (b)). Motion in the Coronal Plane is referred to as abduction (away from the center of the body) and adduction. Further, motion in the Transverse Plane is simply referred to as external rotation and internal rotation. These terms will be used throughout the rest of this thesis in describing the kinematic of the assist wear.

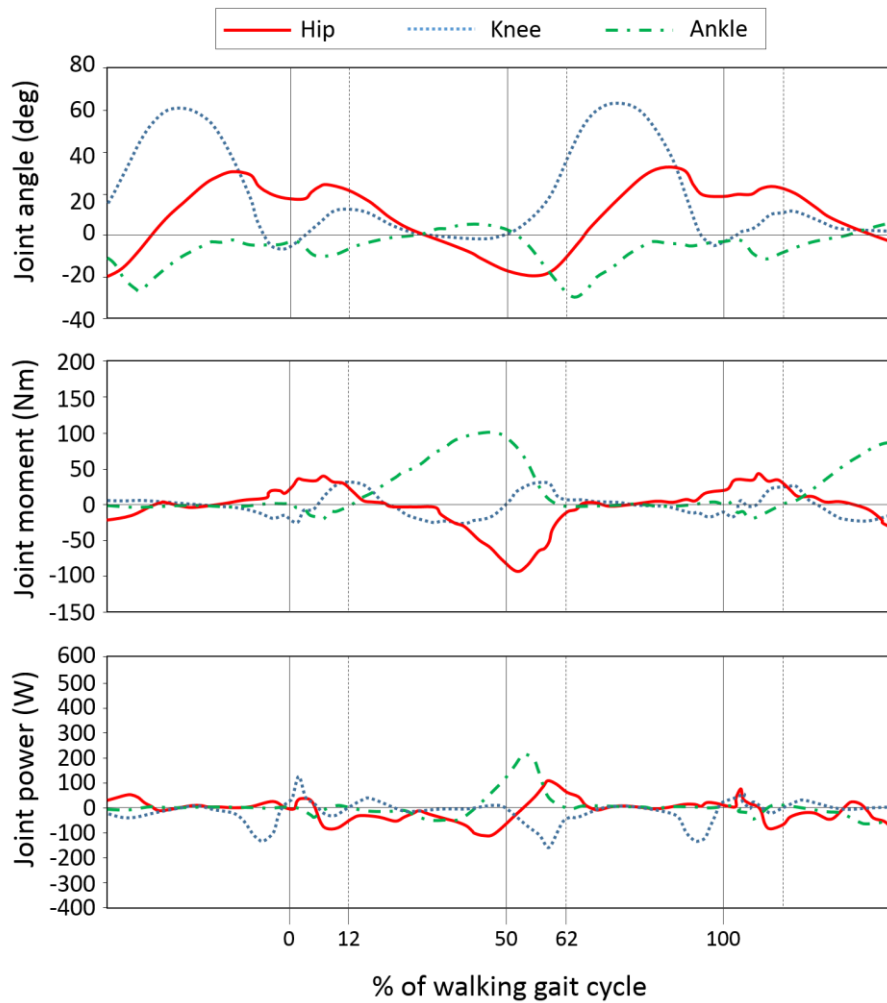


Fig. 3.1.3. Representative angles, moments, and power of the leg flexion/extension joints over the gait cycle. Data are adapted from [4].

3.1.3 Angle, moment and power of lower limb joints

Fig. 3.1.3 shows the joint angle, moment, and power for hip, knee, and ankle flexion/extension motions during level-ground walking in a normal speed which are adapted in [4]. The data may

differ somewhat across subject and condition, but the qualitative nature of the data remains similar [5]-[7]. We can see that, at a normal speed, power at the hip is positive or near zero, power at the knee is predominantly negative, and power at the ankle is evenly split between positive and negative. Therefore, the powered exoskeletons and orthoses developed so far often incorporate means of adding power at the hip, dissipating power at the knee and storing and releasing energy at the ankle using passive elastic structures.

3.2 Proposal of a walking assist wear with PVC gel artificial muscles

For the elderly people, falls are the common and serious problems which are due to multiple factors, such as limitation of joint ROM (range of motion), loss of balance, reduce of muscular strength and so on [8, 9]. In this study, for a preliminary application of PVC gel artificial muscles on walking assistance, we focused on the hip joint motion as it played an important role to control the balance in the stance phase and make an accelerated forward movement with the goal of propelling the body weight forward during the swing phase. A hip joint movement with an extra external assistive force may reduce the muscular activities and make the clearance of the foot big enough to make a step forward to avoid a tumbling during walking.

Fig. 3.2.1 shows the structure of the proposed PVC gel artificial muscles based walking assist wear [10]. It contains three parts: walking motion detector part, assist wear part and the power and controller part. For the assist wear part, several PVC gel artificial muscle modules are arranged along the top of the thigh, connected by some flexible wires and belts. And both sides of the assist wear are fastened at the waist and knee. This structure can be considered as some extra external artificial muscles connected with the biological muscles that around the hip joint in parallel. These artificial muscles could be capable to enhance the healthy muscles or supply the functions that lost in the weakened muscles.

The walking motion detector part is to detect the gait cycle and the power and controller part is to operate the assist wear according to the status of the walking motion. Since the PVC gel artificial muscles have a low impedance without a DC field, the whole assist wear could be flexible and easy to fit the body without impeding the natural motion by this structure. Also, it is easy to adjust the length of the wear by adjusting the length of the belts to fit the body of individuals and easy to put on and take off by oneself.



Fig. 3.2.1. Structure of the proposed walking assist wear with PVC gel artificial muscles.

3.3 Walking assistance method with the assist wear

The aim of our assist wear is to assist the lower limb during the swing phase. The phase is between the toe off phase and the heel strike phase. Fig. 3.3.1 and Table 3.3.1 shows the variation of the activities of the main upper leg muscles during the swing phase. As can be seen that several of the muscles start to work from the moment when the toe leaves the ground and reaches a peak in the initial swing phase. That is, when the toe leaves the ground at the pre swing phase, the flexor group (such as rectus femoris muscle, gracilis muscle and sartorius muscle) of the hip joint works and provides some tensile forces to realize a flexion movement as to step forward. Therefore, in this study, at the moment that the toe leaves the ground, the assist wear generates an extra tensile force outside to support the motion of the hip joint so as to reduce the burden of the muscles in the flexor group, as shown in Fig. 3.3.2.

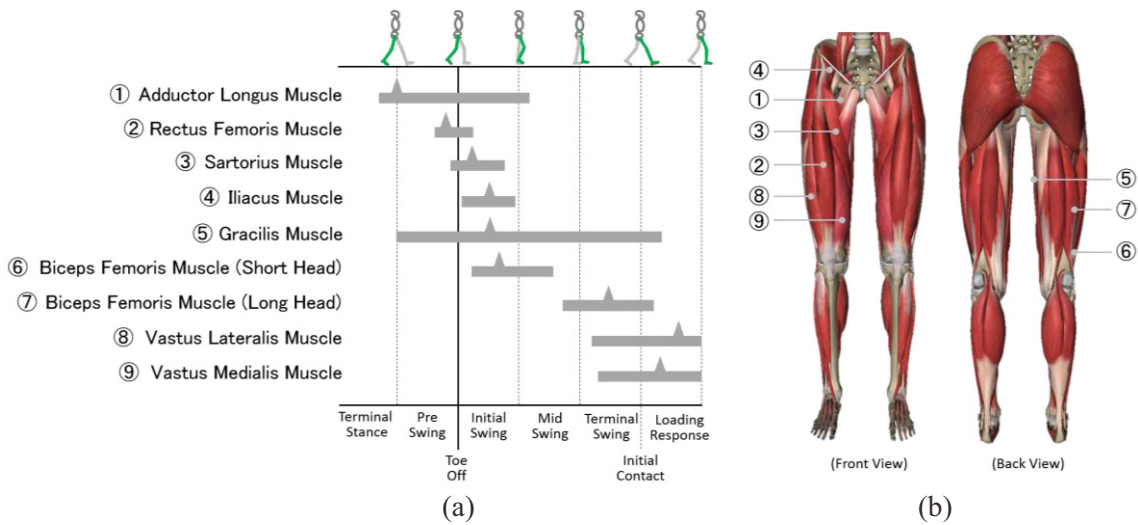


Fig. 3.3.1. (a) Muscular activities variation during swing phase (adapted from [1]). (b) Muscles of the leg.

Table 3.3.1. Muscular activities variation during swing phase (%GC) (adapted from [1])

Muscles	Start moment	Peak value moment	End moment
① Adductor Longus Muscle	46	50	77
② Rectus Femoris Muscle	57	59	65
③ Sartorius Muscle	60	65	71
④ Iliacus Muscle	63	69	74
⑤ Gracilis Muscle	50	69	4
⑥ Biceps Femoris Muscle (Short Head)	65	71	82
⑦ Biceps Femoris Muscle (Long Head)	82	93	5
⑧ Vastus Lateralis Muscle	90	8	16
⑨ Vastus Medialis Muscle	91	4	16

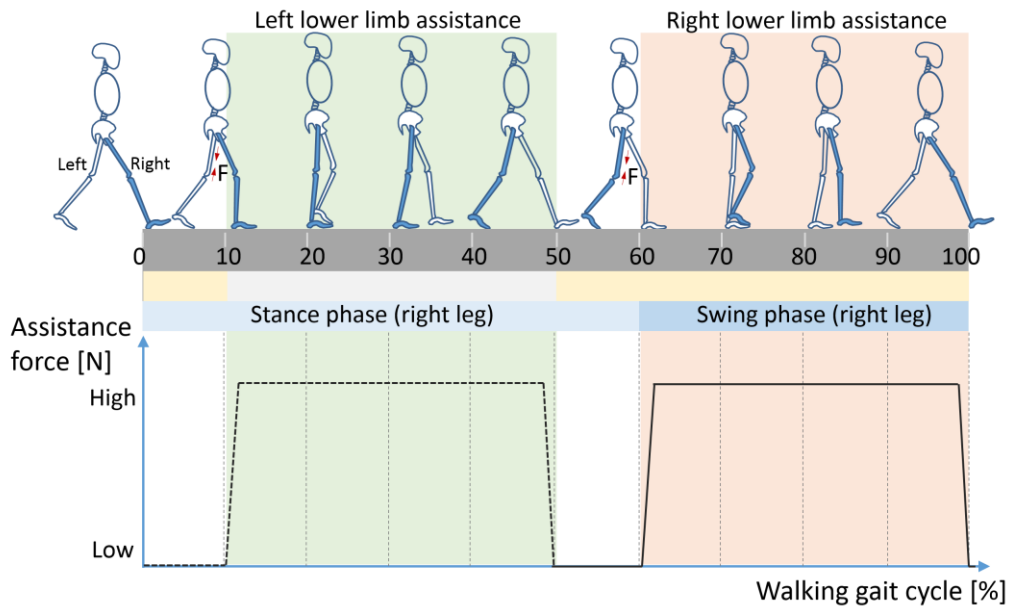


Fig. 3.3.2. Method of walking assistance in walking gait cycles.

That is, when the wearer raises the left foot from the pre swing phase to the initial swing phase, the controller changes the applied electric field to the left part of the assist wear to make a contraction movement and provide a tensile force. And a moment will be created around the hip joint to assist the flexion motion due to the offset of the tensile force from the hip joint center. Then when the left foot steps to the ground at the terminal swing phase, the applied electric field is changed to make an extension movement and decrease the output force of the left part of assist wear to make it easy to extend the left limb. As the same manner, when the wear raises the right foot from the pre swing stance phase to the initial swing phase, the controller changes the applied electric field to the right part of the assist wear to provide a force to the thigh to assist the flexion motion of the right hip joint. Then when the right foot steps to the ground at the end of swing phase, the electric field is changed to decrease the output force of the right part of assist wear to make it easy to extend the right limb.

We expect that the assist wear would be able to lighten the burden of the human muscles and increase the length of the pace during a daily walking.

3.4 Chapter summary

PVC gel artificial muscles have many positive properties which indicates a great potential to construct a walking assist wear for a daily life walking support.

This Chapter proposed a lightweight wearable assistive wear using PVC gel artificial muscles, according to the biomechanics of walking.

The assist wear is to assist the lower limb during the swing phase, from the moment that the toe leaves the ground, the assist wear generates an extra tensile force outside to support the motion of the hip joint until the moment of the heel initially contact to the ground, so as to reduce the burden of the leg muscles in the flexion motion.

Reduction of the burden of the flexor group muscles and increase of the pace length during a daily walking could be expected.

References

- [1] Jacquelin Perry, Judith M. Burnfield, *Gait Analysis: Normal and Pathological Function*, Second Edition, ISBN: 9784263213988.
- [2] <http://www.gla.ac.uk/t4/~fbls/files/fab/tutorial/anatomy/hfgait.html>.
- [3] https://en.wikipedia.org/wiki/Anatomical_plane
- [4] Y. Ehara and S. Yamamoto, *Introduction to Body-Dynamics: Analysis of Gait and Gait Initiation*, 2002, ISBN: 978-4-263-21532-6.
- [5] J. Linskill. (2005). CGA Normative Gait Database, Limb Fitting Centre, Dundee, Scotland [Online]. Available: <http://guardian.curtin.edu.au/cga/data>
- [6] A. J. Van DenBogert, "Exotendons for assistance of human locomotion," *Biomed. Eng. Online*, vol. 2, p. 17, 2003.
- [7] Wang, M., Flanagan, S.P., Song, J., Greendale, G.A., Salem, G.J. Relationships among body weight, joint moments generated during functional activities, and hip bone mass in older adults, *Clinical Biomechanics*, 21 (2006) 717-725.
- [8] Albert B. Schultz, *Mobility impairment in the elderly: Challenges for biomechanics research*, *J. Biomechanics*, Vol.25, No.5, pp.519-528, 1992.
- [9] Kyle C. Moylan, Ellen F. Binder, *Falls in Older Adults: Risk Assessment, Management and Prevention*, *The American Journal of Medicine* (2007) 120, 493-497.
- [10] Y. Li and M. Hashimoto, "A Proposal of a Light-weight Walking Assist Wear using PVC Gel Artificial Muscles", *The 2015 IEEE International Conference on Robotics and Automation (ICRA 2015)*, Seattle, USA, pp.2920-2925, 2015.

Chapter 4

Design and prototyping of the proposed walking assist wear

Chapter 4 Design and prototyping of the proposed walking assist wear

To design a walking assist wear using PVC gel artificial muscles, we have to determine an appropriate size to provide an enough displacement to satisfy the length change of the assist wear during walking, and to provide an assistive force that big enough for creating moments to support the body.

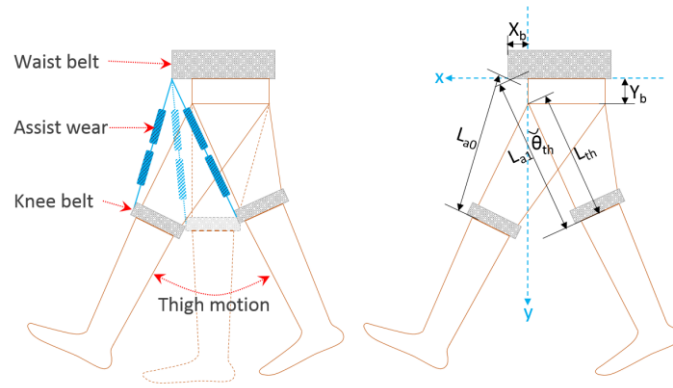
This Chapter will focus on the design and prototyping of the walking assist wear. The challenge of constructing an assist wear using PVC gel artificial muscles is to make the assist wear being robust, compact and lightweight. Moreover, smart and cost effective walking motion detector and controller should be developed.

4.1 Actuation modules

To design a prototype of assist wear using PVC gel artificial muscles, we have to consider the following factors: the output force and displacement to provide a sufficient assistance, the size, shape and weight to make a good fit and comfortable wear, the structure to make a robust assist function, and the insulation treatment for the safety of the wearer.

4.1.1 Specification design of PVC gel artificial muscles

The assist wear is aiming to assist the flexion motion of the hip joint. On the one hand, as shown in Fig. 4.1.1 (a), the length of the assist wear will be changed due to the angle variation of the thigh during walking. This should be realized by the contraction and expansion movement of PVC gel artificial muscles. Therefore, the displacement of the artificial muscles should satisfy the slack (ΔL) of the assist wear. Fig. 4.1.1 (b) shows the results of the amount of slack under different conditions. In this study, considering about 10 mm slack happens to the walking assist wear from the beginning of extension motion to the end of the extension motion and taking into account the average length of human upper leg, we set the displacement of the assist wear is about 20 mm.



L_{a0} : Initial length of assist wear at the terminal swing phase;
 L_{a1} : Length of assist wear during walking;
 L_{th} : Length of thigh (between top tibia bone and Greater trochanter);
 θ_{th} : Angle of thigh during walking;
 X_b : Thickness of edge profile of waist belt;
 Y_b : Height between Greater trochanter and waist belt.

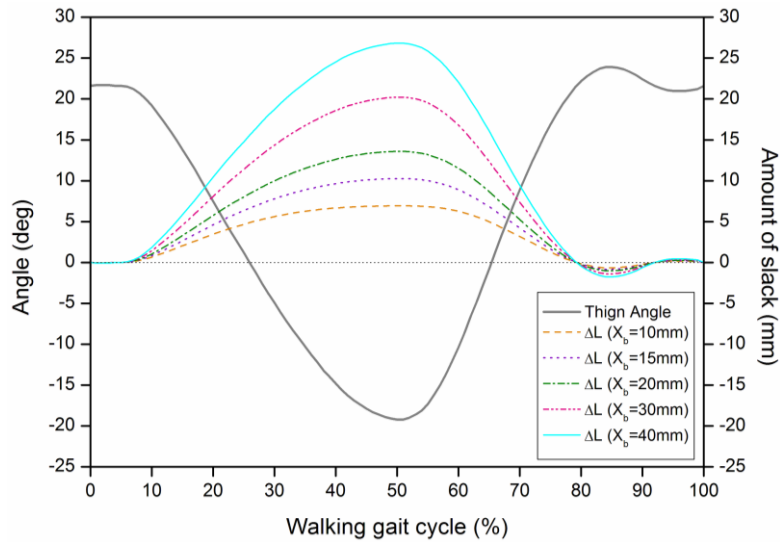
$$\Delta L = L_{a1} - L_{a0}$$

$$L_{a1} = \sqrt{(L_{th} \sin \theta_{th} - X_b)^2 + (L_{th} \cos \theta_{th} + Y_b)^2}$$

$$L_{a0} = \sqrt{(L_{th} \sin \theta_{a0} - X_b)^2 + (L_{th} \cos \theta_{a0} + Y_b)^2}$$

θ_{a0} : Angle of thigh at the end of terminal swing phase.

(a)



(b)

Fig. 4.1.1. (a) Model of human body with the assist wear in the sagittal plane, the length of the assist wear is varying during walking gait cycles. (b) The results of the slack (ΔL) generated during a walking gait cycle with different thickness of the edge profile (X_b) of the waist belt while the height between the Greater trochanter and waist belt (Y_b) is about 20 mm.

On the other hand, for the output force determination, considering the maximum internal hip torque occurs at the terminal stance phase is about 1.0Nm/kg (70Nm for a weight of 70kg) at the pre-swing phase during walking [1, 2]. For the prototype, we consider generating a moment around the hip joint over 10% of the maximum internal hip torque and determine the maximum generation force of the assist wear is about 80N (corresponding to 8Nm as a 10cm offset between the force and the hip joint center for an average thigh size).

To efficiently design the assist wear, we determine the maximum applied DC voltage as 400V. Then the displacement is almost proportional to the number of stacked layers and the force magnitude depends on the area of the single-layer structure artificial muscle. Based on the conditions mentioned above, the area of the single layer artificial muscle is about 0.001 m² and the height of the total artificial muscle is about 200 mm according to the basic characteristics of PVC gel artificial muscles described in Chapter 2.

4.1.2 Structure of the actuation modules

To design the PVC gel artificial muscles for the walking assist wear, it is necessary to avoid a break during walking. As we described in sections 2.4 and 2.5 that the structure of a multilayered PVC gel artificial muscle is just stacked up by the single-layer structure units. If we use the force generated by the contraction movement of the artificial muscles, it would cause a separation among the layers when a certain external stretching force applied due to the non-uniform structure of each layer of artificial muscles. Therefore, in order to avoid the break of the artificial muscles, we used a stretching-type structure unit proposed in section 2.5 to make the assist wear much more robust to external forces (Fig. 4.1.2) [3].

As shown in Fig. 4.1.2 (a), the unit consists of a container and a slide frame with a connector. The PVC gel artificial muscle is encased into the units. When the DC field is applied, the PVC gel artificial muscle contracts and leads the slide frame upward. Then turn off the DC field when it is necessary to generate a tensile force to support the motion during walking.

Furthermore, to reduce the weight of the unit structure and boost the fitness of the assist wear, we introduced the structure as shown in Fig. 4.1.2 (b). We designed the interface of the actuation module as a curved surface shape to fit the body curve according to the average size of the thigh circumference [4, 5] (Fig. 4.1.3 (c)). And an insulating sheet was fixed on the surface for personal safety and protection of the artificial muscles.

As shown in Fig. 4.1.2 (c), by connecting the stretching-type structure units with flexible stainless wires that we can get the flexible actuation modules.

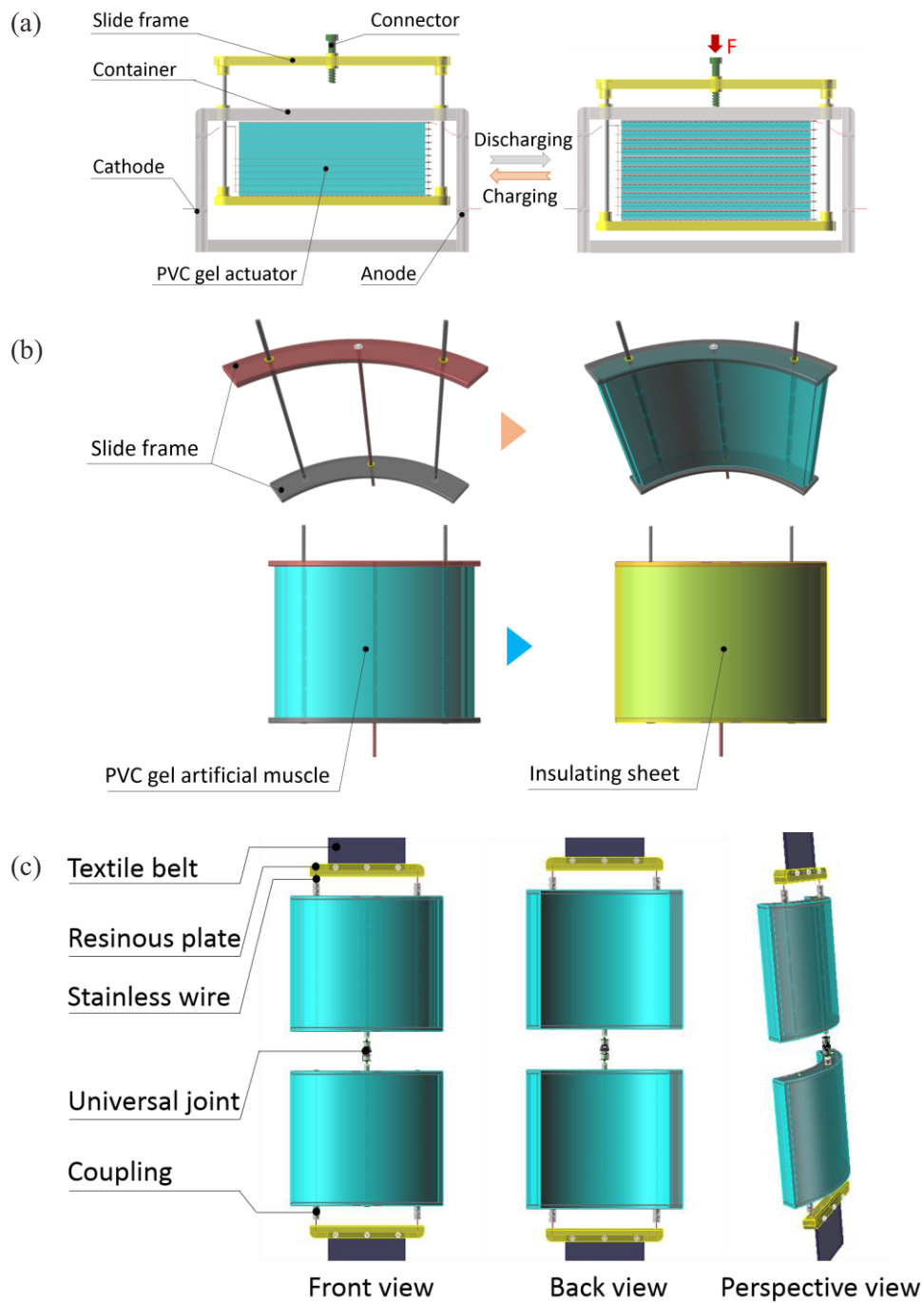


Fig. 4.1.2. Structure of the actuation modules. (a) Mechanism of the movement and generation force. (b) An improved structure to minimize the weight and to fit the body line using a curved surface shape. (c) Designed actuation modules.

4.1.3 Structure of electrodes and wiring

The artificial muscle makes contraction and expansion movement with sliding between the anode electrodes and the shafts. To minimize the effect of friction, we introduced two types of anode mesh electrodes with different diameters of the through holes (Fig. 4.1.3 (a)). The electrodes with the smaller holes were arranged every tens of stacked layers of the electrodes with the bigger holes (Fig. 4.1.3 (b)). Therefore, just several of the electrodes would have a sliding motion with the shafts. By this way, not only the friction between the electrodes and shafts could be minimized to make a fast response actuation but also produce few heat during actuation which might have a negative effect on the characteristics. Fig. 4.1.3 (c) shows the structure and overview of the electrodes used in this study.

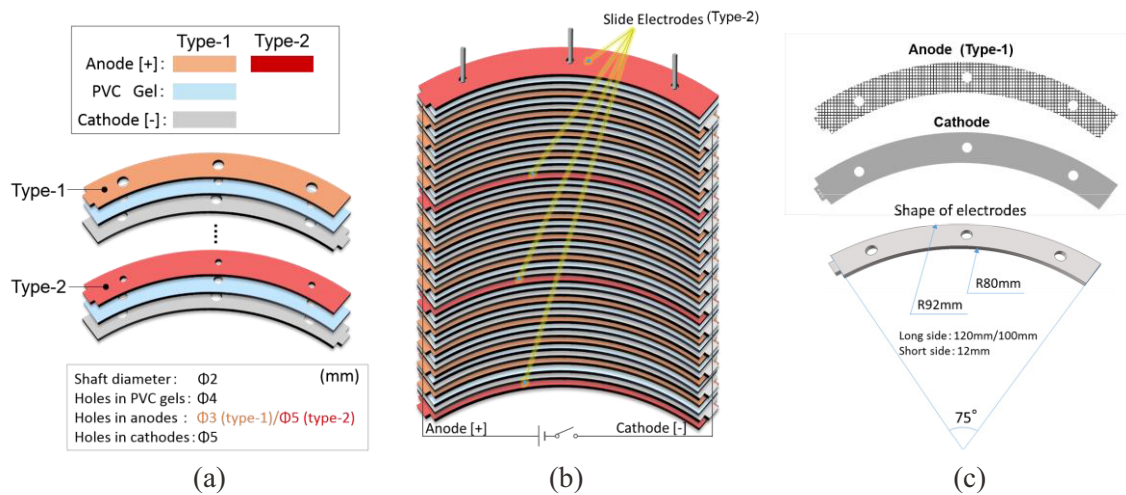


Fig. 4.1.3. Structure of the electrodes. (a) Components of artificial muscles with different through holes. (b) Illustration of the slide electrodes in a multilayered structure. (c) Structure and overview of the fabricated electrodes used in this study.

Since the DC field is simultaneously applied to each layer of the artificial muscles, we connect the anode electrode and cathode electrode of each layer together using wires, respectively. The traditional method (Fig. 4.1.4 (a)) of wiring for a multilayered artificial muscle using a soldering connection that each layer connects to a wire with a welding manner. This could make the artificial muscles be bulky and uneasy to handle when making the actuation modules, especially when a big number of stacked layers needed. In this study, we proposed a new approach of wiring for the multilayered artificial muscles, called as a clinched-wire through connection, as shown in Fig. 4.1.4 (b). This makes the wiring be more compact and much lighter than the

former method, also makes an easy handle of the multilayered artificial muscles (Fig. 4.1.4 (c)). For ensuring the connection of the wires and electrodes, we used three wires connected together, two of which are running through the electrodes in a crossed way (like an X-shape) and the rest one is going through the electrodes straightly in a line. And we investigated the connection state and durability of this new wiring method using several 5-layer PVC gel artificial muscles. We evaluated the displacement, current and output force (using a load cell) variation under different applied DC voltages. Fig. 4.1.5 shows the results of the comparisons between the traditional method and the proposed one. The artificial muscle with the new wiring almost has the same characteristics of the artificial muscle that using the traditional method. Also there is no break happens during a 10 thousand DC field driven (320V) in 2Hz.

As we can see that the proposed wiring method has no influence on the characteristics of PVC gel artificial muscles. Therefore, it is effective to use it in fabrication of the multilayered artificial muscles for the walking assist wear.

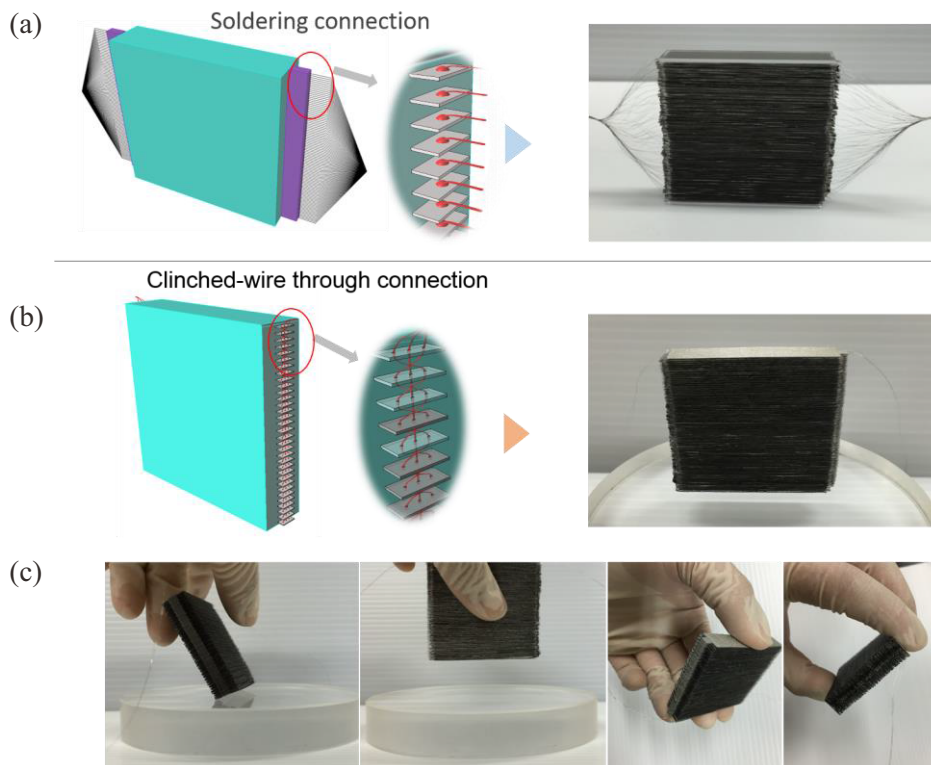


Fig. 4.1.4. (a) Traditional method of wiring for a multilayered artificial muscle, with a fabricated sample (80-layer). (b) Proposed method of wiring for a multilayered artificial muscle, with a fabricated sample (80-layer). (c) Photographs show the easy handle of a 80-layer PVC gel artificial muscle with the new wiring.

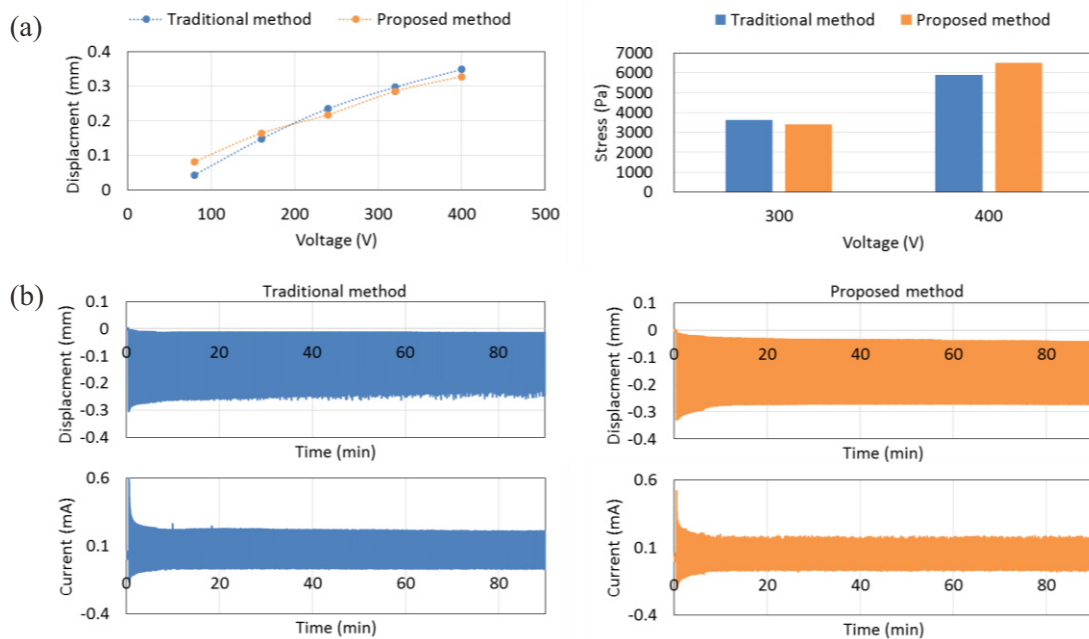


Fig. 4.1.5. Results of the comparisons between the traditional wiring method and the proposed one. (a) Displacement comparison. (b) Output stress comparison (measured by a load cell). (c) Durability variation of displacement and current.

4.1.4 Fabrication of actuation modules

The fabricated PVC gel artificial muscles based actuation modules are shown in Fig. 4.1.6 (a). We divided them into two module units (Fig. 4.1.6 (c)) which are connected with a universal joint. The PVC gel membrane in each layer was about 0.2 mm in thickness, a curve shape with 120 mm and 100 mm length in the long side and short side, respectively. The mesh size of the stainless steel mesh anode was 100 (each inch has 100 wires), with a thickness of about 0.18 mm. And a 0.01 mm thick foil electrode was used as the cathode. The size of the electrodes is the same as the PVC gel membranes.

The artificial muscle makes contraction and expansion movement with sliding between the anode electrodes and the shafts. Fig. 4.1.6 (b) shows the two types of anode mesh electrodes with different through holes to minimize the effect of friction between the electrodes and shafts to make a fast response actuation and to produce few heat during actuation to prevent a negative effect on the characteristics. To ensure the safety of the wearer and to avoid the artificial muscles being contaminated, we fixed some 0.05 mm thick Teflon sheets around the frame of the actuation modules for the insulation and protection (Fig. 4.1.6 (d)). The type and thickness

of the cover sheet can be changeable in a practical use.

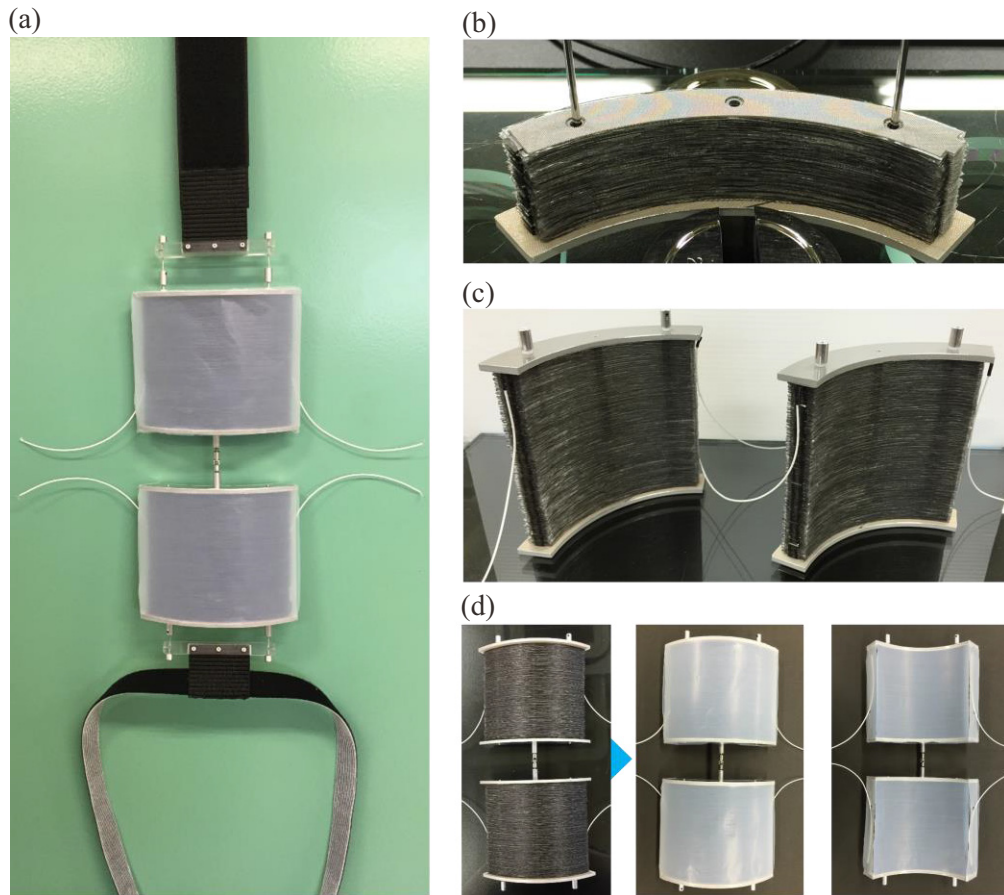


Fig. 4.1.6. The fabricated prototype of actuation modules with PVC gel artificial muscles. (a) Overview. (b) Two types of anode mesh electrodes with different holes to minimize the friction and heat with the slide shafts. (c) Photographs of the module units. (d) Photographs of the connected module units covered with some Teflon insulation sheets (0.05mm thick).

4.2 Walking motion detector

In this study, we have to detect the gait cycle of the wearer during walking to control the output force of assist wear. We have to make the motion detector be smart and cost effective. This section will describe the design and fabrication of the walking motion detector in detail.

4.2.1 Sensors selection and calibration

In this study, we chose the FlexiForce[®] force sensors (Tekscan, Inc.) [6] to detect the gait cycles. Because the FlexiForce[®] force sensors (Fig. 4.2.1 (a)) are very thin (0.2 mm in thick), flexible, with a high response rate (<20μs), good accuracy (±3%) with a large range of measurement of loads and a low cost which can be easily integrated into the insoles for the force measurement.

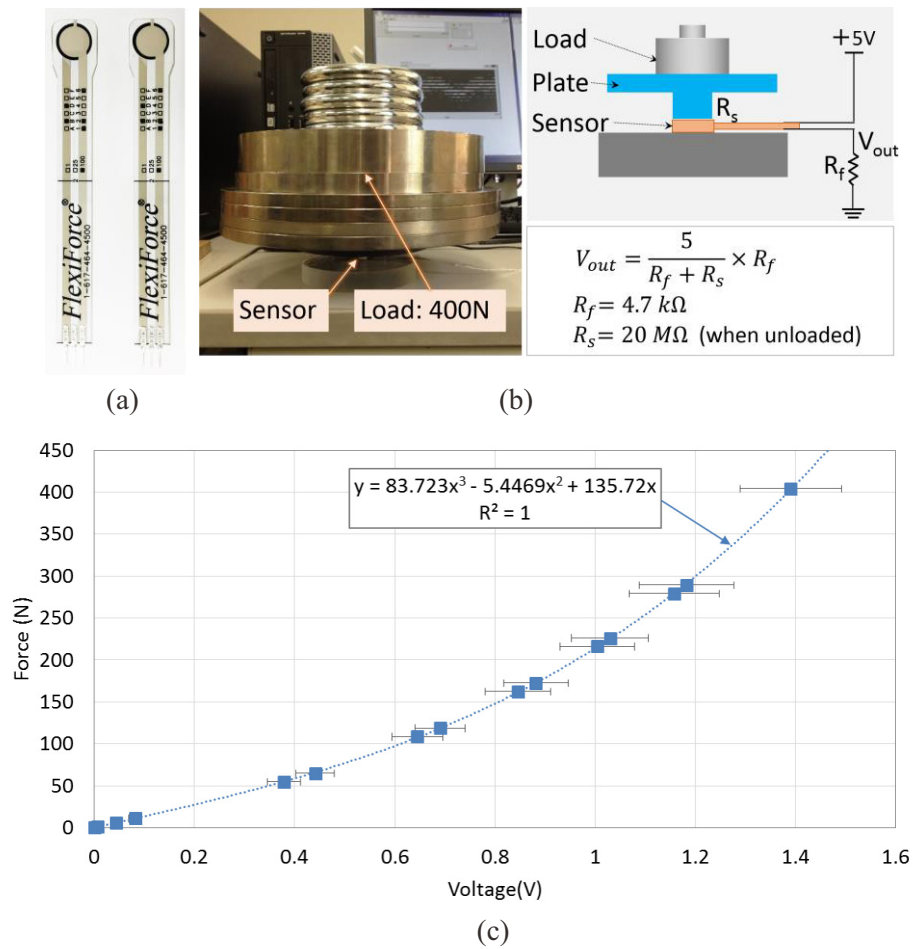


Fig. 4.2.1. Calibration of the force sensors. (a) Photograph of the Flxiforce[®] force sensors. (b) Method of calibration. (c) Results of calibration under different applied loads.

Fig. 4.2.1 (b) shows the calibration of the sensors. The force sensor is a variable resistor R_s which is connected with a reference resistor R_f (4.7 kΩ) in series. We detect the voltage of the reference resistor V_{out} to measure the change of the pressure on the sensor. When there is no

pressure applied, the resistance of the force sensor is very high (up to 20 M Ω) so that the voltage of the R_f is almost zero, and when there is pressure applied on the force sensor, the voltage of the R_f increases. The result of the calibration is shown in Fig. 4.2.1 (c). The relation between the V_{out} and the applied force can be represented by a cubic polynomial as shown in the figure, with a determination coefficient (R^2) of 1.

4.2.2 Design and fabrication of walking motion detector

We use the force sensors to integrate into the insole to make the walking motion detector. Considering the sequence change of the contact area between the foot and ground during the stance phase [7] (Fig. 4.2.2 (a)), we use 4 sensors on each foot to make the insole as shown in Fig. 4.2.2 (b). The accurate position of each sensor is determined based on the average size of skeletal structure of the foot in human body dimension databases [4, 5], as shown in Fig. 4.2.2 (c) and Table 4.1.1. Fig. 4.2.2 (d) shows the structure of the insole. The sensors are sandwiched by some stainless plates (thickness of 1 mm), with diameters of 9.5 mm and 15 mm, respectively. And the stainless plates are fixed in some natural rubber sheets (thickness of 1 mm) by adhesive. Fig. 4.2.2 (e) shows the fabrication process and overview of the fabricated walking motion detector on the most right side. The fabricated insoles are flexible so that they can make a walking be comfortable.

The moment when the wearer raises to make a step from the pre swing phase to the initial swing phase can be detected when the force of the sensor that set at the position of big toe becomes a minimal value. And by using the status of the other sensors, we can get a more accurate estimation of walking gait cycle and also the center of gravity can be estimated to support the assistance.

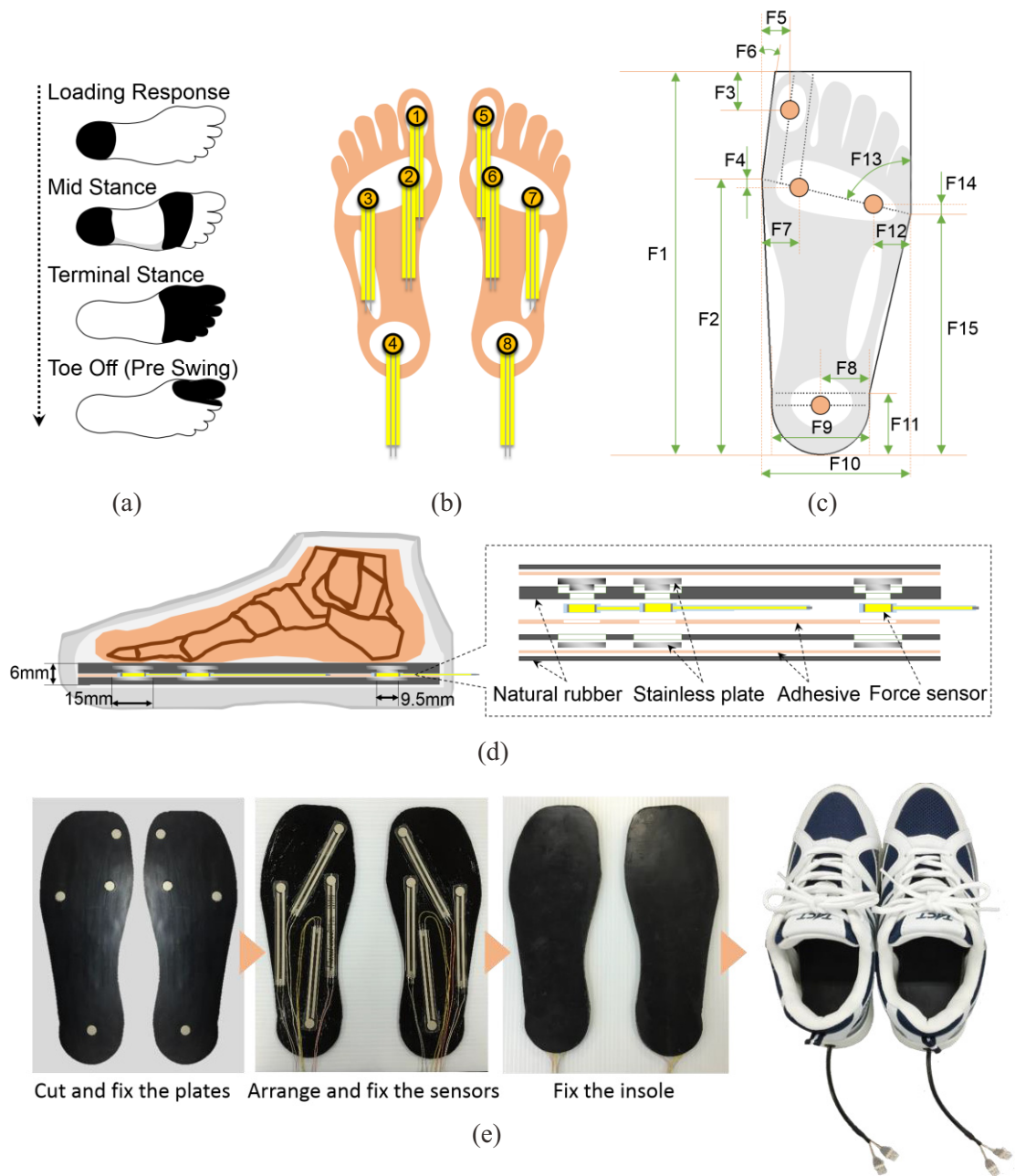


Fig. 4.2.2. Fabrication of the walking motion detector. (a) The contact area changes between the foot and the ground during the stance phase. (b) Arrangement of sensors. (c) Definition of the measurement terms of foot. (d) Structure of the insole with force sensors. (e) Process of fabrication.

Table 4.2.1 Dimension of each portion of foot (items from Fig. 4.2.2 (c)).

Measurement item	For male (cm)	For female (cm)
F1	25.00	23.00
F2	18.00	16.80
F3	2.48	2.22
F4	0.57	0.53
F5	1.81	1.80
F6	7.00° (deg)	9.43° (deg)
F7	2.43	2.18
F8	3.20	3.15
F9	6.40	6.10
F10	9.74	8.74
F11	4.00	3.70
F12	2.43	2.19
F13	76.72° (deg)	76.30° (deg)
F14	0.57	0.53
F15	15.70	14.67

4.3 Controller

In this study, we need a controller that can receive and convert the data of the eight sensors and process the output DC field signals in real time. We use a computer myRIO (LabVIEW, NI) for data acquisition and analog-digital conversion.

4.3.1 NI myRIO and its calibration

The NI myRIO-1900 provides analog input (AI), analog output (AO), digital input and output (DIO), audio, and power output in a compact embedded device. The NI myRIO-1900 connects to a host computer over USB and wireless 802.11b, g, n. Fig. 4.3.1 shows the overview and the arrangement and functions of NI myRIO-1900 components [8].

Three connectors including eight single-ended analog inputs (MXP A/B), six analog outputs (MXP A/B and MSP C) and forty digital I/O lines overall with support for SPI, PWM out, quadrature encoder input which is capable to do the application in this study. Furthermore, the RT and FPGA capabilities along with onboard memory and built-in WiFi allow us to deploy applications remotely and run them without a remote computer connection which could make

the system much more compact and simple in future.

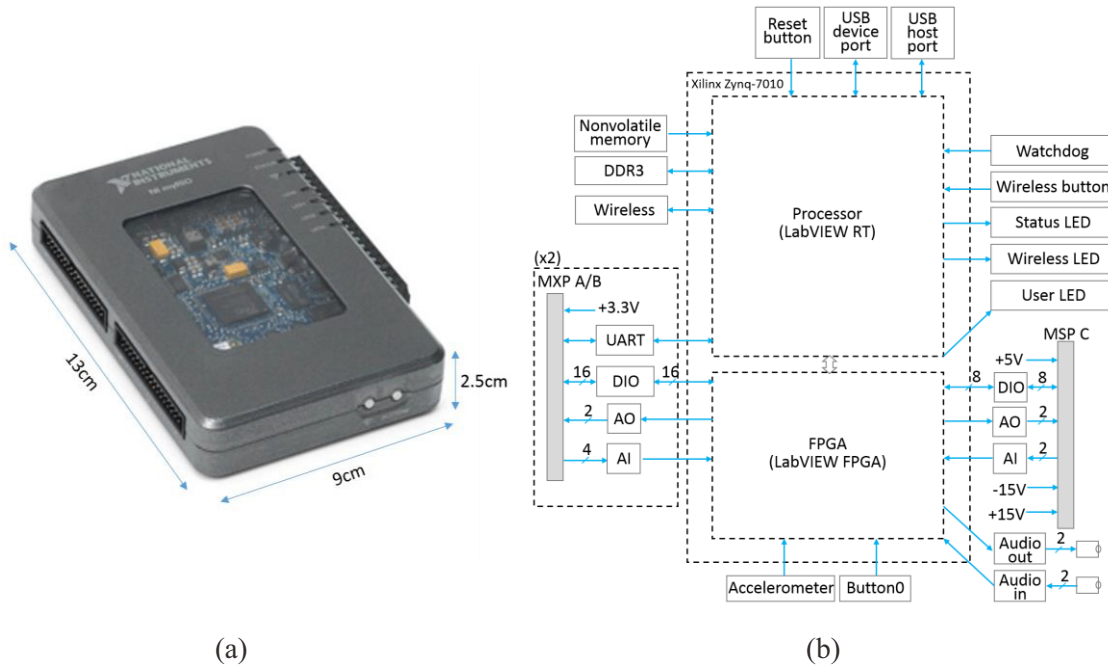


Fig. 4.3.1. (a) Overview of the NI myRIO-1900 device. (b) NI myRIO-1900 hardware block diagram.

In this study, we primarily use the eight analog input channel (MXP A/B in Fig. 4.3.1 (b)) to acquire the data of the insole force sensors to analysis the walking gait cycle change during walking, and use the analog input channel (MSP C in Fig. 4.3.1 (b)) to measure the current of the artificial muscles. Therefore, we calibrated the analog input channel MXP and analog output channel MSP.

MXP connectors A and B have four single-ended analog input channels per connector, AI0-AI3 and BI0-BI3, which can be used to measure 0-5V signals. MSP connector C has two high-impedance, differential analog input channels, CI0 and CI1, which can be used to measure signals up to ± 10 V. We used a function generator (Agilent 33250A) to give some 0-1V and 0-9V sine and square wave signals to the input channels of MXP A/B and MSP C, respectively.

Fig. 4.3.2 shows the results of the calibration. We got a measurement accuracy of about 90% when the input signal is below 0.01mV and a measurement accuracy over 95% when the input signal is over 0.05mV for the channels of MXP A and B, with an average standard deviation of below 1%. And we obtained a measurement accuracy of about 90% when the input signal is below 0.02mV and a measurement accuracy of over 95% when the input signal is over 0.05mV,

with an average standard deviation of about 2%. We think that the measurement accuracy, along with a 667MHz processor speed are sufficient for performing the tasks in our study.

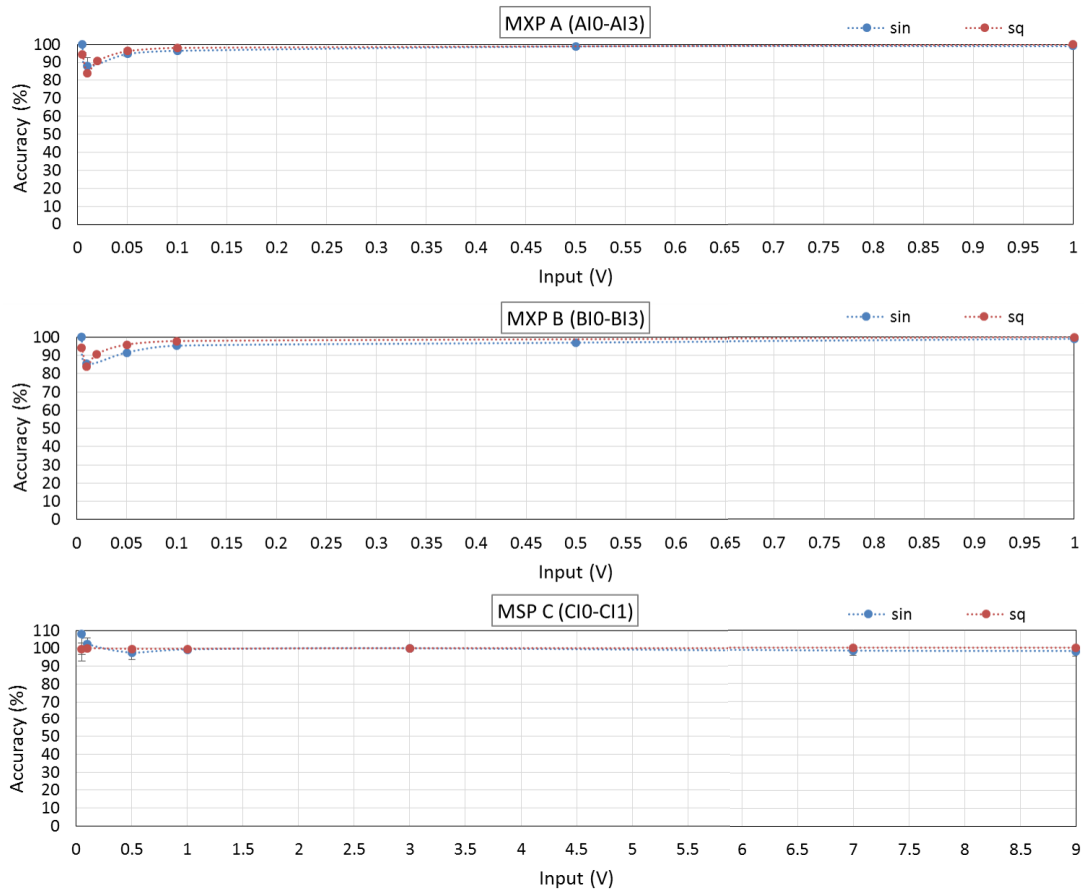


Fig. 4.3.2. Results of calibration of the analog input (MXP A/B) and analog output channels (MSP C).

4.3.2 Control system construction

The structure of the walking assistance system (Fig. 4.3.3 (a)) consists of three parts of gait cycles detection, operation decision and DC field control. The controller part receives the data of the force sensors and estimate the walking status and operate the assist wear according to the status of the walking gait.

The output voltage is amplified by a high voltage amplifier. The fabricated control system is shown in Fig. 4.3.3 (b). The control system is powered by a 12V battery. The whole weight of the power and controller is about 800g.

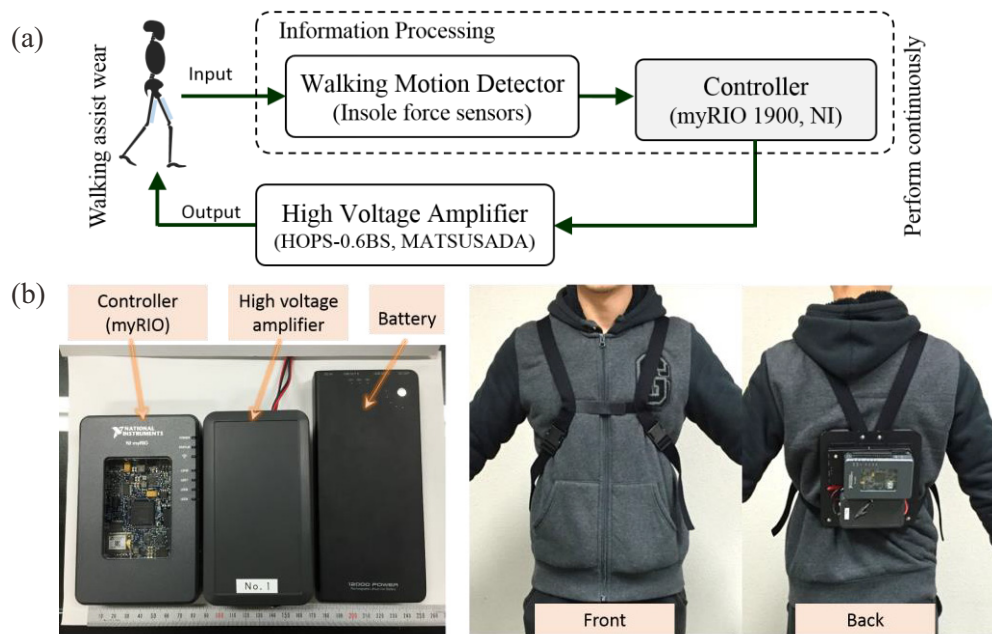


Fig. 4.3.3. Control system of the walking assist wear. (a) System structure. (b) Overview of the controller system.

4.4 Prototype of the PVC gel artificial muscles based walking assist wear

Fig. 4.4.1 shows the designed 3D model and the real fabricated prototype of the walking assist wear with PVC gel artificial muscles. The total weight of the prototype, not including the mass of the shoes and power source, weighs approximately 600 g. As we can see that the assist wear is compact, flexible and has a good fit to the wear's leg. Besides, the structure and interface are simple and the length of the assist wear can be easily adjusted to fit the leg of each individual. Fig. 4.4.2 shows some photographs of several basic motions of an elderly subject (over 60 years) when wearing the assist wear. The assist wear may not impede the natural movements of the wearers even in the directions that no extra assistances are needed, can be wore like a part of clothing for the wearers.



Fig. 4.4.1. Prototype of the walking assist wear with PVC gel artificial muscles. (a) Overview of a 3D model of the prototype. (b) Mechanism of assistance. (c) Overview of the real fabricated prototype, wearing on a model.

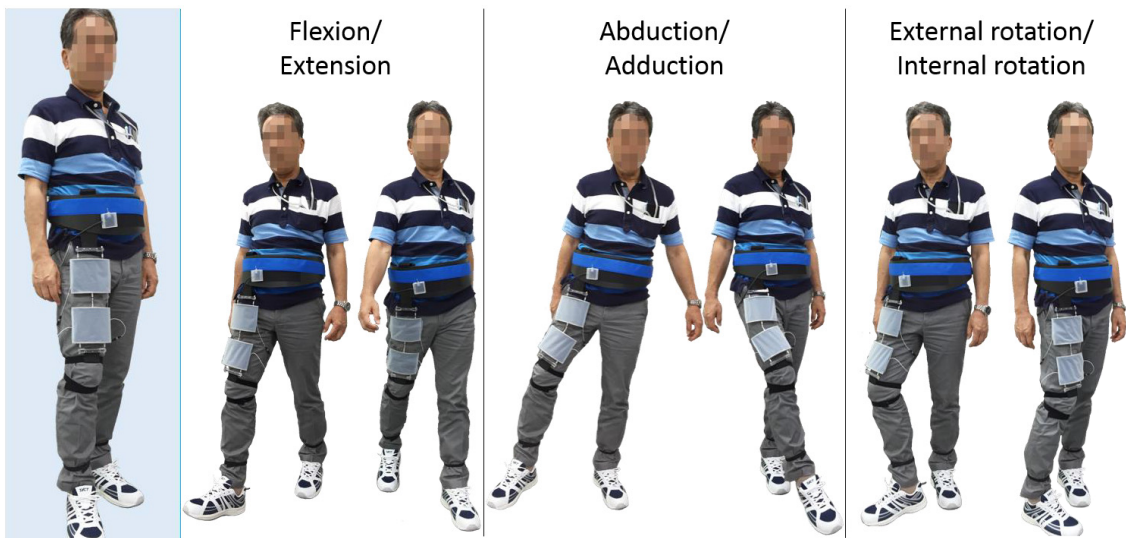


Fig. 4.4.2. Photographs of several basic motions of an elderly subject with the fabricated prototype of assist wear.

4.5 Chapter summary

This Chapter described the design and prototyping of the walking assist wear using PVC gel artificial muscles. The design should deal with the challenge of making the assist wear being robust, compact and lightweight. And making the walking motion detector and controller be smart and cost effective.

For providing an assistance over 10% of the maximum moment on the hip joint during walking, we set the output force of the assist wear as 80N, with a displacement of about 20mm.

A stretching-type structure was introduced to make the assist wear be robust to avoid a break that could be happened among the stacked layers of PVC gel artificial muscles.

Some improvements on the actuation modules, such as a frame-only structure, a curved surface shape and a compact wiring makes the assist wear be more compact, much lighter and better in fitting human body.

Several flexible thin force sensors integrated into the insoles according to human foot skeleton structures, making the walking motion detector be smart and cost effective.

A portable computer NI myRIO was adopted to make the controller be multifunctional and cost effective.

The fabricated prototype weighed about 0.6kg, demonstrated a good fitting to human body, allowed the wearer moving freely in all directions which liked wearing a clothing.

References

- [1] Haggerty M., Dickin DC., Popp J., Wang H., The influence of incline walking on joint mechanics, *Gait & Posture*, 39 (2014) 1017-1021.
- [2] Wang, M., Flanagan, S.P., Song, J., Greendale, G.A., Salem, G.J. Relationships among body weight, joint moments generated during functional activities, and hip bone mass in older adults, *Clinical Biomechanics*, 21 (2006) 717-725.
- [3] Y. Li and M. Hashimoto, “PVC gel based artificial muscles: Characterizations and actuation modular constructions”, *Sensors and Actuators A-Phys.*, Vol 233, No. 1, pp.246-258, 2015.
- [4] National Institute of Technology and Evaluation, Human Characteristics Database, 2002. Available: <http://www.tech.nite.go.jp/human/jp/contents/cindex/database.html>
- [5] M. Kawachi and M. Mochimaru, 2005 AIST Human Body Dimension Database, National Institute of Advanced Industrial Science and Technology, H16PRO 287.
- [6] <https://www.tekscan.com/product-group/embedded-sensing/force-sensors>.
- [7] Barnett CH., The phases of human gait, *Lancet*, 271 (1956) 617-621.
- [8] NI myRIO-1900 User Guide and Specifications, National Instruments, 2013.

Chapter 5

Characterization and performance of the fabricated walking assist wear

Chapter 5 Characterization and performance of the fabricated walking assist wear

A prototype of PVC gel artificial muscles based walking assist wear was designed and fabricated, the effectiveness of the proposed system should be investigated. To evaluate whether the characteristics are consistent with that of the design, we measured the basic characteristics of the fabricated assist wear. Some preliminary results will be presented in this Chapter.

5.1 Basic characteristics of the assist wear

We assumed the displacement, output force, current, and response time of the fabricated walking assist wear [1].

5.1.1 Displacement

The displacement was measured by a laser displacement sensor (IL-065, KEYENCE, JAPAN). No extra load except a frame plate (about 0.1N) was applied to the artificial muscles. The applied DC voltage was from 100V to 400V.

Fig. 5.1.1 shows the results of the displacement with different applied DC voltages. As can be seen that the displacement almost linearly increases with the increase of the applied DC voltage. The displacement at 400V is about 16 mm (with a contraction strain of 8 %) which is a little bit smaller than the displacement 20 mm that we desired. This may due to that with the increase of the stacked layers, the self-weight of the artificial muscles increases and has an effect on the displacement [2, 3]. However, since the displacement is bigger than the peak value of 13 mm slack that happens to the walking assist wear when the thickness of edge profile of the waist belt (X_b) is 20 mm as shown in Fig. 4.1.1 (b), we think it is sufficient to give an assistance during walking.

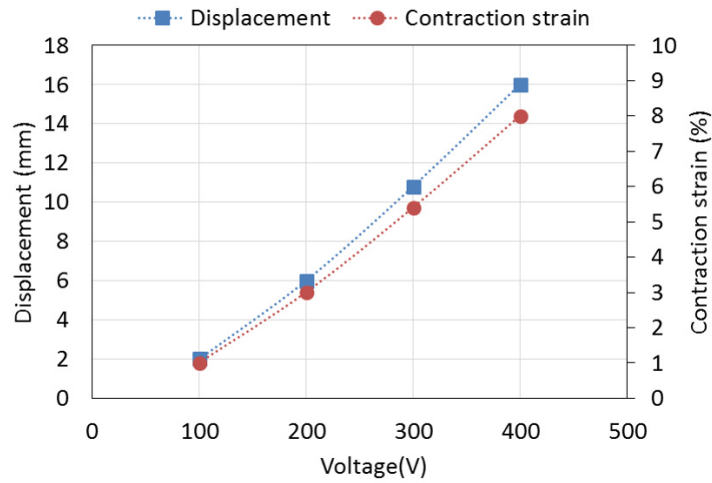
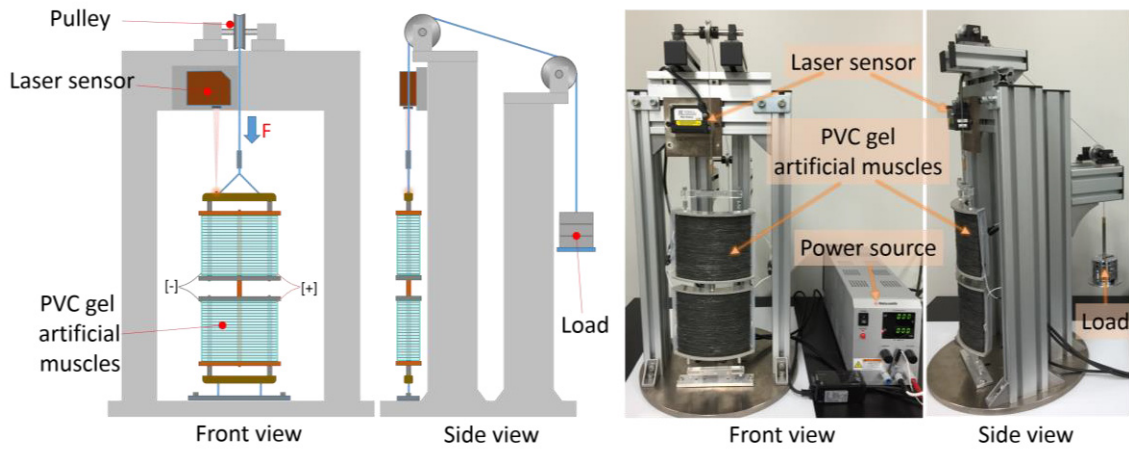


Fig. 5.1.1. Displacement and contraction strain of the assist wear.

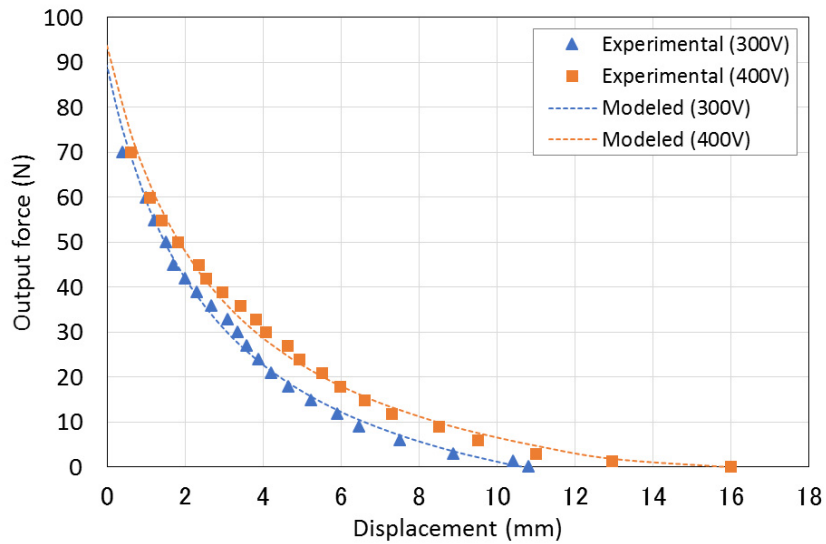
5.1.2 Output force

We use the stretching-type PVC gel artificial muscles [4] for the assistance as shown in Fig. 4.1.2. When the DC field is applied, the artificial muscles contract and the actuation modules extend in the length direction, providing a slack to assist wear which make it easy to make an extension motion in the stance phase. Then, when the toe leaves the ground from the pre swing phase to the initial swing phase, the DC field is turned off and the artificial muscles return to their original shape and generate a recovery force due to the elasticity of PVC gels. We measured the recovery force as the output force of the assist wear.

In this study, we used the displacement-force relation to measure the recovery force [4, 5]. Fig. 5.1.2 (a) shows the method of the measurement. The artificial muscles are stretched by a load through two pulleys. When the DC field is applied, the artificial muscles shrink and the load moves downward by its self-weight. And when the DC field is turned off, the artificial muscles recover to their original shape and the load is uplifted. The displacement of the load was measured by a laser sensor. With the applied load increases, the displacement of artificial muscles decrease. And the maximum recovery force occurs when the displacement becomes zero. We measured the relation between displacement and output force under DC voltages of 300V and 400V. The applied load was from 0N to 70N and the preload was about 1.5N.



(a)



(b)

Fig. 5.1.2. Output force measurement of the assist wear. (a) Illustration of method. (b) Results of the relation between displacement and output force.

Fig. 5.1.2 (b) shows the results of the output force at different displacements of each applied voltage. The force also depends on the applied DC voltage. Since we did not get the maximum output force until the applied load of 70N (a displacement of 0.6mm at 400V), we modeled and fitted the curve using a hyperbolic equation proposed in Chapter 2 to estimate the maximum output force when the displacement is zero [4, 6]. As we can see that the estimated maximum output force at 400V is about 94N which is bigger than 80N that we designed. Therefore, we

think that the characteristics of the fabricated assist wear are almost consistent with the characteristics of the designed ones.

5.1.3 Response time

The response time of the actuation modules of the assist wear was investigated. The response time is defined as the time from 10% to 90% of the contraction displacement (DC filed on) and recovery displacement (DC filed off), respectively (see Fig. 2.5.6).

Fig. 5.1.3 shows the result of the response time of the actuation modules under a DC voltage of 400V. The rise time and fall time of is about 70 ms and 56 ms with the DC field on and off, respectively. We believe that the response time of the actuation modules is sufficient for walking assistance.

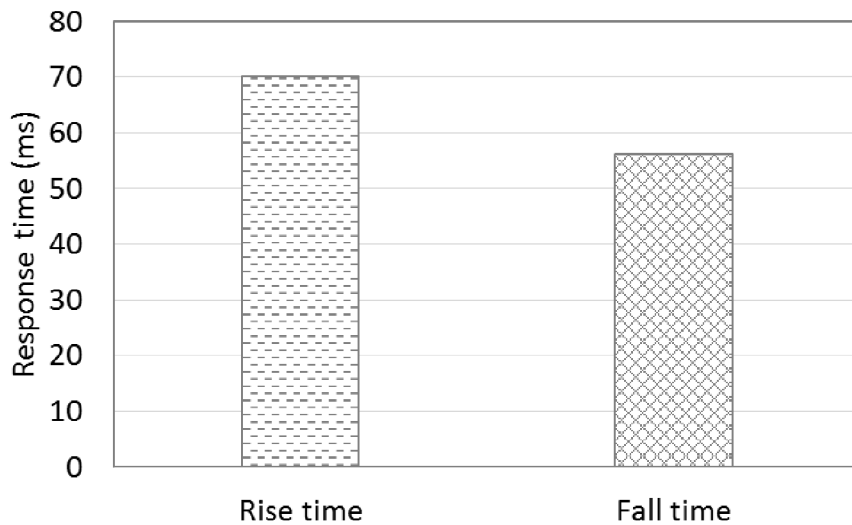


Fig. 5.1.3. Response time of the actuation modules of the assist wear.

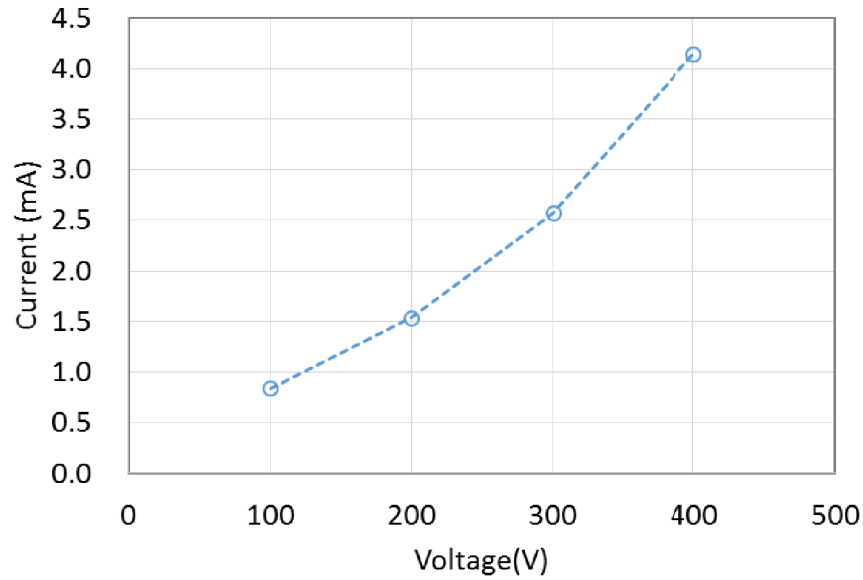


Fig. 5.1.4. Electrical current of the assist wear.

5.1.4 Current

We investigated the electrical current variation of the artificial muscles with different applied DC voltages. We used a 1 k Ω resistor connecting with the artificial muscles in series to measure the current. Since the artificial muscles adopted a new wiring method that all the anode electrodes and cathode electrodes are connected together by several wires, respectively, we have to make sure that each of the layer works well during the fabrication. We measured the current of each layer to confirm that each layer of the artificial muscle works well under the DC voltage. Because there could be a short circuit happens between the electrodes if the samples of the electrodes of PVC gels were damaged beforehand. We have checked all of the layers and get an almost equal value of each layer without any short circuit happened.

Fig. 5.1.4 shows the current of the assist wear. The current increases with the increase of the applied DC voltage. The current of the prototype (when the applied DC voltage is 400V) is about 4.1 mA and the power consumption is about 1.6 W which indicates that the PVC gel artificial muscles based assist wear has a low power consumption.

5.2 Performance of the walking assistance system

5.2.1 Insole force sensors measurement

We measured the performance of the insole force sensors based on the calibration results. As shown in Fig. 5.2.1, a 2 kg weight was applied on the insole at the position of each sensor. The analog signal is obtained by myRIO as a voltage signal, and the measured force is calculated by the cubic polynomial obtained in the force sensor calibration, as shown in Fig. 4.2.1 (c).

Fig. 5.2.1 (c) shows the result of the measured force. We can see that the average result of the measured force of all the sensors is almost the same as the desired force, which indicates that the fabricated insole force sensors could be effective to measure the force change during walking.

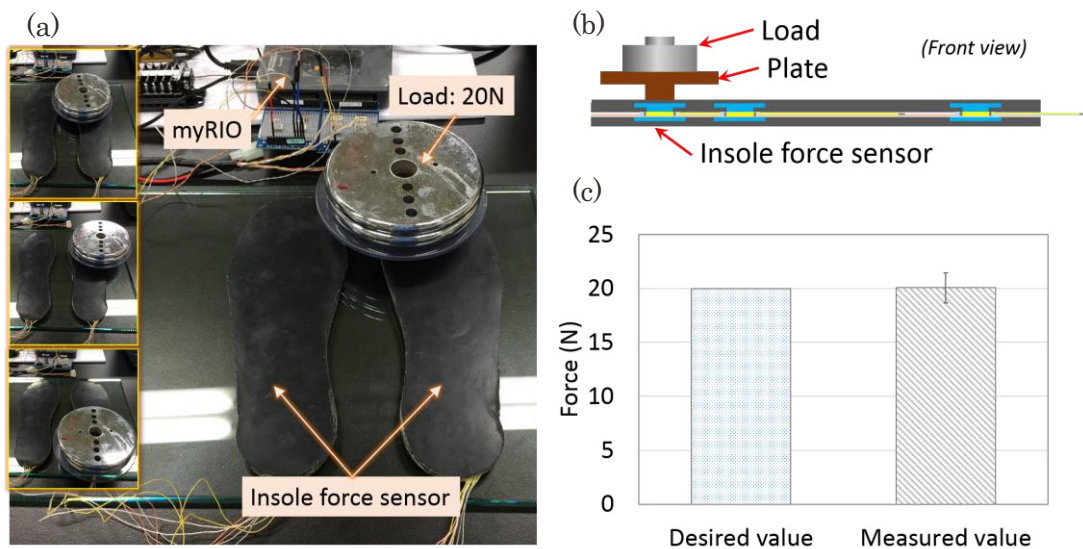


Fig. 5.2.1. Force measurement using the insole force sensors. (a) Overview of the measurement. (b) Illustration of measurement method. (c) Result of the measured force.

5.2.2 Walking gait cycles detection and output control

When the wearer raises the foot from the pre swing phase to the initial swing phase, the controller turns off the applied electric field to the assist wear to make a contraction movement and provide a tensile force to support the flexion motion of the limb. This moment can be detected when the value of the insole force sensor that arranged at the big toe becomes to zero.

Then when the foot contacts with the ground at the terminal swing phase, the applied electric field is charged to make an extension movement and create a slack on the assist wear to make it easy to extend the limb. This moment can be detected when the insole force sensor that arranged at the heel increases from zero. Of course, the values of the sensors in the opposite limb could be a reference.

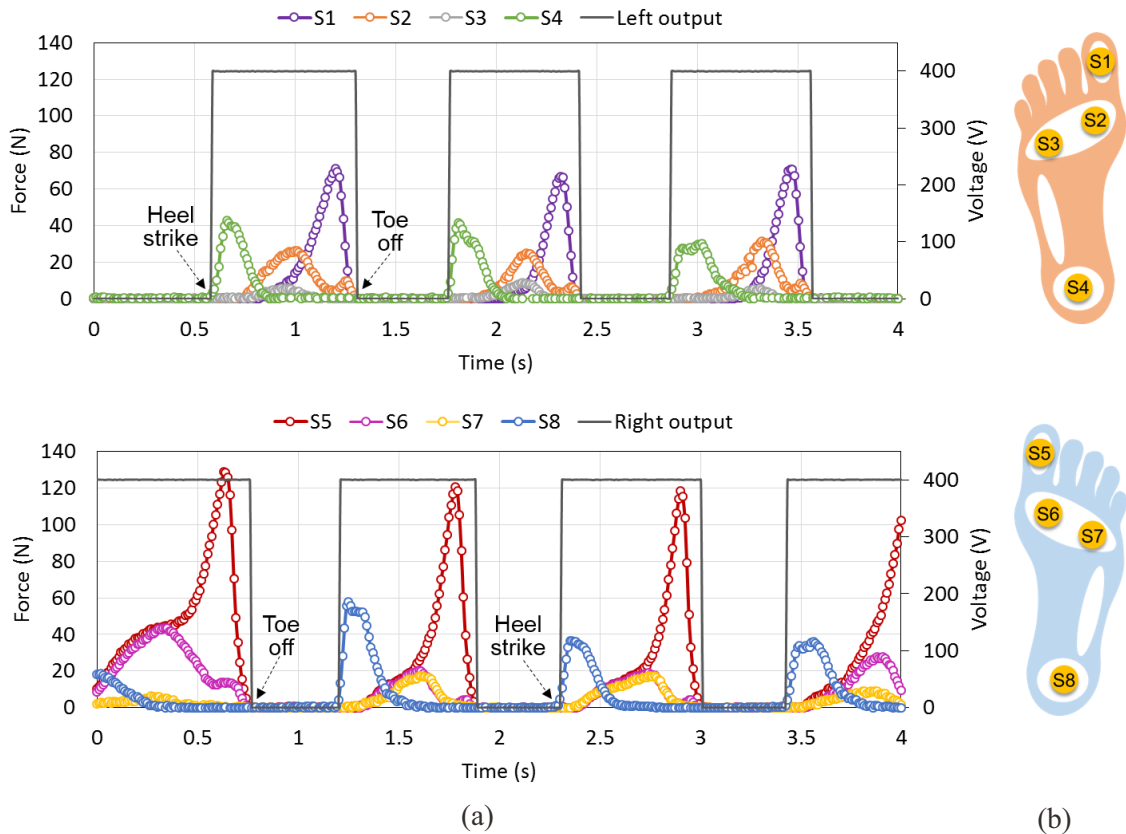


Fig. 5.2.2. Results of the force measurement and output voltage control I . (a) Result of the left and right lower limbs. (b) Arrangement of the force sensors.

We made a program according to the condition that mentioned above and investigated the effectiveness of the control system (denote as C1). We measured the force changes of all the sensors and controlled the output voltage in real time during walking. Fig. 5.2.2 shows the result of the relation between the force changes and the output voltage in the gait cycles. As shown in the figure, the output voltage becomes 0V when the value of the sensor arranged at the big toe (S1 and S5) becomes to 0 together with the other three sensors. And it becomes 400V when the values of the sensor arranged at the heel (S4 and S8) becomes bigger from 0. These results are

consistent with the desired results which shows that the designed control system works well.

Furthermore, considering the response time of the assist wear is about several tens of milliseconds, we designed another strategy to control the assist wear. For a normal working, as we can see the force changes of the sensors arranged at the big toes in Fig. 5.2.2, the elapsed time from the peak to the valley is about several tens of milliseconds. So we made another program to turn off the DC field of the actuation modules at the peak of the sensors arranged at the big toes (denote as C2).

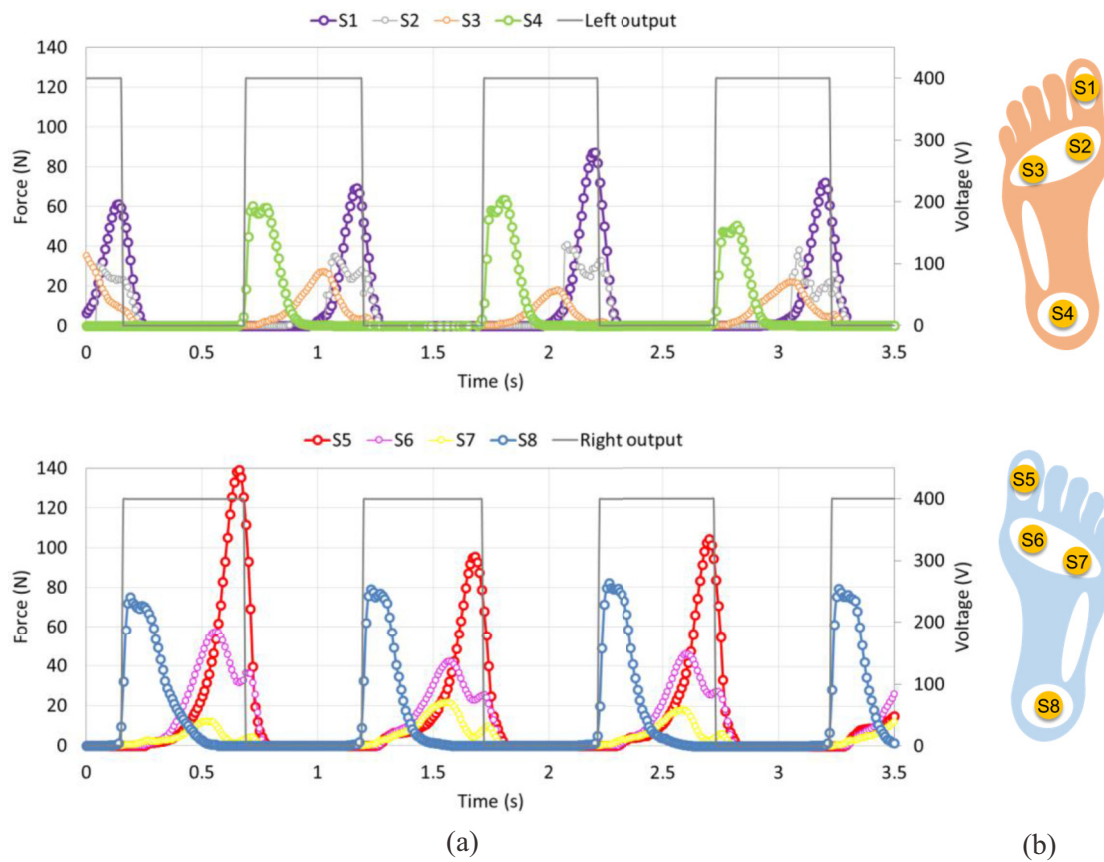


Fig. 5.2.3. Results of the force measurement and output voltage control II. (a) Result of the left and right lower limbs. (b) Arrangement of the force sensors.

Fig. 5.2.3 shows the result of the relation between the force changes and the output voltage in the gait cycles for the second strategy. As shown in the figure, the output voltage becomes 0V almost at the peak value of the sensor arranged at the big toe (S1 and S5). And it becomes 400V when the values of the sensor arranged at the heel (S4 and S8) becomes bigger from 0. These results are consistent with the desired results which also shows that the designed control system

works well.

Fig. 5.2.4 shows the estimation of the assistance force and period for the control C1 and C2. As we can see that the C2 could have a bigger assistance force which is about four times bigger than that of C1, and the assistance period would be increased by 10% of a walking gait cycle compared with C1.

The walking assistance effectiveness with the two patterns of the control strategies should be verified in the walking experiments.

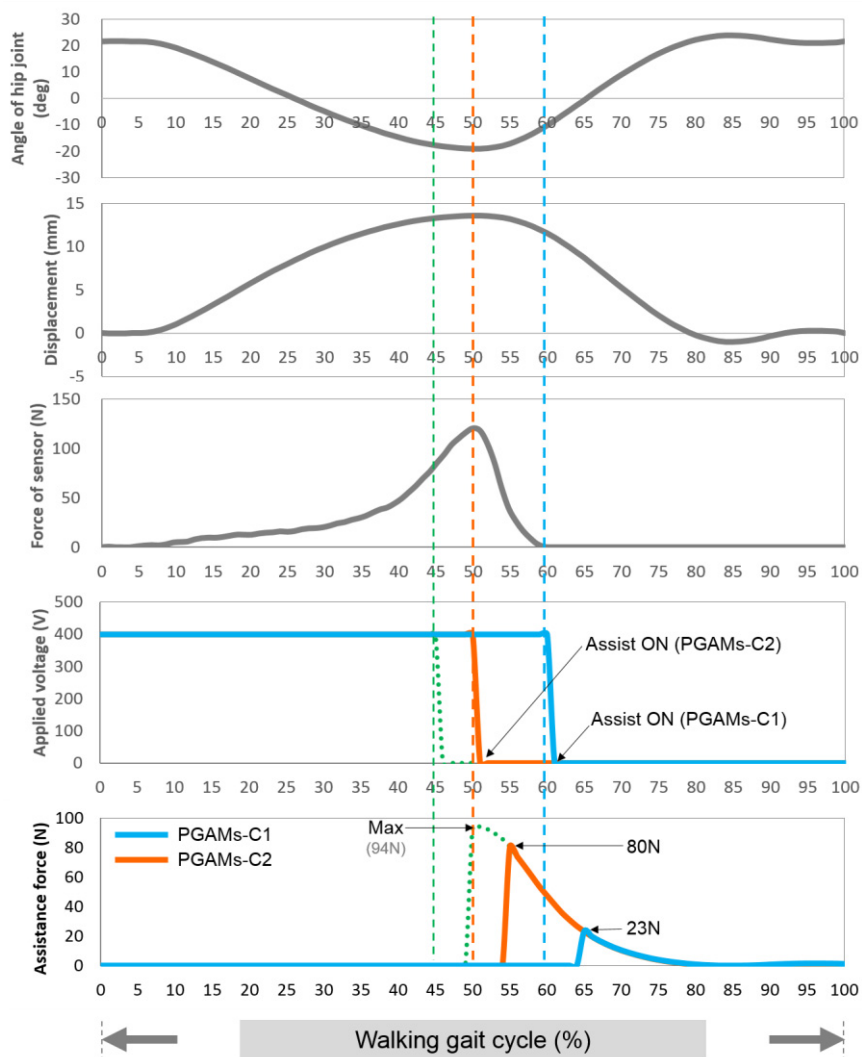


Fig. 5.2.4. Estimation of assistance force of control method C1 and C2 during a walking gait cycle.

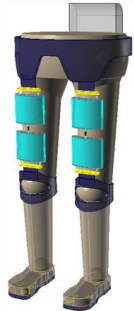
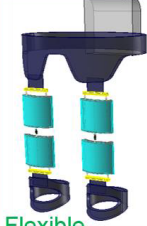
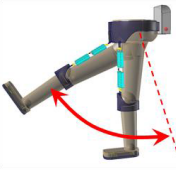


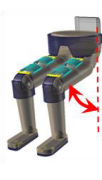


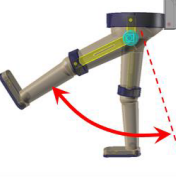


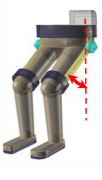
5.3 Comparisons with the other assist wears

Compared to the traditional motors based assist suits, the PVC gel artificial muscles based assist wear has the advantages of light weight, low impedance, high flexibility and low power consumption.

On the one hand, since the PVC gel artificial muscles are soft, so the whole assist wear is flexible, and with high degree of freedom of all motions. On the other hand, for the motors based assist suits, because they have to use some rigid frame to transmit the power. That could bring some restriction to the motions, such as abduction and adduction, external rotation and internal rotation and so on, as shown in Table 5.3.1. Besides, considering to realize the same linear motion with the same arrangement as the proposed assist wear for the DC motors and DC solenoid motors as shown in Table 5.3.2, we estimated the least necessary weight and power consumption to realize the same maximum output force and displacement of the prototype of PVC gel artificial muscles based assist wear in this study. Two DC motors (A-max 32, Maxon motor ag. [7]) and four DC solenoids (S-1512, Shindengen Mechatronics Co., Ltd. [8]) were used to do the estimation. We found that the power consumption of PVC gel artificial muscles based assist wear could be less than about 12% of that for the DC motors and less than 6% of that for the DC solenoids. And the total weight of the actuation modules part could be less than 60%-70% of the DC motors currently. Furthermore, we can make the PVC gel artificial muscles much lighter by using different types of electrodes, for example, we have reduced the weight of the artificial muscles up to 25% by using the conductive meshed fibers electrodes to obtain the same characteristics [9]. Finally, the DC motors based assist wear could be noisy while the PVC gel artificial muscles based assist wear produces no noise.



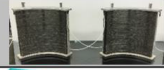
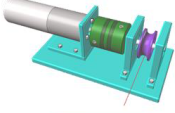

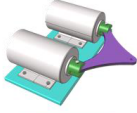

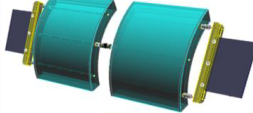

Therefore, we think the proposed assist wear is reasonable for a daily life use, for the advantages of a simple structure, compact and lightweight, flexible, good in fitting and easy to put on and take off. And some positive effects on the wearers could be expected.

Table 5.3.1. Comparisons of the degree of freedom of movement between the PVC gel artificial muscles based assist wear and the motors based assist wear.

Structure		Range of motion (ROM)			
PGAM assist wear		Flexion/ Extension	Abduction/ Adduction	External rotation/ Internal rotation	Squat
 Flexible					
		●	●	●	●
Motors based assist suit		Flexion/ Extension	Abduction/ Adduction	External rotation/ Internal rotation	Squat
 Rigid					
		●	▲	▲	▲

● Without restriction ▲ With restriction

Table 5.3.2. Comparisons of the weight and power consumption between the PVC gel artificial muscles based assist wear and the motors based assist wear.

Output (max)	80N, 20mm, 2Hz, linear motion		
Actuator	DC motor/A-max32 (51:1) (Maxon motor ag) 	DC solenoid/ S-1512 (Shindengen Mechatronics Co.,Ltd.) 	PVC gel artificial muscle 
Structure	 	 	 
Applied voltage	24 V	17 V	400 V
Power consumption	40 W (20x2)	80 W (20x4)	< 4 W (1x4)
Weight	>1.6 kg (0.8x2)	>2 kg (0.5x4)	<1.2 kg (0.3x4)

5.4 Chapter Summary

The prototype of PVC gel artificial muscles based walking assist wear was evaluated to confirm whether the characteristics were consistent with that of the designed ones in this Chapter.

The displacement and output force of the assist wear under a DC voltage of 400V were about 16mm and 94N, respectively. These are almost consistent with the desired results that we designed.

And the current was investigated for each layer of the artificial muscles and almost obtained an equal value for each layer. The current of the assist wear under a DC voltage of 400V was about 4.1mA, with a power consumption of about 1.6W.

The effectiveness of the walking motion detector and the myRIO based controller were evaluated and found that the whole system worked well.

We compared the PVC gel artificial muscles based assist wear with the traditional motors based assist suits, founding that the PVC gel artificial muscles based assist wear has the advantages of light weight, low impedance and high flexibility with a high freedom of motion, no noise and low power consumption.

Therefore, the proposed PVC gel artificial muscles based assist wear could be reasonable for a daily life use, for the advantages of a simple structure, compact and lightweight, flexible, good in fitting and easy to put on and take off.

References

- [1] Y. Li and M. Hashimoto, "Design and prototyping of a novel lightweight walking assist wear using PVC gel soft actuators", *Sensors and Actuators A-Phys.*, 239 (2016) 26-44.
- [2] Y. Li, Y. Shirai, Y. Tsuchiya, K. Yasuda and M. Hashimoto, Relation of Stacked Layers and Characteristics of PVC Gel Actuators, in the JSME conference on Robotics and Mechatronics, 2014, pp. 2A1-K01. (in Japanese)
- [3] Y. Li, Y. Tsuchiya, A. Suzuki, Y. Shirai and M. Hashimoto, Influence of the Number of Stacked Layers on the Performance of PVC Gel Actuators, The 2014 IEEE/ASME International Conference on Advanced Intelligent Mechatronics (AIM2014), 2014, pp. 94-99.
- [4] Y. Li and M. Hashimoto, "PVC gel based artificial muscles: Characterizations and actuation modular constructions", *Sensors and Actuators A-Phys.*, 233 (2015) 246-258.
- [5] Y. Li, Y. Tsuchiya, A. Suzuki, Y. Shirai, R. Sakai and M. Hashimoto, A Characteristics Evaluation Method for PVC Gel Actuators, in the 15th SICE System Integration Division Annual Conference (SI2014), pp. 592-595. 2014.
- [6] Y. Li and M. Hashimoto, Characteristics and Modeling of PVC Gel Actuators, in the JSME conference on Robotics and Mechatronics, 2015, pp. 2A2-A09. (in Japanese)
- [7] <http://www.maxonmotor.com/maxon/view/product/motor/dcmotor/amax/amax32/236662>
- [8] <http://www.shindengen.co.jp/smt/product/lineup/p02.html>.
- [9] Y. Tsuchiya, Y. Shirai, S. Haruyama, K. Yasuda, Y. Li and M. Hashimoto, Evaluation of the characteristics of the PVC gel actuator using a flexible mesh electrode, in the JSME conference on Robotics and Mechatronics, 2014, pp. 2A1-Q03. (in Japanese)

Chapter 6

Walking experiments using the assist wear system

Chapter 6 Walking experiments using the assist wear system

This Chapter will focus on the validation of the walking assistance effect using the prototype of PVC gel artificial muscles based assist wear.

Since the assist wear just have one half for assisting one leg during walking, we asked a hemiparetic stroke patient (paralysis on one side of the body) to participate in the evaluation experiments to investigate the effectiveness of wearing the assist wear during walking. The experiments will be conducted in the physiological (e.g. muscular activity variation), physical (walking speed and pace length calculation) and psychological (e.g. some questionnaire survey) aspects.

The patient gave a signature to consent to the participation, and the local Ethics Committee approved the experiment.

6.1 Purpose and hypotheses

Hemiparesis or one-sided (“hemi”) weakness (“paresis) causes weakness or the inability to move one side of the body. One-sided weakness in the leg can cause a loss of balance, a difficulty walking with limited steps and frequency [1]. In this experiment, we apply the prototype of artificial muscles assist wear on the weakened side of the leg to investigate the effect with and without wearing the assist wear during steady-state level ground walking. We had the hypotheses that there would be some positive effect on the walking status of the weakened leg with the assistance of the artificial muscles assist wear, such as improving the walking speed or increasing the step length and decrease the muscular activity during walking.

6.2 Methods and conditions

6.2.1 Subject characteristics

In this experiment, since the assist wear can just provide an assistance over 10% of the maximum moment on the hip to support the motion of the hip joint during walking, we asked a

hemiparetic stroke patient with a low-level of stroke who can make a walk by himself without any orthoses. Table 6.2.1 shows the detail of the subject in this study.

Table 6.2.1 Characteristics of the subject in the walking experiment.

Items	Characteristics
Sex	Male
Age	74 years
Height	168 cm
Weight	67 kg
Length of upper leg (left/right)	48 cm/48 cm
Thigh diameter (left/right)	46 cm/45 cm
Foot size	25.5 cm
Months since stroke	3 months
Affected side	Right
Walking ability	Independent (without orthoses)
Walking speed	0.8 m/s
Hip joint function limitation	20 degree (internal rotation)
Degree of paralysis (12-grade recovery grading system of hemiplegia)	11
Functional Independence Measure (FIM) score	123

6.2.2 Experimental methods and devices

As shown in Fig. 6.2.1, the subject was asked to do a to-and-fro straight line walking task for about 10m with and without the assist wear. The walking speed, length of steps, the electromyogram (EMG) and the acceleration and angular velocity of the upper body during walking were measured. After the experiment, the subject was asked to answer a questionnaire about the impression of the experiment. The subject was accompanied by a physician during the whole experiment as for his safety.

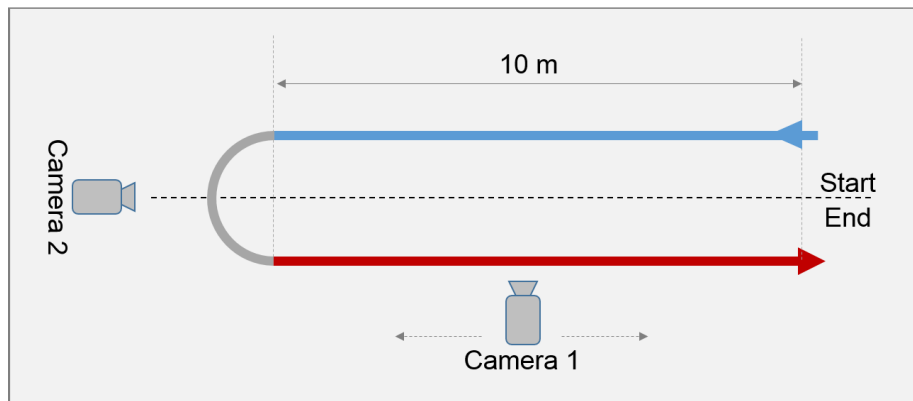


Fig. 6.2.1 Illustration of a to-and-fro straight line walking for about 10m.

The prototype of PVC gel artificial muscles (PGAMs) based assist wear was arranged on the right upper leg of the subject, and the power and controller were on his back. Two types of control methods were used when wearing the assist wear as shown in Fig. 5.2.2 and Fig. 5.2.3, respectively. The first control method (C1) is that when the big toe leave the ground at the end of pre-swing, the DC field is turned off to provide an assistance force on the hip joint to support the motion of lifting the leg up and forward. And the second control method (C2) is that when the force of the sensor arranged at the big toe reach to a peak value, the DC field is turned off to provide an assistance force. Considering the response time of the actuation modules of the assist wear, we think that the C2 can provide a bigger force at the moment when the leg leave the ground to make a step forward and give a more positive effect on the acceleration of the leg than C1.

The EMG of the Rectus femoris muscle, Sartorius muscle, Hamstring and Gastrocnemius were measured by using a wireless EMG logger (LP-MS1002, Oisaka Electronic Equipement Ltd.), as shown in Fig 6.2.2.

The acceleration and angular velocity variation were measured by a Wireless Motion Recorder (MicroStone Corporation) [2]. Two Wireless Motion Recorders were arranged on the chest and waist, respectively (Fig. 6.2.3).

Two digital cameras were used to record the walking motion, arranged at the front and the side, respectively (Fig. 6.2.1). The walking speed is calculated based on the time spent in one way walk and the length of step can be calculated by the number of steps in one way which can be read from the videos.

Furthermore, the subject was asked some impression evaluation questionnaires and some free comments after the experiment.

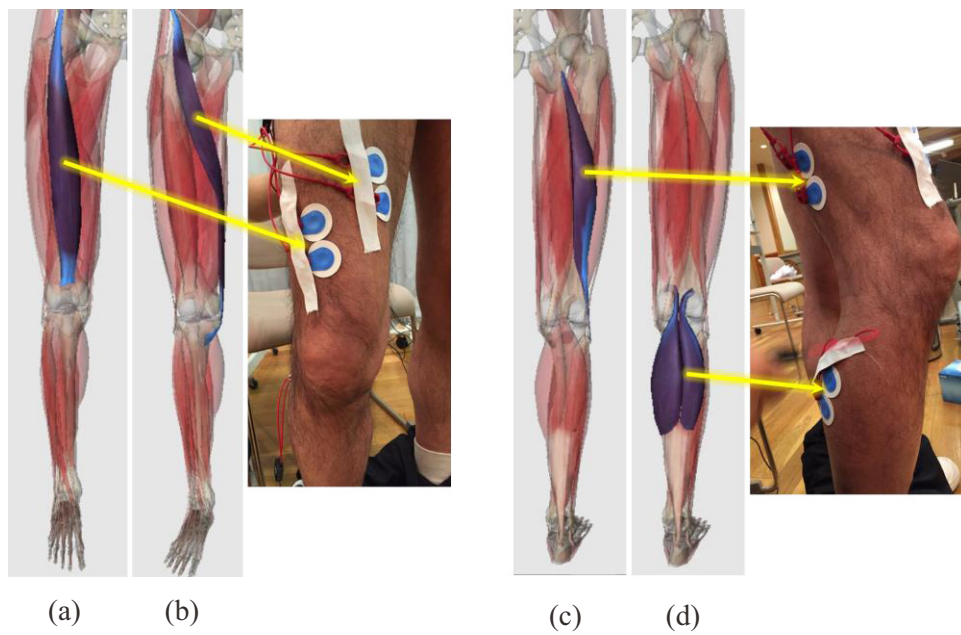


Fig. 6.2.2. Arrangement of the EMG electrodes. (a) On the Rectus femoris muscle. (b) On the Sartorius muscle. (c) On the Hamstring. (d) On the Gastrocnemius.

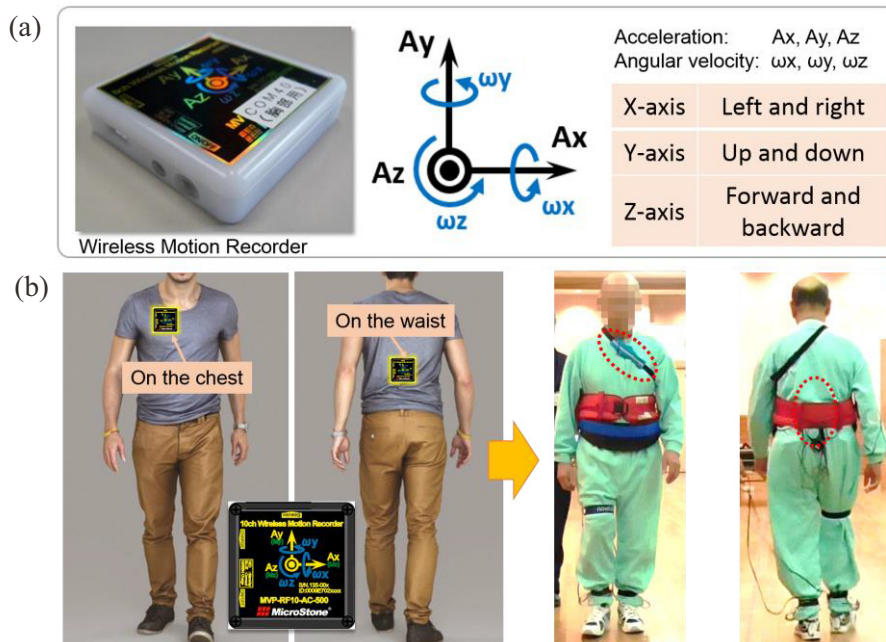


Fig. 6.2.3. Measurement method of acceleration and angular velocity. (a) Overview of the Wireless Motion Recorder, with a definition of directions. (b) Position of arrangement.

The process of the experiment is shown as follows:

- 1) To put and fix the EMG electrodes on the right leg of the subject.
- 2) To measure the maximum myogenic potential of each muscle for the %MVC evaluation.
- 3) To put the Wireless Motion Recorder on the chest and waist of the subject.
- 4) The subject was asked to do the 10m to-and-fro straight line walking task for two times in a normal speed, without the PGAMs assist wear.
- 5) To put the PGAMs assist wear on the subject.
- 6) The subject was asked to do the 10m to-and-fro straight line walking task for two times in a normal speed, with the PGAMs assist wear using the control method C1.
- 7) The subject was asked to answer an impression evaluation questionnaires and some free comments after 6).
- 8) The subject was asked to do the 10m to-and-fro straight line walking task for two times in a normal speed, with the PGAMs assist wear using the control method C2.
- 9) The subject was asked to answer an impression evaluation questionnaires and some free comments after 8).
- 10) Take off the PGAMs assist wear from the subject.
- 11) The subject was asked to do the 10m to-and-fro straight line walking task for two times in a normal speed, without the PGAMs assist wear.
- 12) To save the data and finish the experiment.

Fig. 6.2.4 shows an overview of wearing the PGAMs assist wear and the walking experiment. The belt in red is a safety belt for the subject.

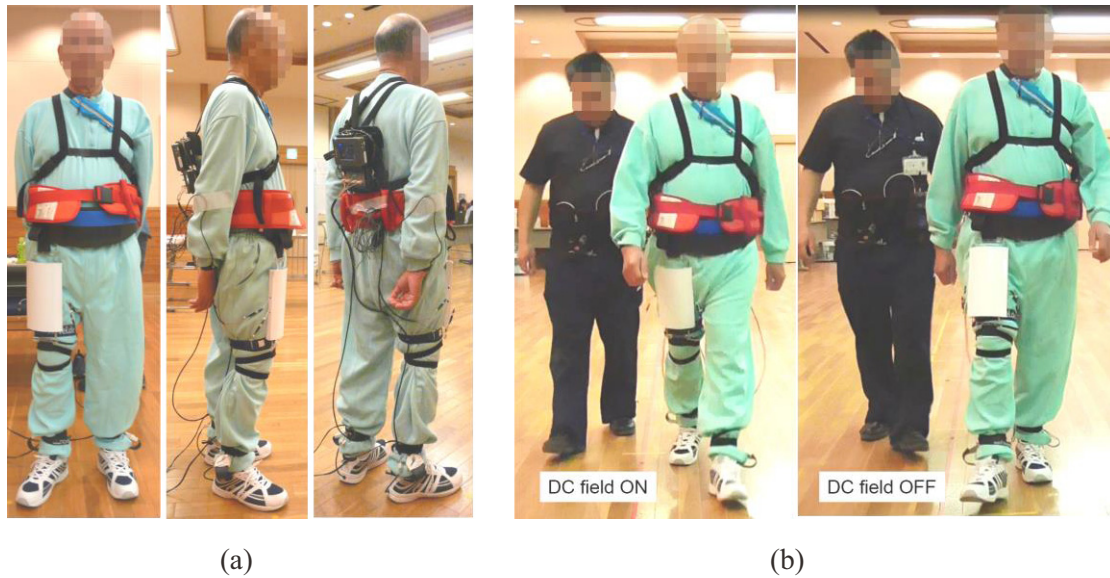


Fig. 6.2.4. (a) Overview of wearing the PGAMs assist wear (the belt in red is a safety belt). (b) Overview of the walking experiment (the subject was accompanied by a physician).

6.3 Results and discussions

6.3.1 Walking motion detection and assist wear control

To verify whether the walking assist wear system worked well or not, we measured the accuracy of the walking motion detection and the assist wear control. As we mentioned in section 6.2.2 that we conducted two types of control algorithms for controlling the assist wear as C1 and C2. We measured the variations of the insole force sensors, the output DC voltage and the current of the artificial muscles to investigate the validation of the system during the walking experiment. Fig. 6.3.1 shows a part of results of the walking motion detection and assist wear control. As we can see that, the phases of the toe off and the heel strike were accurately detected and the output DC voltage was correctly applied at the right moment both for the control C1 and C2. And the current of the actuation modules changes with the variation of the applied DC voltage. These results show that the walking motion detection and actuation modules work well during the experiment.

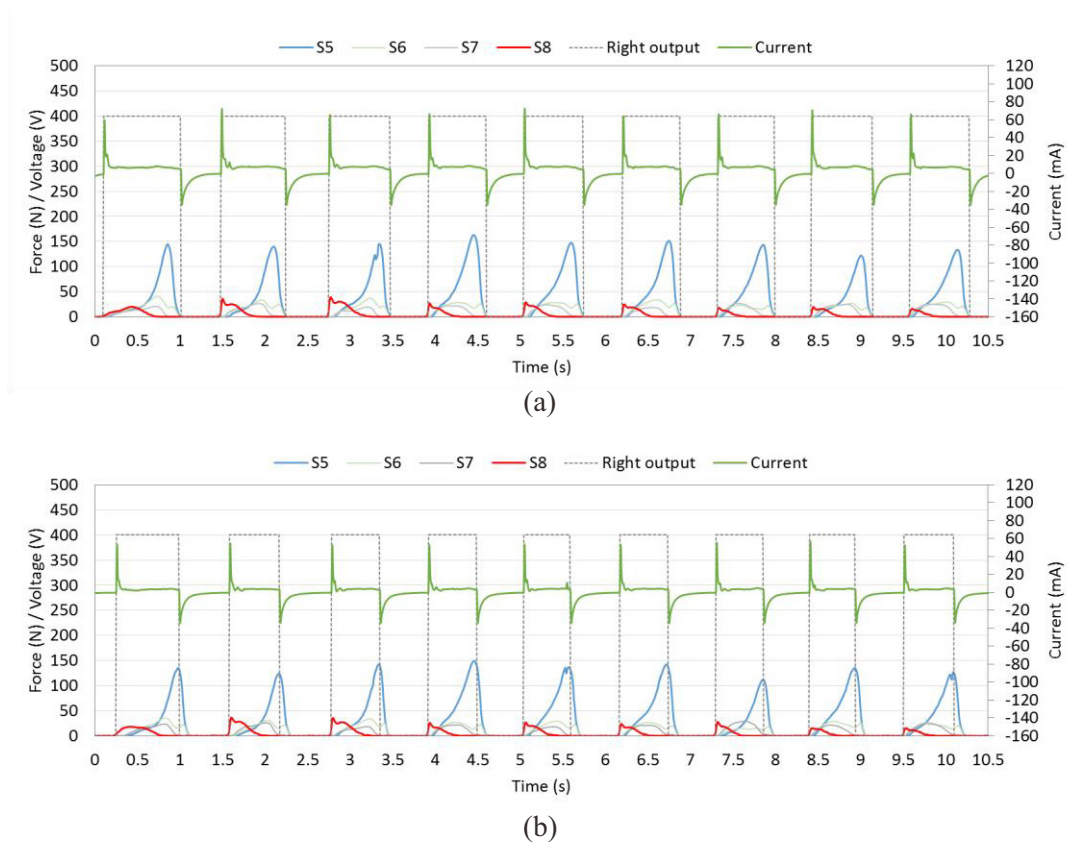


Fig. 6.3.1. Results of the walking motion detection and assist wear control. (a) Result of the control C1. (b) Result of the control C2.

6.3.2 Walking speed and length of steps

Fig. 6.3.2 shows the results of the average walking speed in the four types of walking, as a normal walking before assistance experiment (without assist wear), a walking with PGAMs assist wear using control C1, a walking with PGAMs assist wear using control C2 and a normal walking after assistance experiment (without assist wear). We found that the walking speed with the PGAMs assist wear using control C2 increases about 10% than the normal walking without an assist wear, with a significant difference of 5%. No significant difference for the control C1. This should be due to that the control C2 makes the assist wear providing an assistance force before the leg leaves the ground at the phase of pre-swing which leads to a faster walking pace. The control C1 provides an assistance force after the leg leaves the ground which may not be effective to increase the walking pace. Besides, the generation force of the assist wear decreases with the increase of the hip joint during the swing phase. Therefore, the control C2 can provide an earlier assistance force to support the acceleration of the leg during the initial swing phase.

which would be effective to increase the length of the steps. And we calculated the length of steps of right and left leg by using the number of steps in the to-and-fro walking. We found that the average step length of the right leg (weakened side) increased about 2.8cm with the PGAMs assist wear using control C2, with a significant difference of 5% (Fig. 6.3.3). No significant difference on the left leg (healthy side). And no significant increase of step length was found for the control C1.

These results indicate that the PGAMs assist wear is able to assist the walking by increasing the step length and walking speed.

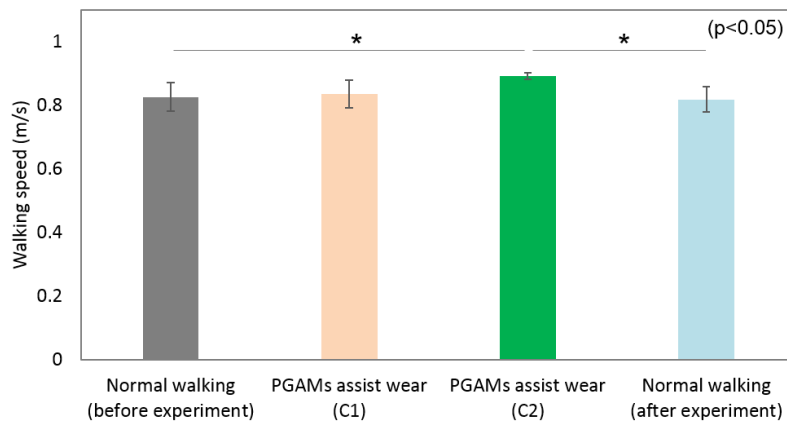


Fig. 6.3.2. Results of the walking speed in the four types of walking.

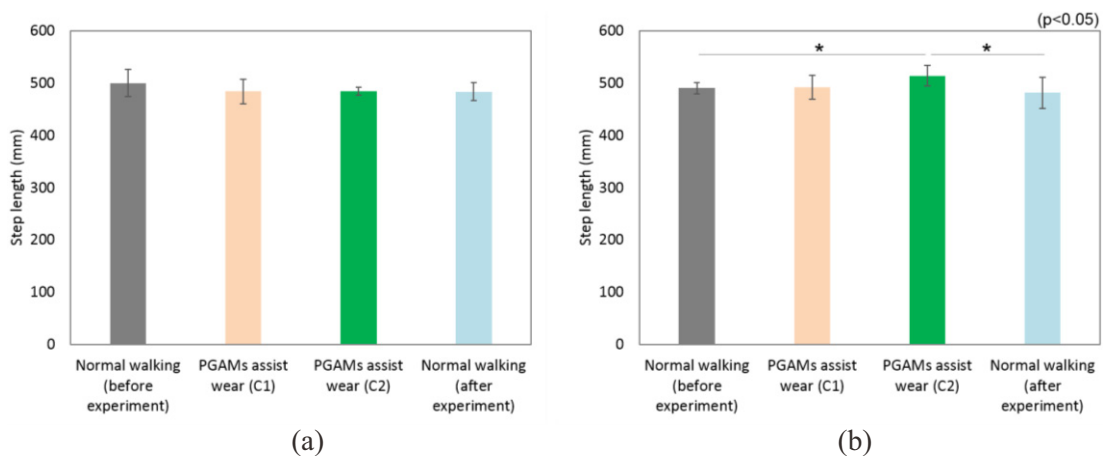


Fig. 6.3.3. Results of the step length in the four types of walking. (a) Step length of the left leg (healthy side). (b) Step length of the right leg (weakened side).

6.3.3 Acceleration and angular velocity of the upper body

Fig. 6.3.4 shows the average results of the acceleration of the upper body during walking. As we can see that, the acceleration in the direction of A_z (forward and backward) is bigger than the acceleration in the directions of A_x (left and right) and A_y (up and down) due to the straight line walking motion. In the direction of A_z , the acceleration becomes bigger when wearing the PGAMs assist wear (C2) than the normal walking, with a significant difference of 5% on the chest and 1% on the waist, respectively. Also there is a significant difference of 5% on the waist for PGAMs assist wear (C1). This indicates that with the assistance of the assist wear, the subject moves faster than that without an assist wear which is consistent with the results of walking speed. And we obtained no significant difference in the other directions, which might indicate that there is fewer negative influence on the balance of the A_x and A_y directions when wearing the PGAMs assist wear.

Fig. 6.3.5 shows the average results of the angular velocity the upper body during walking. On the chest, the angular velocity in the direction of A_x is bigger than that in the other directions. This is due to the body swing for a forward movement. On the waist, the angular velocity in the direction of A_x and A_y is bigger than that in the direction of A_z . And in the direction of A_y , we can see that with the PGAMs assist wear (C2) there is a rising tendency of the angular velocity. We think this might be concerning with the assistance of the weakened leg. However, no significant difference was found for the angular velocity in all the directions.

These results indicate that, with the assistance of the PGAMs assist wear, the subject can move faster forward during the steady-state level ground walking. And fewer negative influence happens on the balance of the body. This means that when wearing the lightweight PGAMs assist wear, the wearer could be able to remain a good balance of the body and move faster during walking which would make the walking be more efficiency.

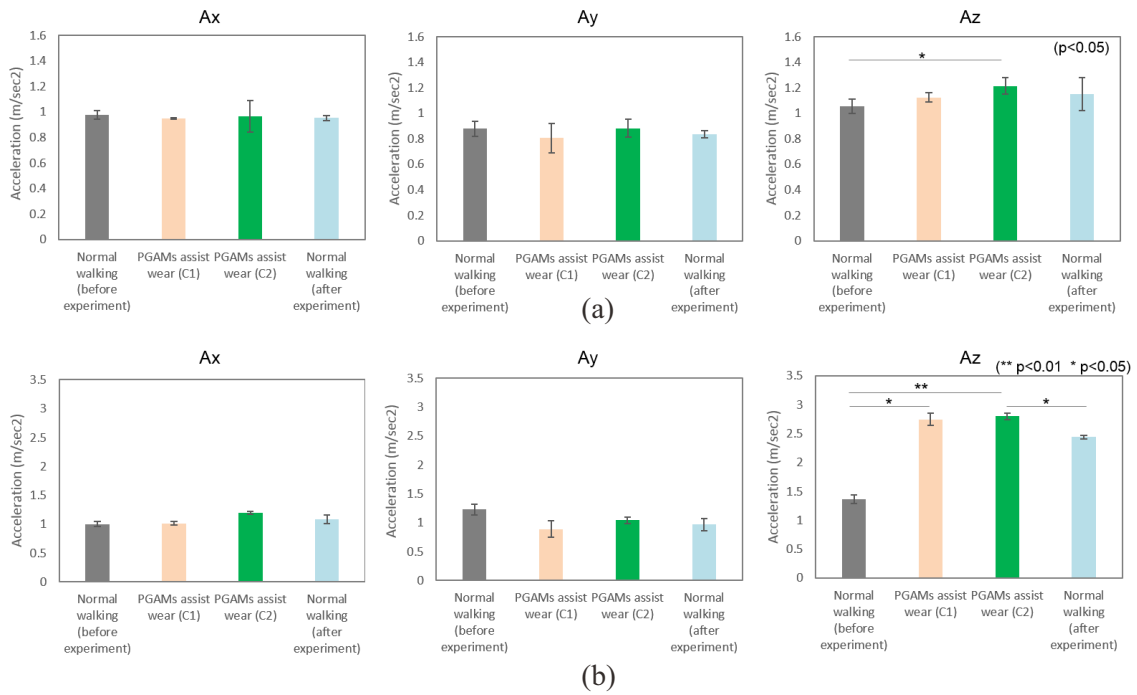


Fig. 6.3.4. Results of the acceleration of the upper body during walking. (a) Acceleration results of the chest. (b) Acceleration results of the waist.

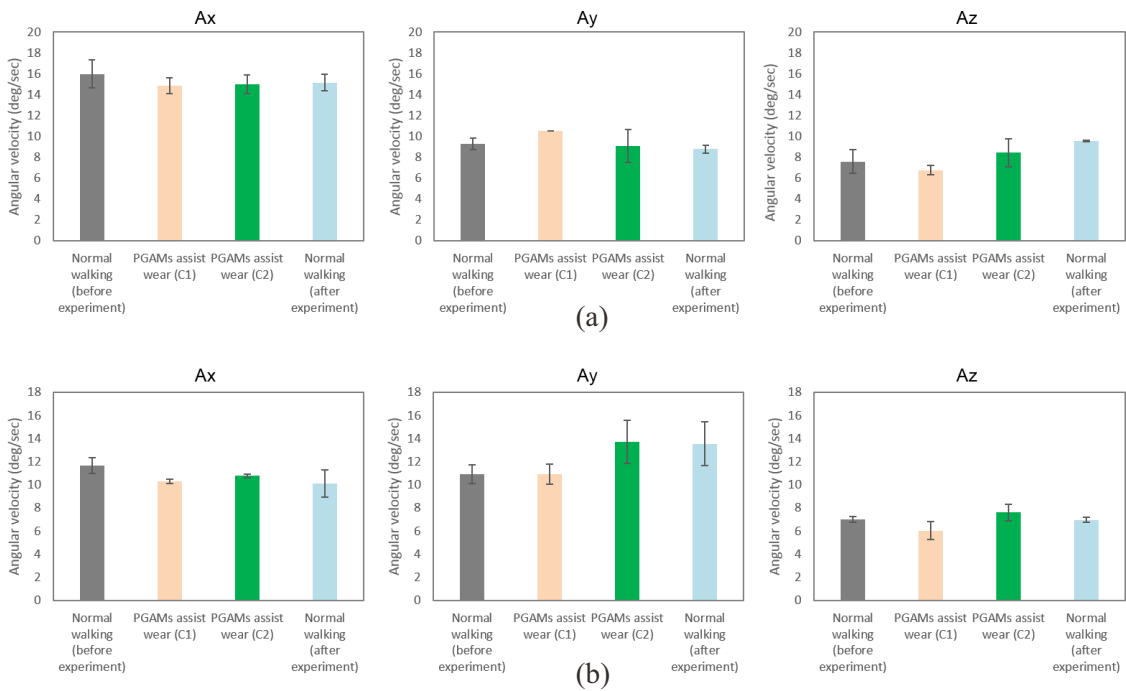


Fig. 6.3.5. Results of the angular velocity of the upper body during walking. (a) Angular velocity results of the chest. (b) Angular velocity results of the waist.

6.3.4 Surface EMG of the muscles

In this experiment, we investigated the EMG variation of the Rectus femoris muscle, Sartorius muscle and Hamstring to find out that whether the PGAMs assist wear can reduce the muscular activity so as to lighten the burden of human muscle during walking. Also we investigated the EMG of the Gastrocnemius to find out that whether the PGAMs assist wear brings a burden to the muscle during the stance phase.

Fig. 6.3.6 shows a result of the integrated electromyogram (IEMG) variation of each muscle during a walking gait cycle. We can see that the IEMGs of the Rectus femoris muscle, the Sartorius muscle and the Hamstring decrease dramatically after 40% of the gait cycle with the assistance of the PGAMs assist wear both in the control C1 and C2. And there is no significant change in the IEMG of the Gastrocnemius. This means that both of the control methods are effective to reduce the burden of the muscles during walking, and seems that the arrangement and fixation of the assist wear brings no notable burden to the muscle of Gastrocnemius.

Fig. 6.3.7 and Fig. 6.3.8 show the average integrated electromyogram (IEMG) and %IEMG (the maximum average IEMG of the normal walking as a reference value) of each step during the four types of walking, respectively. And Fig. 6.3.9 shows the results of the maximal voluntary contraction (%MVC) values of each muscle. As we can see that, the average IEMGs of the Rectus femoris muscle and the Sartorius muscle decreased dramatically when wearing the PGAMs assist wear both in the control C1 and control C2. The same result was obtained for the Hamstring. About 41% maximum decrease of the %IEMG for the Rectus femoris muscle, about 34% maximum decrease for the Sartorius, about 28% maximum decrease for the Hamstring with a significant difference over 5%. This means that the assist wear reduces the burden of the muscles for lifting a leg forward and does not bring a burden to the Hamstring which has the function of control the balance of the body during the terminal swing phase. This may due to the force of the assist wear decreases with the increase of angle of hip joint. And we obtained about 17% maximum decrease of the %MVC for the Rectus femoris muscle, about 11% maximum decrease for the Sartorius, about 5% maximum decrease for the Hamstring with a significant difference over 5%. However, the %MVC for the Gastrocnemius increased about 5% compared with the normal walking after the assistance experiment for both the control C1 and control C2. We think this is due to the lower speed of the normal walking and used less muscular activity of the Gastrocnemius.

These EMG results indicate that, with the assistance of the assist wear, the burden of the muscles on the lower limb can be effectively reduced during walking.

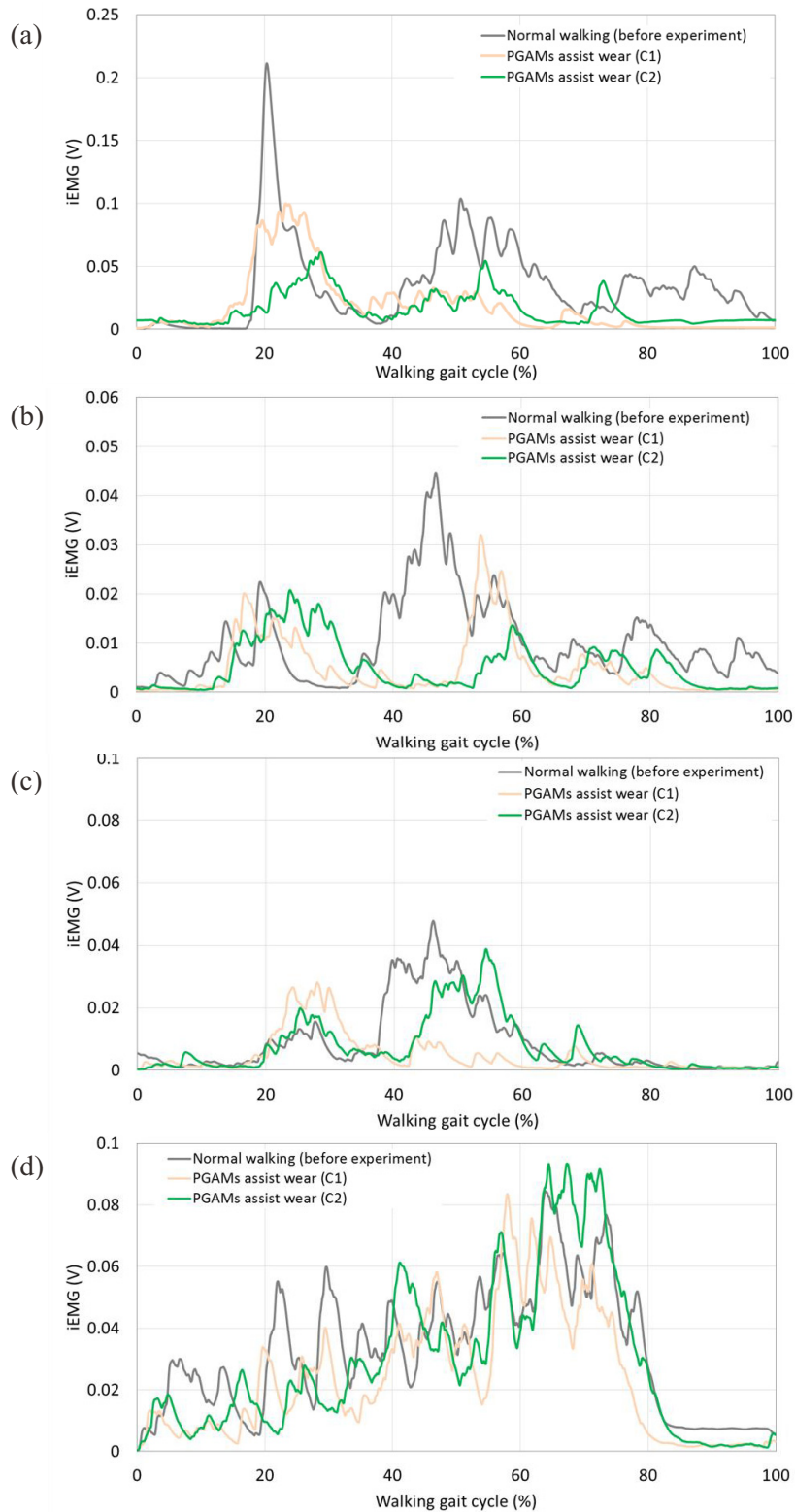


Fig. 6.3.6. Results of the integrated electromyogram (IEMG) variation during a walking gait cycle. (a) IEMG of the Rectus femoris muscle. (b) IEMG of the Sartorius muscle. (c) IEMG of the Hamstring. (d) IEMG of the Gastrocnemius.

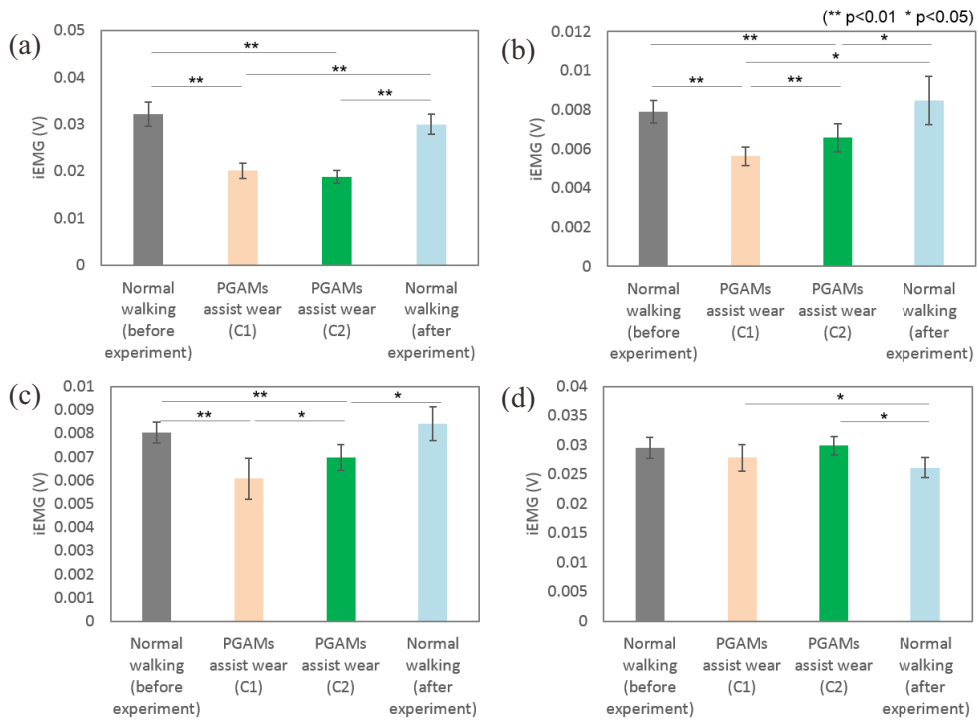


Fig. 6.3.7. (a) IEMG of the Rectus femoris muscle. (b) IEMG of the Sartorius muscle. (c) IEMG of the Hamstring. (d) IEMG of the Gastrocnemius.

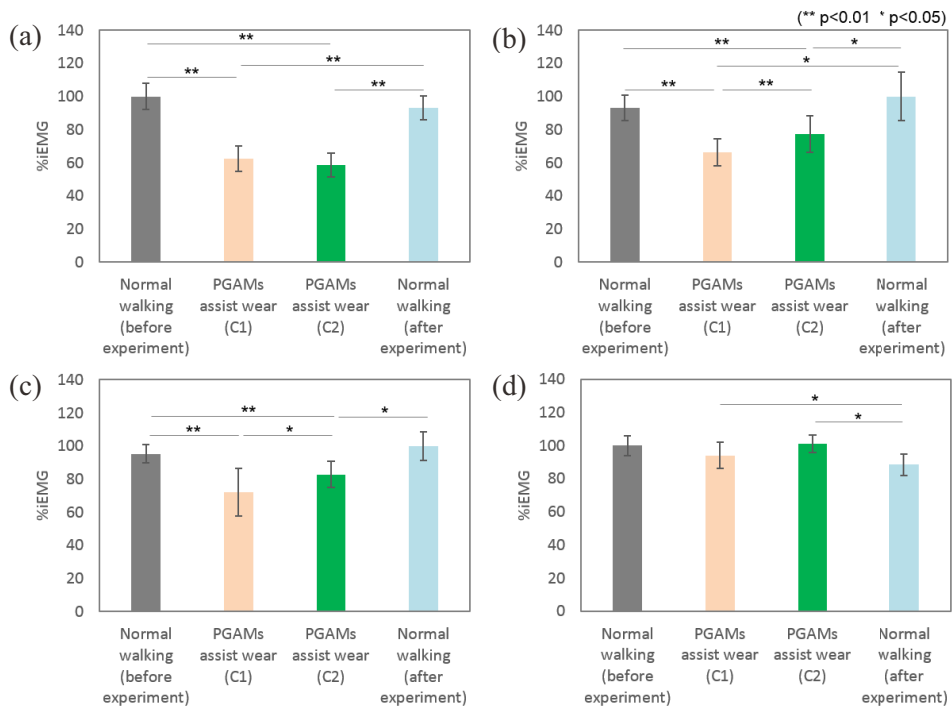


Fig. 6.3.8. (a) %IEMG of the Rectus femoris muscle. (b) %IEMG of the Sartorius muscle. (c) %IEMG of the Hamstring. (d) %IEMG of the Gastrocnemius.

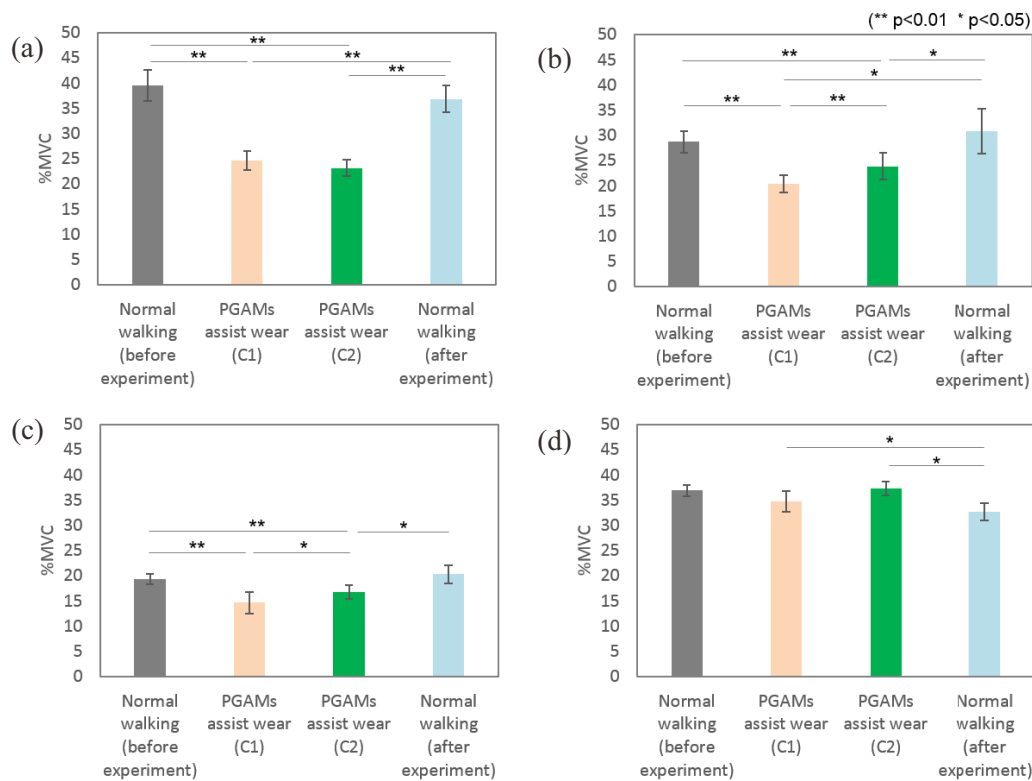


Fig. 6.3.9. (a) %MVC of the Rectus femoris muscle. (b) %MVC of the Sartorius muscle. (c) %MVC of the Hamstring. (d) %MVC of the Gastrocnemius.

6.3.5 Impression evaluation questionnaires

Some items of impressions of the experiment were designed and each item was evaluated in five degree with a score from -2 to 2, as shown in Fig. 6.3.10. The subject was asked to answer three question about the impression of the walking after each type of experiment with the assist wear (C1 and C2) and finally to answer the impression of the weight of PGAMs assist wear. Tab. 6.3.1 shows the result of the questionnaire survey after the experiments with the PGAMs assist wear. As we can see that, the PGAMs assist wear has a positive score on the items of walking freely with the control C1, feeling being assisted with the control C2 and thinking the whole assist wear is lightweight. These results are consistent with all the physical results that obtained before.

As a summary, the PVC gel artificial muscles based assist wear is compact, lightweight and flexible and showed no impedance to the natural movement of the wearer during walking, it makes the wearer walking freely like a clothing, making the walking being easier and more

efficient and reducing the burden of the leg muscles during walking. This indicates that the proposed PVC gel artificial muscles based assist wear could be feasible to use in a daily life for supporting human motions.

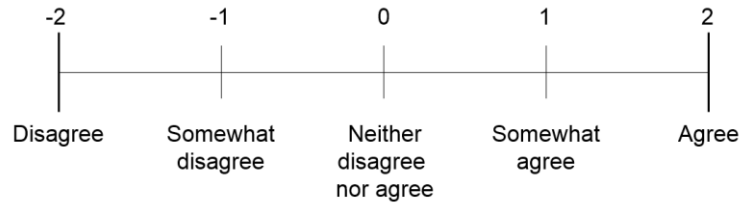


Fig. 6.3.10. Five degree with a score from -2 to 2 for impression evaluation questionnaires.

Table 6.3.1. Result of the impression evaluation questionnaires.

Items	Score
Do you think you walked freely with PGAMs assist wear using control C1	1
Do you think you have been assisted (or walking easier) by the PGAMs assist wear using control C1	-2
Do you feel you would be going to lose a balance during walking with PGAMs assist wear using control C1	-2
Do you think you walked freely with PGAMs assist wear using control C2	0
Do you think you have been assisted (or walking easier) by the PGAMs assist wear using control C2	1
Do you feel you would be going to lose a balance during walking with PGAMs assist wear using control C2	1
Do you think the PGAMs assist wear (including the power and controller) is light weight	2

6.4 Chapter summary

In this Chapter, we conducted an experiment to investigate the effectiveness of wearing the PVC gel artificial muscles based assist wear during steady-state level ground walking.

Since the assist wear just have one half for assisting one leg during walking, we asked a hemiparetic stroke patient (paralysis on one side of the body) to participate in the evaluation experiments. The experiments were conducted in the physiological (e.g. muscular activity variation), physical (walking speed and pace length calculation) and psychological (e.g. some questionnaire survey) aspects.

It was found that with the assistance of the PVC gel artificial muscles based assist wear the walking speed increased about 10% and the step length of the assisted leg increased about 2.8cm during walking.

Also we obtained about 17% maximum decrease of the %MVC for the Rectus femoris muscle, about 11% maximum decrease for the Sartorius, about 5% maximum decrease for the Hamstring with a significant difference of 1%.

And the assist wear is compact and lightweight which allowed the wearer walking freely like a clothing. All the results agrees well with the hypotheses that we made at the beginning of this Chapter.

Those results have already indicated some feasibilities of using the PVC gel artificial muscles based assist wear for a daily life walking support.

However, some further researches on several aspects, such as assist wear design, control algorithms optimization, system effectiveness validation for more subjects with different types should be considered in the future work.

References

- [1] <http://www.stroke.org/we-can-help/survivors/stroke-recovery/post-stroke-conditions/physical/hemiparesis>.
- [2] http://www.creact.co.jp/category/measure/pressure/pressure-novel/pedar_n/
- [3] <http://www.microstone.co.jp/product/mvp-rf10-ac.html>

Chapter 7
Conclusion

Chapter 7 Conclusion

In this Thesis, a novel lightweight, flexible wearable walking assistive wear using PVC gel artificial muscles has been developed, with the aim to meet new demands and needs for a daily life walking assistance for the elderly or the people with some mobile disabilities. Compared to other prior motors based wearable assistive devices, the proposed assist wear had the features of no rigid mechanical structures, minimal weight, and high flexibility and easy to put on and take off which made the assistive device possibly be wearable like a clothing. The main works and results are concluded as follows.

We have improved the characteristics of PVC gel artificial muscles from several aspects, from the gel membranes to artificial muscle fabrication to make it almost close to the level of the biological muscles, in terms of the stable contraction strain, response rate and the maximum output stress. These advantages along with the satisfactory cycle life (over 5 million times) indicate that the PVC gel artificial muscles have a great potential to be a candidate of the new generation artificial muscles in the practical use.

We have proposed an improved approach to measure the output force of PVC gel artificial muscles that can accurately measure the characteristics than the former method which made a great sense in present and future development of PVC gel artificial muscle technologies.

We have proposed three types of modular constructions in this study to make the PVC gel artificial muscles become robust actuation devices for different kinds of applications, which are very important elements for the standardization of PVC gel artificial muscles (as one element for commercialization). Furthermore, the model of the static characteristics developed in this study which showed a good agreement with the experimental data could be an effective element for the specific design and control of the proposed modular constructions in an application.

We have proposed a novel lightweight wearable assistive wear using PVC gel artificial muscles, according to the biomechanics of walking. The assist wear is able to assist the lower limb during the swing phase, from the moment that the toe leaves the ground, providing an assistance over 10% of the maximum moment on the hip to support the motion of the hip joint until the moment of the heel initially contact to the ground, so as to reduce the burden of the leg muscles in the flexion motion.

We have designed and prototyped the walking assist wear using PVC gel artificial muscles, and developed a smart and cost effective walking motion detector and a competent controller. We faced the challenges to make the assist wear being robust, compact, lightweight and

powerful. We used a stretching-type structure to make the assist wear be robust to avoid a break that could be happened among the stacked layers of PVC gel artificial muscles due to the external tensile forces and obtained a high output force that over fifteen times bigger than that in a previous study without any break. A frame-only structure, a curved surface shape and a compact new wiring design of the actuation modules makes the assist wear getting a good fitting to the body and makes it more compact. And we used some cheap but smart insole force sensors to construct a walking motion detector for supporting the control of the assist wear, together with a portable computer NI myRIO to make the system be multifunctional and cost effective.

The characteristics evaluation experimental results of the system were almost consistent with the desired results which indicated the effectiveness of the designed walking assistance system with PVC gel artificial muscles. The fabricated prototype weighed about 0.6kg, demonstrated a good fitting to human body, allowed the wearer moving freely in all directions which liked wearing a clothing. And a low power consumption made the system much more efficient compared to the other prior assistive devices.

And we have conducted experiments to validate the effectiveness of the walking assist wear system, founding that, with the assistance of the PVC gel artificial muscles based assist wear the walking speed increased about 10% and the step length of the assisted leg increased about 2.8cm during walking.

Also we obtained about 17% maximum decrease of the muscular activity for the Rectus femoris muscle, about 11% maximum decrease for the Sartorius, about 5% maximum decrease for the Hamstring with a significant difference of 1% which shows that the assist wear can reduce the burden of the muscles of the lower limb during walking.

And the assist wear is compact and lightweight, showing no impedance to the natural movement of the wearer during walking, and it allowed the wearer walking freely like a clothing.

Therefore, the proposed PVC gel artificial muscles based assist wear could be reasonable for a daily life use, for the advantages of a simple structure, compact and lightweight, flexible, good in fitting and easy to put on and take off.

Future work prospects are extremely wide, and they should be reasonably start with the control algorithms optimization, system effectiveness validation and improvement.

The main contribution of this Thesis can be briefly concluded as follows:

1. A critical review and analysis of the existing artificial muscles and human assistance device technologies.

2. Development and improvement of the PVC gel artificial muscle technology from several aspects to make it much more applicable in a practical application.
3. Propose of a novel lightweight assist wear for a daily life support using the PVC gel artificial muscles.
4. Design, construction and fabrication of a new walking assist system, including the assist wear, walking motion detector and controller.
5. A comprehensive evaluation of the characterizations of the system.
6. An experimental effectiveness validation with a deep analysis of the proposed novel assist wear system.

Finally, we believe that this soft artificial muscles based design concept and structure will give a big inspiration for future wearable robots and soft artificial muscle technologies for human motion assistance and rehabilitation. And we also believe that the PVC gel artificial muscles will play an important role in the field of mechatronics, robotics, biomimetics and biomedicine in the future.

Acknowledgement

Time flies, I have spent another three years in Japan. I can still clearly remember the day I came here, with the dream of the Ph.D. In the past fullest three years, I met many kinds of challenges on the study and work, I experienced many frustrations and also got some grow, and finally arrived to this new important goal in my life. This Thesis is dedicated to all the people who have helped me. I'd like to express my sincere appreciation to all those who have offered me help in any way during the last three years.

My deepest gratitude goes first and foremost to my supervisor, Professor Minoru Hashimoto, who has supported me throughout my two-year master study and the three-year PhD course. With his profound knowledge, constant encouragement and guidance, I have overcome many difficulties in my study and work. I would like to say that without his consistent and illuminating instruction, this thesis could not have reached its present form. Furthermore, he always generously gave me his kindly help and considerations to my foreigner life in Japan. Here, I'd like to give my heartfelt appreciation to him. His positive and rigorous attitude towards work will be a constant inspiration in my life.

I should also give my sincere gratitude to my vice-supervisors and Thesis reviewers, Professor Li-bao Min, Associate professor Hiroaki Yoshida, Professor Atsushi Nishikawa and Professor Taro Nakamura for their time, support and constructive advices and comments in helping me to complete this Thesis.

I would like to represent my great gratitude to my tutor, Associate professor Michihiro Koseki, who has given me many helpful advices, encouragements and supports both on my study and life in the three years study.

I will give my special thanks to Dr. Tsuneaki Yamabe and researcher Kazutoshi Kusano, who have given me a big support on the measurement devices fabrication and many constructive advices and comments to my study, which pushed me to grow. I'd like to say that without their great effort, some important experiments in this study cannot be going on smoothly.

I also want to show my heartfelt thanks to all the colleagues of our research group to support me in daily work and life. They are Mr. Yoichiro Tsichiya, Ms. Aya Suzuki, Ms. Manami Yamaguchi, Ms. Izumi Yoda, Ms. Rina Yokotsuka, Ms. Yoshiko Shirai, Mr. Ryo Sakai, Mr. Keigo Yasuda and Mr. Hikaru Iwano. I cannot finish this Thesis without their support and effort. Besides, I also owe my sincere gratitude to all the colleagues in the other research groups in our laboratory. I enjoyed with them and had a very happy time with them during my three years study. I'd like to give many thanks Ms. Shizue Takeuchi, Mr. Mikio Tetsuya, Mr. Takuma Ohya

for all the supports for the final experiment and helps to my study and life. With the same gratitude to Ms. Hanako Niwa, Ms. Saeko Awazaki, Ms. Hiromi Tokoro and Mr. Hiroharu Arima.

I also want to give my gratitude to Mr. Yasuhiro Maeda for his hard work and important research contribution on walking assist wear which gave me a great inspiration on my own study.

A special thank should give to Shinshu Medical Industry Association (SMIA) of Japan and The Japan Society for the Promotion of Science (JSPS) KAKENHI (15K18002) for the great financial supports.

Finally, my thanks would go to my beloved family. First are definitely my parents, Li Dehua and Jiang Qin, who are always giving me encouragement and incommensurable support in all my studies. Then, I sincerely thank my lovely wife Liu Xiaoyan and my lovely son Li Zifan, for their continuously understanding and support throughout these years. Last but not least, I'd like to give my heartfelt gratitude to my beloved sister Li Rong, who is always giving me encouragement and support all through these years. This thesis would not have been possible without their continuously loving considerations, great support and confidence in me throughout all my studies.

List of publications

(1) Peer reviewed articles

1. Y. Li and M. Hashimoto, "Design and prototyping of a novel lightweight walking assist wear using PVC gel soft actuators", *Sensors and Actuators A-Phys.*, 239 (2016) 26-44.
2. Y. Li and M. Hashimoto, "PVC gel based artificial muscles: Characterizations and actuation modular constructions", *Sensors and Actuators A-Phys.*, 233 (2015) 246-258.
3. Y. Li, Y. Maeda and M. Hashimoto, "Light-weight, Soft Variable Stiffness Gel Spats for Walking Assistance", *International Journal of Advanced Robotic Systems*, Vol. 12, No. 175, pp. 1-11, DOI: 10.5772/61815, 2015.
4. Y. Li, M. Hashimoto, "Emotional Synchronization-based Human-robot Communication and Its Effects", *International Journal of Humanoid Robotics*, Vol. 10, No. 1, pp1350014, 2013.
5. Y. Li, P. He, Q. Li, Z. Dou, J. Li, "The Design of Intelligent Sheep Detector", *Journal of Agricultural Mechanization Research*, Vol.2, pp182-183, 2009. (in Chinese)

(2) International conference (Peer reviewed full paper):

1. Y. Li and M. Hashimoto, "A Proposal of a Light-weight Walking Assist Wear using PVC Gel Artificial Muscles", *The 2015 IEEE International Conference on Robotics and Automation (ICRA 2015)*, Seattle, USA, pp.2920-2925, 2015. (IEEE Robotics and Automation Society Japan Chapter Young Award (2015))
2. Y. Li, Y. Tsuchiya, A. Suzuki, Y. Shirai and M. Hashimoto, "Influence of the number of stacked layers on the performance of PVC gel actuators", *IEEE/ASME International Conference on Advanced Intelligent Mechatronics (AIM2014)*, Besacon, France, pp.94-99, 2014.
3. Y. Maeda, Y. Li, K. Yasuda and M. Hashimoto, Development of variable stiffness gel spats for walking assistance, in: *The 2013 IEEE/RSJ Int. Conf. on Intelligent Robots and Systems (IROS2013)*, Tokyo, Japan, 2013, pp.5404-5409.
4. Y. Li, Y. Tanaka, M. Ono and M. Hashimoto, "Interaction Design of an Animated Robotic Interface in Vehicle", *5th International Congress of International Association of Societies of Design Research (IASDR2013)*, Tokyo, 2013, pp. 4903-4907.

(3) Japan domestic conference (in Japanese):

1. Y. Li and M. Hashimoto, “Application of Expansion Type PVC Gel Artificial muscles to Walking Assist Wear”, in the 21th Robotics Symposia, pp. 5D2, 2016. (with peer review)
2. Y. Li and M. Hashimoto, “Fabrication and Evaluation of PVC Gel Artificial Muscles based Walking Assist Wear”, in the 16th SICE System Integration Division Annual Conference (SI2015), pp. 1H1-7, 2015.
3. H. Iwano, A. Suzuki, Y. Li, M. Hashimoto, “Development of a PVC Gel Sheet Actuator with Flexible Electrodes”, in the 25th Annual Meeting of MRS-Japan 2015, pp. A4-09-002, 2015.
4. Y. Li and M. Hashimoto, “A light-weight Walking Assist Wear using PVC Gel Artificial Muscles”, in the 20th Robotics Symposia, pp. 477-482, 2015. (With peer review)
5. Y. Li and M. Hashimoto, Characteristics and Modeling of PVC Gel Actuators, in the JSME conference on Robotics and Mechatronics, pp. 2A2-A09, 2015
6. Y. Li, Y. Tsuchiya, A. Suzuki, Y. Shirai, R. Sakai and M. Hashimoto, A Characteristics Evaluation Method for PVC Gel Actuators, in the 15th SICE System Integration Division Annual Conference (SI2014), pp. 592-595, 2014.
7. Y. Li, Y. Shirai, Y. Tsuchiya, K. Yasuda and M. Hashimoto, Relation of Stacked Layers and Characteristics of PVC Gel Actuators, in the JSME conference on Robotics and Mechatronics, pp. 2A1-K01, 2014.
8. Y. Li and M. Hashimoto, “PVC Gel Spats for Walking Assistance using Variable Stiffness”, in the 19th Robotics Symposia, pp. 319-424, 2014. (in English, with peer review)
9. Y. Li and M. Hashimoto, “Construction of an Expansion Type PVC Gel Actuator”, in the 14th SICE System Integration Division Annual Conference (SI2013), pp. 2478-2479. 2013.
10. Y. Meda, K. Yasuda, Y. Li and M. Hashimoto, “Development of a variable stiffness gel spats for walking assistance”, in the JSME conference on Robotics and Mechatronics, pp. 2P1-F08, 2013.